PŘÍLOHA č. 1

ECOHYDROLOGY
Ecohydrol. (2013)
Published online in Wiley Online Library
(wileyonlinelibrary.com) DOI: 10.1002/eco.1453

An appraisal of the effectiveness of nature-close torrent control methods – Jindrichovicky Brook case study

Pavel Kovar,[1]* Frantisek Krovak,[1] Vit Rous,[1] Michal Bily,[1] Miroslav Salek,[1] Darina Vassova,[1] Michaela Hrabalikova,[1] Vaclav Tejnecky,[2] Ondrej Drabek,[2] Tereza Bazatova[1] and Jitka Peskova[1]

[1] *Faculty of Environmental Sciences, Czech University of Life Sciences Prague, Prague, Czech Republic*
[2] *Faculty of Agrobiology, Food and Natural Resources, Czech University of Life Sciences Prague, Prague, Czech Republic*

ABSTRACT

Discharge fluctuation and extreme bed load movement, i.e. erosion and sedimentation occurring on short upper reaches of the river, are characteristic features of torrential rivers. This paper presents a biotechnical appraisal of a torrent catchment for implementing revetments methods, focusing on selected hydraulic characteristics of the flow. The Infiltration and Kinematic wave hydrological model (KINFIL) hydrological model (for design discharges) is used to verify these variables and also the Hydrologic Engineering Centre's River Analysis System and Sedimentation and River Hydraulics Two-Dimensional hydraulic models for channel flow. Data and computation for proposing nature-close remedial measures are demonstrated in a case study of the Jindrichovicky Brook, a mountain torrent located in the Ore Mountains (Czech Republic).

Particular attention is given to appropriate adaptation of the river for the invertebrate community. The hydraulic analysis is carried out in two sections of the river (section A: 'nature-close', restored in 2008, and section B: 'old style', regulated in the 1970s). The aim is to compute the major hydraulic characteristics (depths, velocities, shear stress values etc.). Then, a hydrobiological investigation is carried out in both sections to find how much the invertebrate communities extended their diversity and abundance as a consequence of better geomorphological diversity after restoration. It was found that, from the hydraulic point of view, the old section B is sufficiently robust and stable. However, it is clearly evident that this section can hardly be populated by fauna and if so, then only very sparsely and impermanently. Section A meets both priorities, hydraulic stability and an acceptable living environment for the benthic community. Copyright © 2013 John Wiley & Sons, Ltd.

KEY WORDS torrent control; hydro-technical appraisal; shear stress; migration permeability; diversity and abundance of invertebrates

Received 12 February 2013; Revised 24 October 2013; Accepted 24 October 2013

INTRODUCTION

Restoring small rivers and thereby also improving environmental conditions for the biota have been a trend over the past several decades. Instead of keeping a robust engineering works, in close to nature revitalization measures, we prefer to reconstruct natural obstacles in the river channels, even in the torrent reaches, in order that the river remains open to biota migration. The main objective of this work is to give examples of how traditional torrent control structures, usually insurmountable for fish and the benthic community, can be replaced by more biota-friendly constructions that allow migration. This paper supports an objective comparison of hydraulic properties between old style bed drops and the system of step/chute-pools open to biota.

Sudden changes in discharge occurring during rainstorms are characteristic for torrential rivers. The increase in the discharge is abrupt and of short duration, and after reaching its maxima, it quickly diminishes. This is due to the small catchment area, often impacted by heavy rains, and also the high gradient of the catchment and the flow (Beven, 2006). Another important consideration is that the greatest damage is caused not by large volumes of water overflowing the banks and subsequent flooding of large tracts of land, as is common in lowland catchments, but rather by devastation of specific sections of the catchment and of structures situated in the vicinity of the catchment, due to the significant shear stress that impacts the river bed and the banks through the masses of flowing water. This research on changes in shear stress values fluctuation has recently provided good practical results in the USA (e.g. Chin *et al.*, 2009). The accumulation of moving bed loads in the lower sections of the catchment is another important factor. On the basis of this experience (Kovar and Krovak, 1998, 2002), it is necessary to propose torrent control measures that can not only meet purposeful requirements, influencing the river basin capacity and its resilience to stress, but also fulfil ecological requirements

*Correspondence to: Pavel Kovar, Faculty of Environmental Sciences, Czech University of Life Sciences Prague, Kamycka 129, 165 21 Praha 6, Suchdol - Prague, Czech Republic. E-mail: kovar@fzp.czu.cz

concerning the environmental character of the torrent and biotechnical revetment methods.

Today, the traditional alpine approach to torrent control (reaching back almost 150 years) raises many issues, particularly concerning the utility of allegedly superfluous and excessively large structures. For years, classical torrent control lay within the domain of forestry engineering. However, because of present-day purpose-oriented ecological requirements, specifically migration permeability of the flow for fish, and nature-close remedial measures, the natural character of the bottom substrate and the planting of riparian vegetation have become a part of torrent control methodology (Novak *et al.*, 1986; Just *et al.*, 2005). In contrast to lowland waterways, torrents are closely connected with their catchment, both morphologically and from the hydrological point of view. This is corroborated by the means for identifying them, i.e. setting the index of torrential character, where the characteristics of the torrent catchment are applied for determining its discharge (e.g. Wilcox *et al.*, 2008). Management of torrent catchments, i.e. implementation of erosion control measures, should include measures for safeguarding environmental biodiversity, i.e. fauna and flora. Today, this has become a very important issue (Lange and Lecher, 1993; Chin and Gregory, 2001). The trend is requiring the removal of obstacles that block fish and invertebrate migration, as seen in classical (old-style) torrent control structures. This is also stipulated in the European Union (EU) Water Directives (COUNCIL DIRECTIVE 98/83/EC, 1998; WFD EC 2000/60/ES, 2000) and has been recommended by several authors in journals of ecology and hydrobiology (Brookes and Shields, 1996; Gordon *et al.*, 1996; Waal *et al.*, 2000).

The EU Water Framework Directive (WFD EC 2000/60/ES, 2000) generally defines fish, macroinvertebrates and phytoplankton as target organisms for improvement in aquatic environments. Improvements are not only important for the survival of these species: hydraulic structures must be made in a way that allows them to migrate in the torrent environment. These target groups of invertebrates thrive even in the source area of the torrent. Therefore, from the very first hundred metres of concentrated flow, biotic migration and its revival must be taken into account. The construction of elevated steps and obstacles should be avoided. The same holds for the bottom pavement. Stabilizing structures have been built in the past for erosion control purposes. The question may be raised whether today's society would approve structures of that kind, which restrict the development of biotic communities, whereas modern structures offer feasible alternative measures that support biotic diversity and abundance. This is the issue that is specifically dealt with in our paper.

The restoration of a classical in-line torrent control structure was practically tested in a case study carried out on the Jidrichovicky Brook, in the Ore Mountains, Czech Republic. The KINFIL hydrological model (Kovar *et al.*, 2002; Vrana *et al.*, 2012) was used for determining the *N*-year run-off. Two hydraulic models were used for designing the new structures: first, the Hydrologic Engineering Centre's River Analysis System (HEC-RAS computer program, 2001; Cook, 2008; Brunner, 2010), and parallel to it, the more recent Sedimentation and River Hydraulics Two-Dimensional (SRH-2D) model (Lai, 2008; Aquaveo, 2010). The idea behind our study was to explore the possibilities of applying integrated modelling, hydrological and hydraulic models in a geographic information system (GIS) environment, with the aim of determining core restoration measures. Two experimental sections were selected on the Jindrichovicky Brook (Figure 1). The lower section B is situated downstream the outlet of the catchment at the uppermost bottom drop (1·8 m high). This was built in 'old-style' torrent control during the 1970s in a stable slope with all robust drops, and the river bottom was paved with flat stones (granite). Section A is above section B, and it was fully restored from the 'old-style' torrent control technology in 2008. Hydraulic model computations were used for implementing the restoration measures with a system of hydraulic structures combining chute-pools or step-pools with a free river bottom between them. The differences in benthic population in A and B reaches indicate connectivity and habitat conditions characterized by reduction of flow velocities and heterogeneity of bed material. However, we have to admit that these differences could be even larger when the longitudinal river continuum would be re-established (which should occur in the near future).

In addition, an assessment of the impact of the newly formed channel on stream macroinvertebrates (benthic animals larger than 0.5 mm, Wetzel, 2001) was tested by making a comparison with the former torrent control regulated channel. Macroinvertebrates were chosen for the analysis, because this group is known to be strongly influenced by the substrate of the stream bottom; also, benthic communities of streams and rivers are classified according to the nature of the flow bottom (Lellak and Kubicek, 1991). A number of recent studies have described the effect of stream or river restoration on macroinvertebrate communities (e.g. Jahring and Lorenz, 2008; Sundermann *et al.*, 2011). However, there is still a deficiency of such studies on small torrential brooks.

METHODS

Nature-close torrent control or revitalization measures usually dramatically alter the initial design variables of the torrent basin. A new design of hydraulic variables should therefore focus on

- stability of the river bottom and banks against the impact of erosion caused by flowing water shear stress;
- the impact of biotechnical measures on the water flow type in the channel and in the riparian zone;

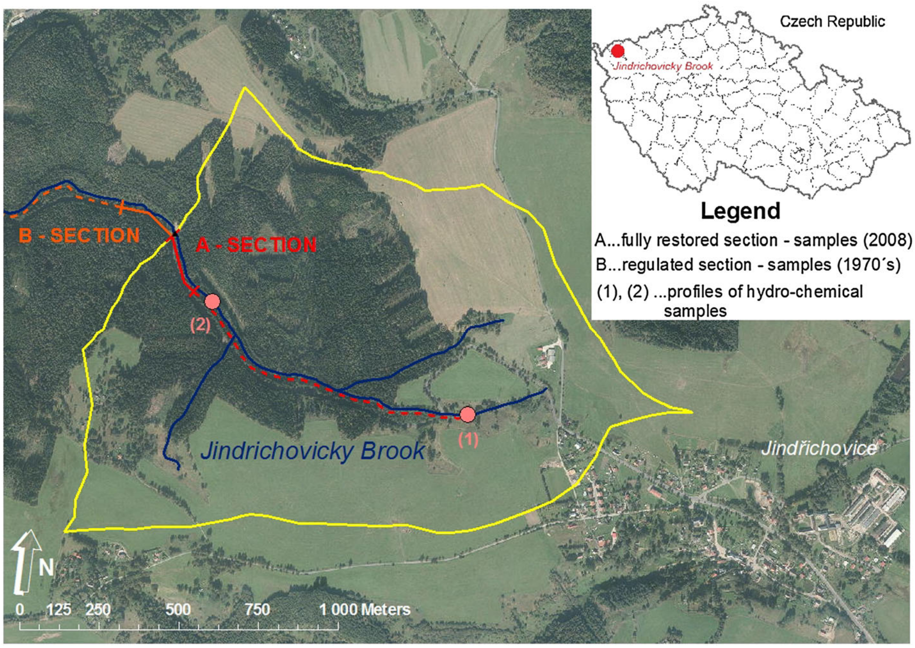

Figure 1. Location of the study area.

- the nature-close character of the bottom substrate (sediments);
- depth, velocity, water volume and possibilities of a change in the morphology of the torrent basin during low discharge that will have an important effect on the biotic population;
- reduction of torrential erosion by adapting the sediment regime; and
- torrent basin capacity, with reference to the design capacity discharge, particularly in urban areas.

The most important design data and derived variables concern design discharges. These are selected with regard to open landscape or urbanized sections and their infrastructure.

N-year discharges, as set up by the Czech Hydrometeorologic Institute (CHMI), are usually used; in the case of small catchments, with run-off conditions altered because of anthropogenic activities, rainfall-run-off models can be applied, e.g. MIKE SHE (Abbott and Refsgaard, 1996), US Army Corps of Engineers' Hydrologic Modeling System HEC-HMS (USACE, 2000) or others. In our study, the KINFIL model (Kovar, 1992; Kovar *et al.*, 2002; Vrana *et al.*, 2012) was used.

Structure of the KINFIL hydrological model

The KINFIL hydrological model (Kovar, 1992; Kovar *et al.*, 2002) is based on a combination of the theory of infiltration and transformation of direct run-off by a kinematic wave, which proved to be useful in small experimental catchments in model simulations of historical flood events. The model uses physiographic and hydraulic parameters of the catchment, which can easily be determined from maps in the absence of direct observation, taking into account the impacts of anthropogenic activities in the catchment. The model is particularly useful in determining the design discharges in various scenarios and land use changes, e.g. deforestation and urbanization. The current version of the KINFIL model is based on the infiltration theory of Green and Ampt, with regard to the Morel-Seytoux (Morel-Seytoux and Verdin, 1981) flooding concept. Soil saturated hydraulic conductivity and the sorptivity parameter (at field capacity) are the major parameters for solving problems related to infiltration. Their correlation with run-off curve numbers (CN) (USDA SCS, 1972; U.S. SCS, 1986; Morgan and Nearing, 2011) can also be used.

The second component of the KINFIL model is a direct run-off transformation. The equation describes the unsteady flow of water approximated by the kinematic wave on a cascade of planes. The differential kinematic wave equation is transferred to the final differences and solved through the explicit numerical scheme of Lax and Wendroff (Singh, 1996). For practical solutions, the catchment is usually fragmented by components, cascades of plane segments, of rectangular planes and/or of river reaches, in order to simulate the natural topographic configuration. The use of the KINFIL model has been described in several studies (e.g. Vrana *et al.*, 2012).

For this hydrological model, it is necessary to analyse the geography of the catchment, using GIS for the geometry of the morphological variables, determining the hydraulic properties of the soil, land use and data for setting the run-off CN.

Structure of the HEC-RAS and SRH-2D hydraulic models

The mathematical HEC-RAS hydraulic model (Brunner, 2010), version 4.1, was selected for calculating the required output data for the Jindrichovicky Brook. HEC-RAS uses the integrated MS Windows environment with an excellent graphic user interface, with detailed representation of the flow hydraulics in open river channels in artificial and natural streams.

The system contains a one-dimensional river analysis for (1) stable flow; (2) unstable flow; (3) sediment movement; and (4) water quality analysis.

The calculation requires the assignment of three main categories of data: geometry of the basin and structures, hydraulic loss coefficients and boundary conditions. It is possible to use the connection to computer-aided design and GIS in 3D presentation. Two principles can be applied for a hydraulic assessment of the capacity of open channel systems and their hydraulic structures for maximum run-off:

1. Deal with the passage of the design flood wave by means of a hydraulic model based on a numerical solution of the unstable flow. This method requires knowledge of the form of the entry design wave in the upper closing profile of the assessed section of the flow and, similar to the next principle, a detailed description of the geometric and hydraulic variables of the basin. This approach is demanding from the computational point of view, and it is usually not applied to streams of local significance.
2. Use the stable hydraulic flow method for determining the longitudinal profiles of the water table, with reference to each design of *N*-year discharges. This method does not function in unstable conditions; however, it has the advantage that a more detailed expression can be made of the flow through hydraulic structures situated in the stream.

The program deals separately with hydraulic regimes of sub-critical and/or super-critical flow. The flow over hydraulic structures can be analysed in detail and solved for various hydraulic regimes. It guarantees reliable assessment, mainly in locations where the hydraulic regime of the structures is influenced by the flow in the river basin. This is the case for the Jindrichovicky Brook. The stable model offers higher values for solving the water table regime; its results are on the side of a safety design.

The system allows stable non-uniform flows in natural open channels to be dealt with, and it is also possible to describe widely used hydraulic structures in the catchment. A big advantage is the cost-free use of the model, its large scope of application and the number of analogue situations and examples. For these reasons, the program application of HEC-RAS was used in this study to assess the capacity of the river basin and the structures.

In this study, HEC-RAS was first used to assess the capacity of the basin and the structures; subsequently, the results of the calculations of depths, velocity and shear stress were compared with the results from the more up-to-date SRH-2D model, which deals with hydraulic events in the stable flow regime.

A digital elevation model was created in accordance with the restoration plan for the Jindrichovicky Brook and was used for testing the two-dimensional SRH-2D model, developed by the US Bureau of Reclamation (Lai, 2008), and for verifying the hydraulic character of the basin. The SRH-2D model is comparable with other two-dimensional models, but it has the advantage that it can be applied in a flexible network of calculation elements and that it is an overall robust model.

A calculation domain in the AQUAVEO Surface-Water Modeling System (SMS), counting over a hundred thousand elements, was created for restoring the Jindrichovicky Brook. The size of the rectangular computational elements was $0{\cdot}5 \times 0{\cdot}4$ m, and when inundated, this amount was $1{\cdot}0 \times 0{\cdot}8$ m. A digital elevation model of the terrain was created in the AUTOCAD Civil 3D 2012 program (Autodesk, 2012) from surveying land measurements and design cross-section profiles from the HEC-RAS program.

Hydrobiological and hydrochemical methods

Sections A and B were studied and compared (Figure 1). These two sections were selected because of similar flow rate and space proximity. It can be assumed that the differences in the composition of the benthic fauna in the two sections are determined mainly by the different torrent control concepts. The most evident difference between the styles of torrent control on Sections A and B is that the old-style (B) has a stone-paved bottom, which provides reliable protection against scouring but makes it hard for benthic communities to survive. In addition, the system of robust bottom drops (1·5–2·5 m in height) in this section can form a bottleneck for biota. Section A, which is as nature-close as possible, provides conditions for full restoration with free bottom almost natural revetments (a stone chute-pool), local riparian vegetation, geomorphological diversity in situation, longitudinal and cross-section profiles and so on.

Hydraulic parameters (Doledec *et al.*, 2007) as well the type of bottom substrate (Allan, 1995; Wetzel, 2001) can play a role in the occurrence of stream macroinvertebrates. The type of bottom substrate was chosen as the parameter characterizing the different types of restoration in our study sites. Macroinvertebrates were sampled in October 2011. There were 15 sampling sites located in section A and 15 sampling sites in section B. One sample was taken at each sampling site.

The sites were situated within the longitudinal direction of the stream. In section A, the position of the sampling sites was primary chosen to represent all three main types of bottom substrate present in this section of the channel. These were

1. stretches that are close to the natural character of the flow, named for this purpose as 'natural' substrate;
2. sandy deposits, occurring principally in the pools under the chute/steps ('sand' substrate); and
3. bottom composed of stone slab compounds ('stone' substrate).

Each of these three types of environment was represented five times in the series of 15 samples in section A. Each two sampling sites were approximately 10 m apart.

In section B, the prevalent type of bottom is composed of consistent stone pavement, covered in some places by sand and gravel deposit. Only in some specific locations (several metres beneath the stone steps), we can find sand deposits similar to 2 in section A. The 15 sample sites in section B were placed regularly on the flow, within a distance of 10 m. In section B, a total of 13 sites are of stone pavement type, and two are of sandy deposit type.

The sampling was done according to the standard methodology with a Surber sampler (Peckarsky, 1984), with mesh size 0·5 mm and a $30 \times 33{\cdot}5$ cm frame. Each sample represented $0{\cdot}1\ m^2$ of bottom. The sample was transferred in the net of the sampler: (1) loose substrate (sand and gravel) was collected at a depth of approximately 5 cm (where such a layer existed); (2) stones smaller than the sampler area were collected directly; and (3) the surface of big stones, solid stone pavements, if present (i.e. in test section B), were swept into the net with brushes. The procedure allowed us also to collect substrate samples under the freely disposed, removable stone slabs. By using this combination of three methods, quantitative sampling of relevant benthic fauna was ensured in all habitats in the sampled areas. All collected materials were washed in the net in running brook water and transported in bowls. The macroinvertebrates were extracted from each sample, fixed in a 70% ethanol fluid and further processed in the laboratory. Abundance (number of individuals) was counted for each sample. Individuals were identified at family level, except higher taxa of Nematomorpha (one specimen) and Hydracarina (15 specimens). Some Trichoptera pupas also remained without family determination. Two abundance categories were therefore distinguished: (1) numbers without Trichoptera pupas in the analysis, which paired each individual to the relevant family, and (2) the total count in the remaining analysis.

For an assessment of the effect of the torrent control type on benthic fauna, we evaluated the taxonomic richness (represented by the number of identified families) and the faunal abundance (the number of specimens) in the samples. Firstly, we tested the strength of the relationship between taxonomic richness and faunal abundance in the samples within sections A and B, by using linear regression; prior to this procedure, we checked the two variables for normality (Kolmogorov–Smirnov test, both $d < 0{\cdot}15$, $P > 0{\cdot}05$). Student's *t*-test was used to assess the difference in taxonomic richness between sections A and B. These procedures were performed using R 2.9.2 software (R Development Core Team, 2009). The effects of torrent control (new restoration or old regulation type) and substrate (natural, sand, stones and paving) on the composition of the benthic communities were explored using direct gradient analysis (canonical correspondence analysis) to summarize the relationships between occurrences of the taxonomic groups and the variables. Using detrended correspondence analysis, we checked that the groups responded unimodally to the predictors and that the use of a weighted averaging method was appropriate (ter Braak and Smilauer, 2002). A Monte Carlo permutation test with 4999 unrestricted permutations was applied to test the importance of the predictors and the canonical ordination axes. A manual forward selection procedure was utilized from an empty model to a more complex model, with stepwise ranking of the variables by their importance computed by CANOCO (Software for Cannonical Comunity Ordination) for Windows 4.5 (ter Braak and Smilauer, 2002). In all analyses, we adopted significance level $P = 0{\cdot}05$ for hypothesis rejection.

Water samples [taken from profiles (1) and (2), see Figure 1] were analysed for their anion and cation contents. Before chemical analysis, each sample was filtered through a nylon membrane filter with 0·45 μm pore diameter. The main inorganic anions (F^-, Cl^-, Br^-, NO_2^-, NO_3^-, PO_4^{3-} and SO_4^{2-}) were identified by means of IonPac AS 11-HC ion chromatography (Dionex, USA). A pre-column and analytic column IonPac AS11-HC (Dionex, USA) was used for separating the analysed samples. For the mobile phase, a 28·8 mm solution KOH and discharge mobile phase in 1 ml min^{-1}. An ASRS 300 4 mm self-regenerating suppressor (Dionex, USA) was used to reduce the conductivity of the mobile phase. Detection of the analysed samples was operated by means of conductometry. Prevalent free cations (Na^+, K^+, NH_4^+, Ca^{2+} and Mg^{2+}) were identified by means of ICS CS16 ion chromatography (Dionex, USA). A pre-column and analytic column IonPac AS11-HC (Dionex, USA) was used for separating the analysed samples. A 35 mm solution of methansulfonic acid and discharge mobile phase in 1 ml min^{-1} for the mobile phase. A CMMS 300 mobile phase suppressor (Dionex, USA) was used to reduce the conductivity. A 100 mm solution of hydroxide tetrabutylammonium was used as a suppressing agent. Detection of the analysed samples was operated by means of conductometry. The total quantity of dissolved Fe and Mn in the water samples was determined by

AA80FS atomic absorption (Varian, Australia) in standard analytic conditions. Quality control and quality assurance were carried out according to Tejnecky *et al.* (2013).

Catchment characteristics

The Jindrichovicky Brook, situated in north-west Bohemia, in the Ore mountains region, is a left-side tributary of the river Rotava, at 2·0 km downstream. The brook, with an average slope of 4%, has the character of a torrent, with the following conditions: catchment area $<35\,km^2$, elevation $H > 200$ m above sea level, slope gradient $J > 3\%$ varies considerably, with supercritical flow, enormous erosion, transport and sedimentation of solid deposits, rock boulder bed, current shadows and hideaways, and populated mostly by trout in the lower parts of the torrent. Table I and Figure 2 indicate the catchment characteristics. Average monthly temperatures and precipitation are indicated in Table II.

Table I. Hydrological characteristics of the Jindrichovicky Brook catchment.

Hydrological catchment number	1-13-01-114
Total catchment area	5·964 km^2
Length of river reach A	0·290 km
Length of river reach B	0·180 km
Forested catchment area	47%
Length of catchment	1·62 km
Length of water divide	4·35 km
Catchment shape coefficient	$A = 0{\cdot}653$
Catchment shape	Fan-shaped without developed hydrographic network
Torrent index	$K_T = 0{\cdot}118$
Slope of catchment	0·044 (–)
Slope of river reach A	0·023–0·038 (–)
Slope of river reach B	0·040 (–)

As far as the relief of the terrain is concerned, it is part of an area of interest in the Ore Mountains, with deep-cut valley waterways. The slopes mostly face the north-west. The stream source of the brook is situated below the village of Jindrichovice, and after about 2 km, it flows into the Rotava river. The Jindrichovicky Brook does not have any significant tributaries. Forested areas make up 47% of the catchment. The valley flood plain is overgrown with mixed forest, with mainly pine and spruce trees. The undergrowth is composed of herb vegetation, with plenty of shallow puddles and ruderal vegetation.

Transmissivity is the basic quantitative characteristic of the hydro-geological environment. This designates the capacity of the aquifer to transmit a certain quantity of groundwater and approximately determines its hydrological use. The transmissivity value for the given locality is $T = 10^{-3}$–$10^{-4}\,m^2\,s^{-1}$, which represents a medium level. The prevalent soil genetic groups are podzolic soil and podzols of mountainous regions, with prevalent clay-loamy soils and clays.

Table III presents data from the CHMI, concerning *N*-year and *M*-day discharges to the closing profile of the Jindrichovicky Brook (catchment area = 5·964 km^2).

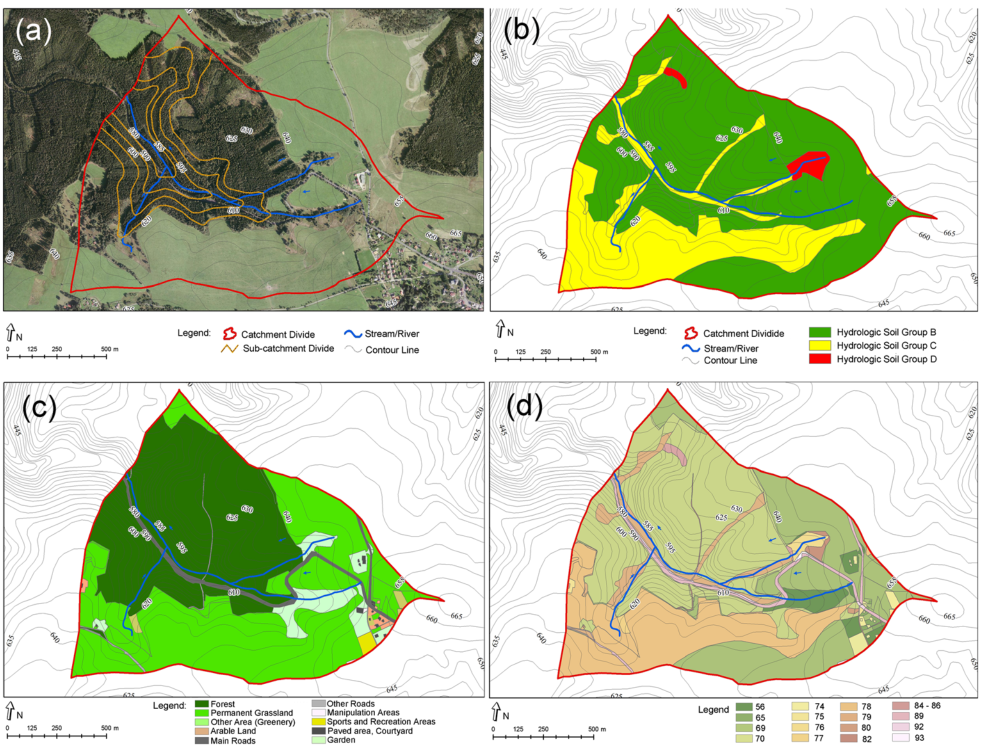

Figure 2. The Jindrichovicky Brook catchment: (a) orthophotomap, (b) hydrological soil groups, (c) land use, and (d) curve numbers.

Table II. Average monthly temperature and precipitation on the Jindrichovicky Brook catchment.

Month	I	II	III	IV	V	VI	VII	VIII	IX	X	XI	XII	I–XII
Temperature (°C)	−2·5	−1·6	2·2	6·4	11·6	14·6	16·4	15·4	12·0	7·1	2·0	−1·4	6·8
Precipitations (mm)	63	54	46	52	60	68	84	80	52	54	55	60	728

Table III. *N*-year and *M*-day discharges of the Jindrichovicky Brook catchment (restored reach beginning profile).

N (years)	1	2	5	10	20	50	100
Q_N (m^3 s^{-1})	0·9	1·2	2·2	2·9	3·7	5·4	6·9
M (days)	30	90	210	330	364	—	—
$Q_{M\mathrm{d}}$ (l s^{-1})	40	25	12	6	3	—	—

The present design quantities (in Table III) do not differ significantly from those used in the traditional methods. Because of the slightly changed land use in the catchment (permanent grassland instead of arable land), the present design discharges were computed as the lesser values (reduction 5–7%).

Initially, the improved river reach was devastated by extensive bank and bottom ruptures, with many stone outcrops, exposed by bed erosion. In certain sites, 2·5–3·0 m deep gulches appeared, which endangered the adjacent road. The bottom of the channel was stony with upper sediment layer granularity of 5–10 cm and with boulder lower layer granularity of 20–30 cm. Where ruptures appeared, the bed was exposed up to the bedrock; where the velocity of the flow was smaller, extensive sandy ripples appeared.

In the design for mitigating torrent erosion, the rule of using all options including biota transfer possibilities was applied (Chin, 2003; Chin *et al*., 2009). This modern ‘chute/step-pool’ procedure meets the restoration requirements and, at the same time, solves the sediment transport problems by reducing the causes of their occurrence. The cascade of combined double hydraulic structures of this kind (with positive or even negative inclination of the pool bed) reduces the occurrence of extreme local velocity and high shear stress values in the regressive process of bottom scour, including bank foots (Figures 7 and 8). The already restored reach of the Jindrichovicky brook followed up its old regulated reach with cross-section barriers impermeable for migrating organisms built in the 1970s in the form of high-drop structures and river bed pavement. Future restoration of this reach (section B) is under discussion.

Nature-close proposal

The proposed trajectory of the Jindrichovicky Brook very closely follows the natural trajectory of the basin, which flows rapidly and, because of the relatively high inclination of the slope, does not meander. The total length of the restored reach is 1·055 km, of which 0·078–0·166 km, 0·206–0·221 km and 0·805–0·815 km are sharp erosive irregularities that have been replaced by free standing arches. The bank ruptures and bottom scours were used to create pools beneath the chutes and steps. They were stabilized with the help of cross-section structures made of stone rip-raps.

The cross-section profile has a saucer-shaped form; the bottom width is 1·0–2·0 m, with bank slopes about 1 : 1·5–1 : 2 up to the bank edges, with the exception of the pool section. The bank foot of this reach is built from stones reinforced with rock fill, and the remaining part of the slope above the abutment is overgrown with grassland. Because of a major longitudinal slope and thus greater shear stress, it was necessary to design the slope lines. A number of basic chute/step-pool gradient structures (U.S. SCS, 1986), as well as cross-section sills, in wood and stone, were built. The construction work and the adaptation of the hydraulic structures were done in such a way as to enable migration in both directions. They do not exceed 0·4 m in height, and the transversal section of the chute table ensures run-off in a consistent water jet. These structures are designed to be hydraulically effective for capacity discharge – the material being stone, which copies the natural gradient drops in the torrents. To minimize the reinforcement between the transversal structures, these sections were designed with a stable slope, which corresponds to the given granulation of the deposits, based on the critical shear stress. The nature-close construction was finished in 2008.

In the restored section A, there are a few short sections with boulders placed on the bottom, where the slope is very steep. However, there are much longer reaches with a free bottom covered by a gravel-sandy surface, mostly formed by sediment. For a closer assessment of the design restoration elements in contrast to the original situation, the computation domain was reduced in a way that corresponds to the surfaces (sections A and B) for the withdrawal of hydrobiological samples. The computation of the hydraulic characteristics was made more precise by condensing computation of the elements from 0·5 × 0·4 m to 0·15 × 0·1 m. This hydraulic computation and the benthos sampling have been carried out in 2011 to 2012.

Design rains and water discharges

For computing the *N*-year discharge, it is necessary to know the depths of the design rains. The depths of short-term rains for the Jindrichovicky Brook catchment (Table IV and Figure 3) were determined from the data collected at the Jachymov raingauge station, using the DES_RAIN program (Vassova and Kovar, 2011), which is based on the one-day maximum rainfall reduction method (Hradek and Kovar, 1994):

$$P_{t,N} = P_{1\mathrm{d},N} \cdot a \cdot t^{1-c}$$

where $P_{t,N}$ represents the rainfall for duration t and average occurrence N, $P_{1\mathrm{d},N}$ is one-day maximum rainfall for occurrence once within N years, t is duration of the design rain, and a and c represent regional parameters.

The KINFIL model computed the N-year design discharges from the design rainfalls applied to the Jindrichovicky Brook catchment. The model is particularly intended to determine the discharge after various human interventions, e.g. change of land use, clear cut and urbanization. It has several options for ungauged catchments, such as this case study of the Jindrichovicky Brook. Various run-off CN data, widely used throughout the world, were applied (U.S. SCS, 1986; Ponce and Hawkins, 1996). The transformation of direct run-off was solved by a kinematic wave according to the geometric and hydraulic properties of each sub-catchment (Kovar and Krovak, 2011). The results are presented in Table V, where the results from the KINFIL model can be compared with the N-year discharge data, supplied by CHMI. The N-year discharge hydrographs acquired through the KINFIL model are indicated in Figure 4.

Hydraulic computations using the HEC-RAS model

The channel capacity and its shear stress were assessed for two scenarios: for section B, old-style regulation measures (B-OLD) and for section A, new 'restoration style' measures (A-NEW), using the HEC-RAS hydraulic model. The difference between them is the paved bottom and the high bottom drops in Section B. In both scenarios, the computation was made for a 30-day discharge, while some of the project-relevant N-year discharges (i.e. from $Q_{30\mathrm{d}}$ to Q_{100}) were determined by the KINFIL model. Geomorphological data

Table IV. Depths of design rainfalls $P_{t,N}$ (mm) for various return periods N = 2–100 years and duration t = 10–300 min for the Jachymov station (648 m a. s. l.).

Return periods N (years)	Depths of design rainfalls $P_{t,N}$ (mm)*	Duration t (min)				
		10	20	30	60	90
2	40·8	13·48	16·59	18·73	21·66	23·46
5	53·5	18·77	23·30	26·44	31·76	34·40
10	61·6	22·17	28·14	32·35	38·64	41·85
20	70·1	26·64	34·01	39·22	47·11	51·03
50	80·5	32·24	41·43	47·98	58·25	63·09
100	88·6	36·35	47·14	54·88	66·49	72·02

*Taken from Samaj *et al* (1983).

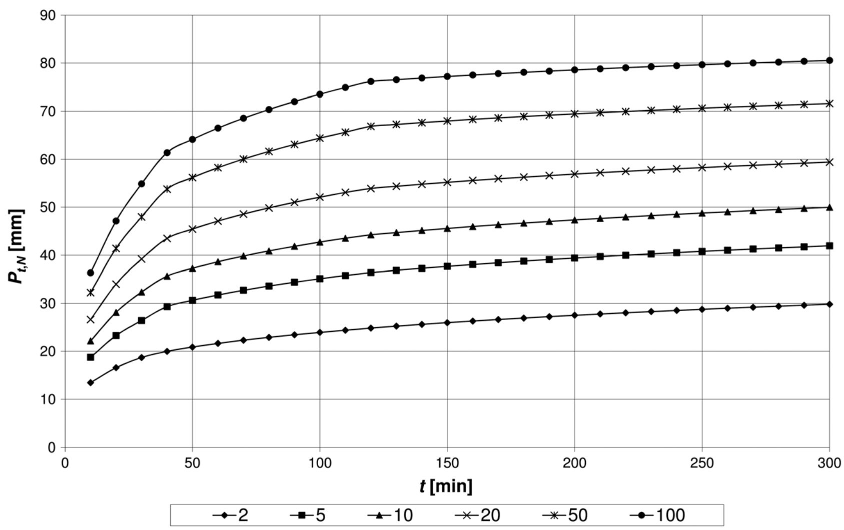

Figure 3. Depths of design rainfalls for duration t = 10–300 min and return period N = 2–100 years for the Jachymov station.

Table V. Design discharges at the outlet of the Jindrichovicky Brook catchment (restored reach beginning profile).

N (years)	1	2	5	10	20	50	100
Q_N CHMU ($m^3 s^{-1}$)	0·9	1·2	2·2	2·9	3·7	5·4	6·9
Q_N KINFIL ($m^3 s^{-1}$)	0·98	1·3	2·39	3·15	4·02	5·85	6·51

input concerning the geometry of the channel and the hydraulic structures, based on detailed measurements of the longitudinal and cross-section profiles, was included in the computation. These structures have a decisive influence on the water level regime and on the channel shear stress. The basic hydraulic characteristic of the channel is the Manning roughness coefficient n. Because of the material composition of the original channel and the structures, various values were selected and determined, in accordance with the HEC-RAS manual and on the basis of local investigations, which were made individually for each cross-section profile.

Computations in the non-uniform steady flow regime were made for the downstream regulated reach of the old regulated channel (B-OLD) and also for the restored upstream new channel (A-NEW). From these computations, it appears that, with regard to the channel capacity for the design discharge, no significant changes were assessed. Flooding events of design discharges take place only in a few specific solitaire locations, and harmless flooding spills in the floodplain. However, there is a clearly observable impact of changes in the longitudinal bottom slope and cross-section structures (chute/step-pool) in the channel on the change in shear stress. The proposed measures will definitely reduce the velocity and the shear stress. The proposed measures, by using a number of cross-section hydraulic structures, can be expected to have a major influence on the retention capacity of the channel. The volume of retained water during lower discharge is much greater. Because of the limited scope of this paper, only selected outcomes (hydraulic depths) are indicated, as summarized in Figures 5 and 6.

Hydraulic computations with the SRH-2D model

Two-dimensional models are particularly useful in situations where prismatic water flow in the channel is not expected and where the physical structure of the land is complex, e.g. a parallel channel with hydraulic structures in it, complex interactions with the flooded area and generally, in a natural river bed. In comparison with 1D models, a disadvantage of 2D models is that they have high demands on data characterizing the terrain and high computation complexity. For the Jindrichovicky Brook, a computation domain was created in the AQUAVEO Surface-Water Modeling System, comprising more than 100 000 elements.

The outcomes of the SRH-2D program are a data text file containing data for all elements in the computation domain. The outcome data consists of water levels, water depths, velocities and their vectors, Froude's numbers and shear stress (Lai, 2008). The flow was assessed at the levels of $Q_{30d} = 0{\cdot}04\, m^3 s^{-1}$, which is known as 'channel formation discharge'. In lower flows, i.e. Q_{330d}, known as 'ecological discharge', computation errors occurred, and these flows were therefore not assessed.

The velocity vectors are important outcomes of the 2D model. They can illustrate the formulae for water movements in the channel. Changes in the direction of the flow vectors indicate increased geomorphological diversity, which is an important condition for the ecological quality of the flow (Comiti *et al.*, 2007). In the case of the Jindrichovicky Brook, it appears that the standard discharge (Q_{30d}) has a quasi-laminar character in most sections of the channel, and changes in the direction of the vectors are observable only at specific individual steps or chutes.

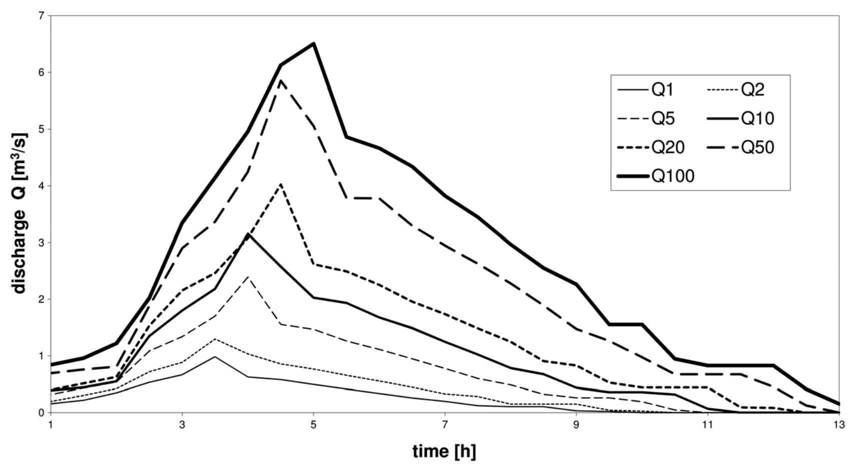

Figure 4. Design hydrographs Q_1–Q_{100} computed by the KINFIL model.

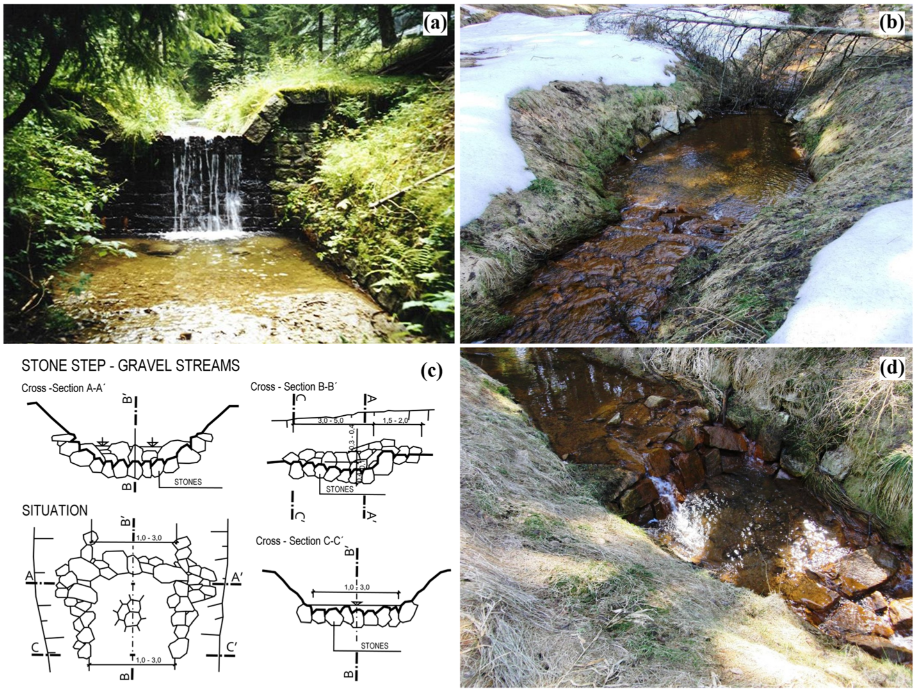

Figure 5. (a) The 'old-style' bottom drop (1·8 m high) from the 1970s, (b) the recently nature-close restored 'chute-pool' structure, 2008, (c) the design proposal for the 'chute-pool' structure, 2008 and (d) combination of 'step-pool', 2008.

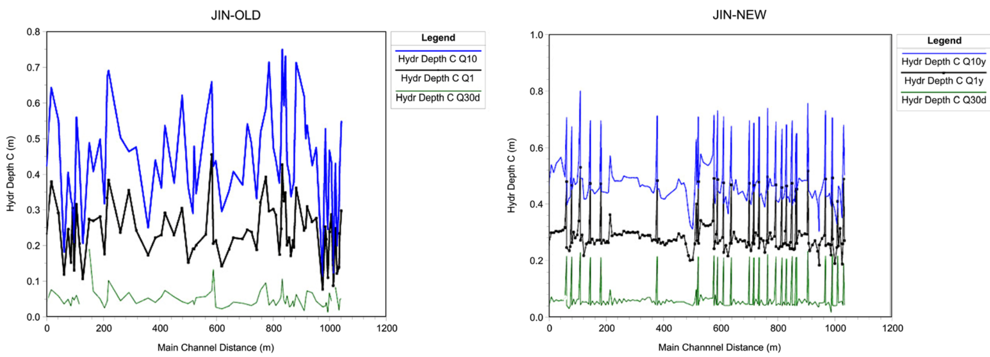

Figure 6. Hydraulic depths of flow simulated by the Hydrologic Engineering Centre's River Analysis System model (a) for Q_{30d}, Q_1 and Q_{10} for the 'old-style' (regulated) channel and (b) for the 'new-style' (restored) channel.

For increasing morphological diversity of the flow and thus for its ecological potential, it would therefore be useful to create even more nature-close steps in the flow, preferably based on criteria derived from assessments of the natural torrent morphology (Lenzi, 2002; Comiti *et al.*, 2007; Chin *et al.*, 2009).

These artificial yet nature-close steps stabilize the longitudinal profile of the flow and retain bed loads in the same way as hard measures in the field of torrent control but simultaneously create a potential habitat for water organisms appearing in the natural surroundings of unregulated torrents (Roni *et al.*, 2006; Comiti *et al.*, 2009; Yu *et al.*, 2010). A good solution is to set up stop planks within the flow from dead wood. This not only changes the morphology of the flow but may also provide a nutrition receptacle for many water invertebrates.

Another important characteristic, from the point of view of the ecological quality of the flow, is the depths of the water. Because of the relatively large distance between the individual steps (approximately 50 m and more), the larger part of the flow has uniform depths, longitudinally and also in the cross-section profiles. The water depths at Q_{30d} vary between 0·05 and 0·10 m and can reach as much as 0·3 m only in the pools beneath the steps. Water depth is one of the main characteristics for assessing the quality of the habitat for most organisms living in water, and thus, its flatness limits the ecological potential of the flow (Diez-Hernandez, 2008; Pasternack *et al.*, 2008; Hauer *et al.*, 2009; Kozarek *et al.*, 2010). Small water depth diversity in the longitudinal profile is illustrated in Figure 9. Restoration measures, as described in the preceding text, can also be used to improve this flow characteristic. Only selected outcomes are indicated in the graphs (Figures 7, 8 and 9).

A closer analysis of sections A and B shows that the resultant variance value of section A was 0·0015 m and in Section B, the value was 0·0005 m. This again indicates much smaller dispersion of values in the given surface and also major uniformity in the environment of this channel. Because of the relatively low depth of the water column in the discharge under investigation Q_{30d} – average depth 0·05 m – the values in each section would most probably increase if the calculation points were condensed, and a much more precise model of the river bed would be created, reflecting even small unevenness (mini ripples) on the channel bottom.

Results of hydrochemical and hydrobiological analysis

Hydrochemical analysis. Table VI presents the results of a hydrochemical analysis of water samples to illustrate the quality of the aquatic biota environment.

The values clearly exhibit the chemical parameters of the water samples collected in the studied environment of the Jindrichovicky Brook; the samples originate from the upper and lower parts of the brook. The main negative influence on biota in the studied ecosystem could be attributed to elevated values of Mn determined in the upper part of the brook. These values apparently exceed the guideline limits for drinking water and also for surface waters (Czech acts No. 252/2004 Sb. and No. 428/2001 Sb. and also EU Council directive No. 98/83/ES).

The amounts of Cl^{-}, SO_4^{2-} and also cations are significantly higher than the amounts found in the streams located in the near vicinity of the Jindrichovicky Brook (Kram

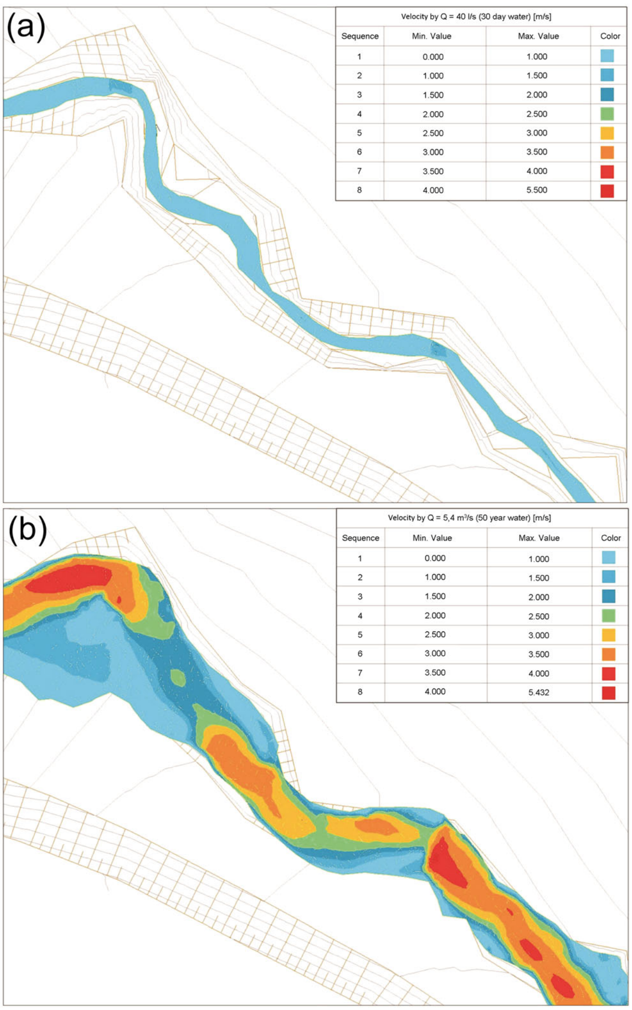

Figure 7. Flow velocities in the restored channel simulated by the Sedimentation and River Hydraulics Two-Dimensional model (a) for Q_{30d} and (b) for Q_{50d}.

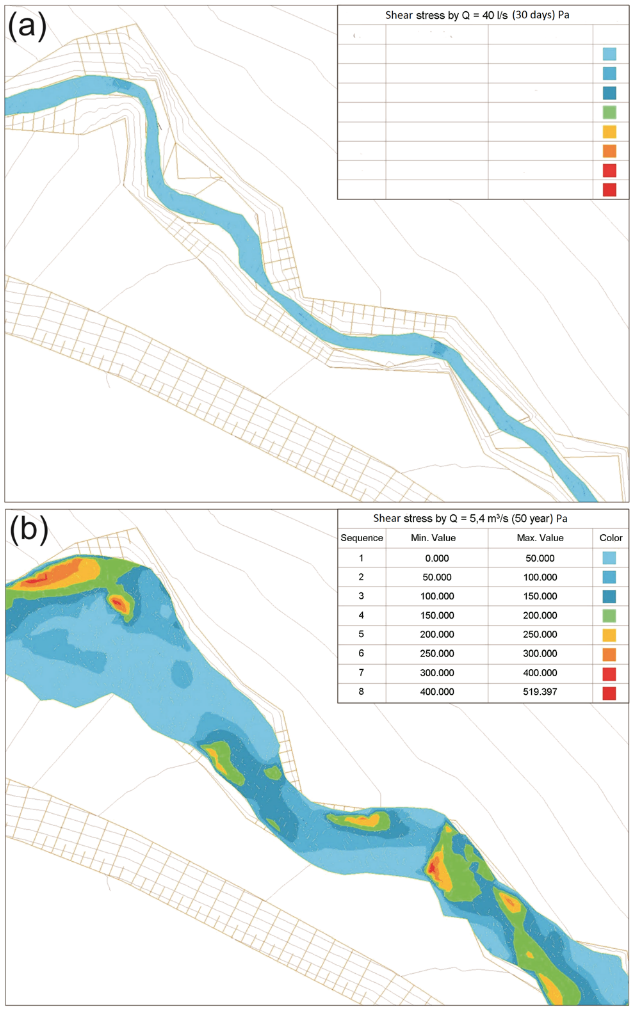

Figure 8. Shear stress in the restored channel, simulated by the Sedimentation and River Hydraulics Two-Dimensional model (a) for Q_{30d} and (b) for Q_{50d}.

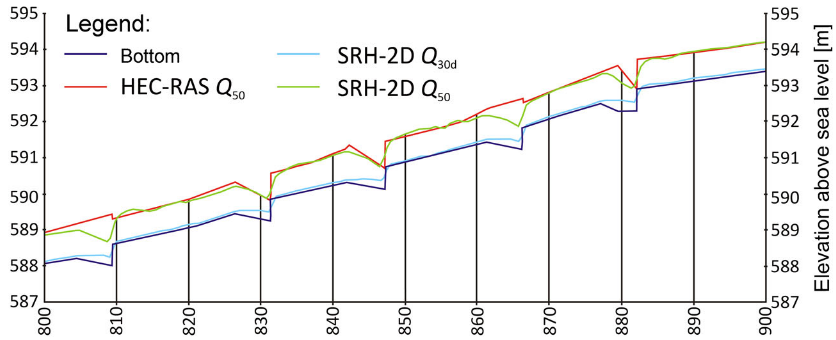

Figure 9. The longitudinal profiles 0·800–0·900 km Hydrologic Engineering Centre's River Analysis System (HEC-RAS) and Sedimentation and River Hydraulics Two-Dimensional (SRH-2D) for Q_{30d} and Q_{50d}.

Table VI. Mean and standard deviation of chemical parameters of stream-water samples (three replicates).

Compound	Unit	1 Mean	1 SD	2 Mean	2 SD
pH		6·12	0·02	6·76	0·02
Conductivity	$\mu S\ cm^{-1}$	444	46·3	239	26·7
NO_2^-	$mg\ l^{-1}$	<0·01		<0·01	
F^-	$mg\ l^{-1}$	0·09	0·00	0·10	0·00
Cl^-	$mg\ l^{-1}$	156	0·65	64·0	0·08
Br^-	$mg\ l^{-1}$	0·03	0·00	0·02	0·00
NO_3^-	$mg\ l^{-1}$	0·99	0·01	1·15	0·01
PO_4^{3-}	$mg\ l^{-1}$	0·01	0·00	0·01	0·00
SO_4^{2-}	$mg\ l^{-1}$	75·3	0·16	35·3	0·04
Na^+	$mg\ l^{-1}$	46·7	0·04	28·8	0·01
NH_4^+	$mg\ l^{-1}$	0·09	0·02	0·04	0·00
Mg^{2+}	$mg\ l^{-1}$	15·6	0·24	7·92	0·06
K^+	mg^{1-1}	4·39	0·24	2·63	0·08
Ca^{2+}	$mg\ l^{-1}$	24·0	0·18	12·7	0·03
Al	$mg\ l^{-1}$	0·18	0·05	0·10	0·04
Mn	$mg\ l^{-1}$	0·54	0·00	0·05	0·02
Fe	$mg\ l^{-1}$	0·21	0·06	0·10	0·00

SD, standard deviation.

et al., 2012). However, it should be mentioned that the streams described by Kram *et al.* (2012) are located in an area less affected by human activities. Thus, we can assume that the elevated values are caused by the nearby road and human settlement. The excessive amount of Cl^- is most likely caused by the extensive use of antifreeze salt (used to keep the road surface clear in winter months), as has also been reported, e.g. by Ramakrishna and Viraraghavan (2005).

Hydrobiological analysis. A total of 30 samples from four substrate types were collected. The total number of samples of each substrate type, irrespective of section (A or B), were pavement (n = 13), sand (7), natural (5) and compound stones (5).

A significant relationship between taxonomic richness and faunal abundance was revealed in section B (Pearson correlation coefficient r = 0·85, $P < 0·0001$, $R^2 = 70·8\%$, n = 15), whereas no such pattern was found in the new section A (Pearson correlation coefficient r = 0·13, P = 0·64, $R^2 = 5·9\%$, n = 15). This difference is due to the fact that several common taxa such as Trichoptera (Sericostomatidae and Hydropsychidae) and Oligochaeta (Tubificidae) varied highly in abundances among the samples in the A section. In contrast, these taxa almost absented in the B section. As at least one of the aforementioned relationships was statistically significant, we used only taxonomic richness for statistical testing of the effect of a type of channel restoration on benthic fauna richness. This approach based on a more conservative parameter reduces the effects of microhabitat proportions on particular sites where the animals preferring appropriate habitat could concentrate. On the other hand, the approach with emphasis on abundance could mask the species richness. The effect of channel type on taxonomic richness was found significant (*t*-test: t = −3·73, df = 27·9, $P < 0·001$) as the mean taxonomic richness achieved 12·5 ± standard error (SE) 0·76 in section A but only 6·8 ± (SE) 0·93 in section B. Similarly, skewed differences were obtained for faunal abundances [60·7 ± (SE) 5·62 in section A vs 23·9 ± (SE) 5·81 in section B], all suggesting much richer and more abundant invertebrate benthic communities in the stream revitalized by the new method (Figure 10). The mean values (bars) and SEs (whiskers) are indicated.

In addition, an analysis was made of the effects of substrate type (paving, natural, stones and sand) on taxonomic richness and faunal abundance. The richest was the 'natural' habitat, as 14·8 ± (SE) 1·48 families were found in this environment, followed by stones [12·6 + (SE) 0·36] and sandy habitats [the same number of 13 families was found in the two sites available in section B and 10·2 + (SE) 0·87 in section A]. The poorest pavement was inhabited by only 5·8 + (SE) 0·81 (Figure 11).The only sandy habitat was present in both the newly restored section A ('sand new') and the old-style treated section B ('sand old') in Figure 11. In the natural habitat, the most represented (numerous) group was Plecoptera, with more

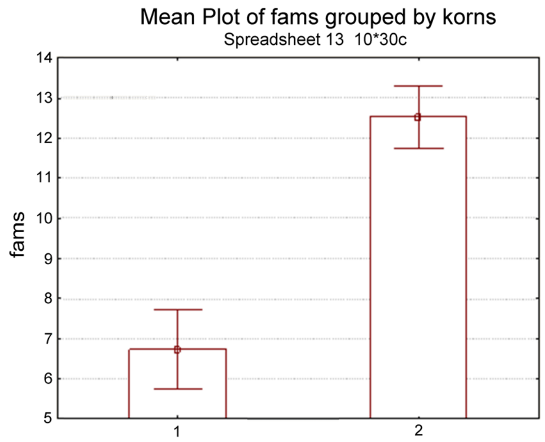

Figure 10. Numbers of detected families of benthic invertebrates at 15 sampling sites on the 'old-style' treated reach (1) and on the newly revitalized reach (2) in the Jindrichovicky Brook, October 2011.

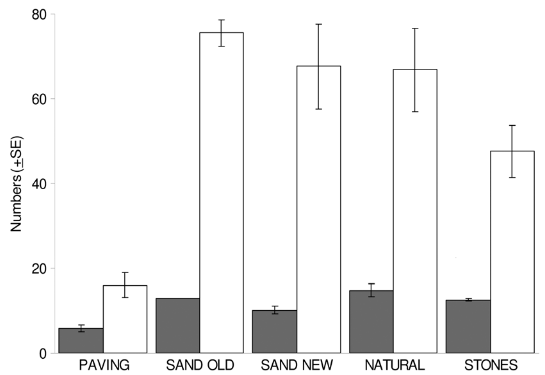

Figure 11. Numbers of families (dark bars) and specimen abundances (white bars) found in the samples collected in the Jindrichovicky Brook, October 2011.

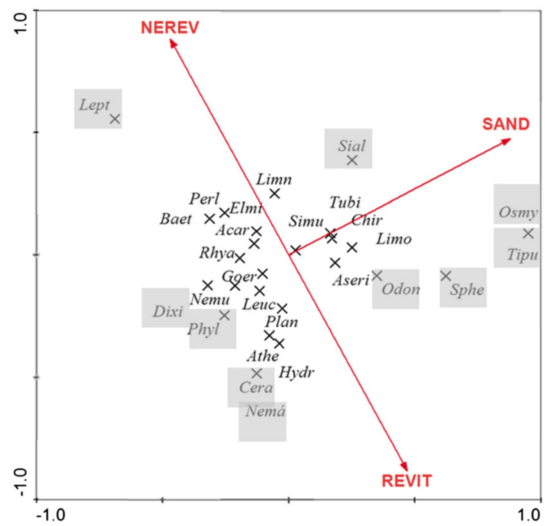

Figure 12. Ordination diagram of canonical correspondence analysis describing associations between the composition of benthic invertebrate communities, restoration type and habitat in the Jindrichovicky Brook, October 2011.

than one half of all collected specimens. Similarly, Chironomidae dominated in the sandy habitat. However, Plecoptera and Ephemeroptera rarely appeared in the sand habitat. Trichoptera occurred across all the habitats.

The habitats also differed in abundance numbers. While the average total abundance value was 65–75 specimens, one sample $0{\cdot}1\,m^2$ in the natural and sand habitats containing around 48 specimens on $0{\cdot}1\,m^2$ was found in the stone habitat and only about 16 specimens on $0{\cdot}1\,m^2$ in the pavement habitat (Figure 11).

Finally, we tested the effects of restoration type (new or old) and also substrate type (natural, sand, stones and paving) on the composition of the benthic communities. In this analysis, restoration type and sand substrate were found to be key factors explaining the variation in family occurrence (Table VIII). The compounded stones, paving and natural, played a minor role in our data. The importance of sand is due to the high occurrence of some Diptera larvae (Chiromidae and Limoniidae*)* and Olicocheeta (Tubificidae) in this habitat.

Some less abundant taxa (Odontoceridae and Sphaeridae) also showed an affinity with the sand substrate. Baetidae, Limnephilidae and Perlidae showed an association with the not fully restored type B (Figure 12). The centroids of the animal taxa positions in Figure 12 are indicated using abbreviations (full names available in Table VII). The groups marked in bold type had dominance >1%. The directions of significant variables (sandy habitat 'SAND' and restoration type 'NEW' vs 'OLD') in the framework of the first two ordination axes are visualized. A global permutation test for all canonical axes showed a significant result (for the statistical output, see Table VIII).

DISCUSSION

This paper has two interconnecting parts: hydraulic and ecological. The hydrological and hydraulic conditions form environmental conditions for benthic communities. We do not speak about living conditions for fish, as the study area is the bead water of the Jindrichovicky Brook, where its upper part is still cut off by the lower edge of section B. This section is not yet open for fish, because of the insuperable bottom drop system. Therefore, the relations between sections A and B concerning the hydraulics and the hydrobiology of macrozoobenthos can be discussed. The depiction of the course of the water table in longitudinal profile (Figure 9) offered an interesting comparison of the simulation results for the two applied models. Figure 9 shows some differences in the computation of the water table, which appear in each step (steps 1 and 4 in the direction opposite to the water flow). In this profile, we may also identify the difference in computed water table height, where it is shown

Table VII. A list of the macroinvertebrate taxa identified in the samples.

Order/*higher taxonomical unit	Family	Number of individuals
Plecoptera	Perlodidae	15
	Nemouridae	45
	Leuctridae	118
Ephemeroptera	Baetidae	126
	Leptophlebiidae	1
Diptera	Chironomidae	293
	Tipulidae	1
	Simuliidae	26
	Dixidae	5
	Ceratopogonidae	1
	Limoniidae	71
	Athericidae	19
Trichoptera	Sericostomatidae	170
	Odontoceridae	11
	Goeridae	21
	Limnephilidae	50
	Hydropsychidae	28
	Rhyacophylidae	18
	Phylopotamidae	10
	unidentified pupas	76
Megaloptera	Sialidae	6
Neuroptera	Osmylidae	1
Tricladida/*Turbellaria	Planaridae	42
Veneroida/*Bivalvia	Sphaeriidae	8
*Oligochaeta	Tubificidae	63
*Hydracarina	—	15
*Nematomorpha	—	1
Total		1269

that the HEC-RAS model indicates mostly higher values (though the difference is very small). We may also identify wave undulation computed by means of the SRH-2D model beneath each step, which of course could not be assessed in the 1D model. From the distance between each of the steps, it may be assessed that the HEC-RAS model records the course of the water table development adequately. An advantage of the SRH-2D model, despite its complexity in calculation, is only seen when the flow manifests higher morphological diversity (e.g. steps in close succession with pools of different depths and obstacles to flow directly in the channel) or in a detailed study of the hydraulic structure of each cross section.

Hence, a complicated unsteady flow can be solved much better by a 2D (SRH) model, when a wide spectrum of flow (from Q_{330d} to Q_{100}) can be simulated and nature-close hydraulic structures can be designed adequately for local conditions. Concluding, HEC-RAS as a 1D model is neither able to simulate reliably flow velocities, water depth and shear stress in complex cross sections nor in sections with hydraulic jumps downstream of weirs or drops. SRH-2D would definitely yield more profound results.

The differences in the composition and the quantity of benthic fauna between the two channel types are evident. Both the metrics are positively skewed towards higher values in new, semi-natural torrent improvement, although the torrent control was implemented less than 5 years ago there, whereas the interventions in the old section were carried out much earlier (in the 1970s). As far as the presence of microhabitats is concerned (sand deposits and heterogeneity of the bottom caused by disturbances), these should theoretically be much more developed in the old channel than in the new channel. This could be the reason why some groups (Baetidae and Limnephilidae) occupy the paving substrate in the old channel with relative high density. A thin sand layer, locally established on the surface of the paving in the old channel, is a particularly attractive habitat. It can be assumed that the newly modified channel will also continue to develop and that the differences in the composition of the macrozoobenthos will increase in years to come.

Sites with different bottom substrates showed different compositions of benthic fauna. Especially, the sandy deposits differed from the other habitats. This is in harmony with Wetzel (Wetzel, 2001), who characterized porous sediments

Table VIII. Summary results of the forward selection procedure in canonical correspondence analysis of the effect of the predictors on the taxonomic composition of benthic communities in the studied system.

Ordination axis			1	2	3	4
Variance explained by species data			0·151	0·078	0·185	0·149
Predictor	F[a]	P[a]	Predictor – axes correlation matrix			
Non/revitalized section	1·98	0·0050	0·357	−0·733	−0·167	−0·070
Sand	3·03	0·0020	0·733	0·282	0·265	−0·042
Natural	1·20	0·2378	−0·336	−0·603	0·271	−0·214
Paving	0·92	0·5144	−0·492	0·635	−0·187	−0·093
Stone	0·69	0·8332	0·062	−0·291	−0·391	0·369
Test of model			Axis 1		All axes	
F-value			3·354		1·841	
P			0·001		0·0008	

[a] Results of a Monte Carlo permutation test.

as an environment where the maximum macroinvertebrate density is commonly found. Thus, the presence of sandy pools under the embankments proved to be favourable for the variety and complexity of the benthic community. Stones contributed less to the faunal richness of a new channel, and their contribution to the whole fauna variability is similar to the contribution of a natural bottom. However, this habitat is substantially better for fauna than 'old paving'. We recommend this way of stabilizing the channel, when necessary.

The differences among fauna from separate habitats are caused not only by the bottom substratum. Other abiotic factors (e.g. Froude number, water velocity and water depths) can also play an important role (Doledec *et al.*, 2007; Pastuchova *et al.*, 2010), but they have not been analysed here because of their close connection with the habitats. In conclusion, the presence of different stretch types in a restored stream channel proved to be important for increasing the taxonomical richness of the benthic community, and each of the habitats contributed to its beta diversity. Our study has shown that suitable improvement of the bottom structure during restoration is important not only in bigger rivers and streams but also in small low-order streams such as the Jindrichovicky Brook.

The hydrobiological analysis results fully reflect the assumption from the hydraulic simulation of the flow conditions in sections A and B, computed by the SRH-2D model. More uniform geomorphological conditions in section B expressed by hydraulic properties, i.e. depths, velocities and shear stress values, undoubtedly diminish a biodiversity of water organisms.

CONCLUSIONS

The initial aim of the nature-close adaptation measures when restoring a torrential river was to maintain the biota in the water environment of the Jindrichovicky Brook and also to stabilize the water direction and the water level of the channel. From our hydraulic computations, we deduced that the changes in the channel variables (longitudinal slope, hydraulic structures and roughness) have an impact on discharges that are less than Q_{50}. There are no further changes. In the proposed design, the depth and dimensions of the former channel were maintained, and hydraulic structures were selected in a way that would ensure biota migration and achieve higher biodiversity.

The depth of the water increases, because of the smaller longitudinal slope and the higher level of roughness. This will be demonstrable mainly in *M*-day discharges, which are the most important for biota. The flow velocity and the shear stress were decreased with regard to these changes. The volume of water increased because of the more articulated longitudinal profile and the deeper water level. The longitudinal profile followed the natural 'wavelike' longitudinal profile more closely, with alternating chutes and pools (step-pool profile). The pools above and below the cross-section structures create refuges for species during low level water situations.

Water aeration in frequent overfalls and particularly on boulder chutes, to some extent, increases the self-purifying capacity of the flow. The migration mobility is maintained thanks to the low hydraulic structures and their structural arrangement. The aesthetic character of the landscape is a significant factor in a hydro-ecological assessment of the state of the water flow.

The macroinvertebrate sampling showed that the new type of channel adaptation is much more effective than the old type. The taxonomic composition and also the quantity of benthic fauna in the newly adapted river bed decisively outnumbers the same variables in the river bed with old improvements, mainly due to the occurrence of nature-close sections on the bottom, composed of a rich variety of habitats (sand, gravel and smaller and bigger stones). In addition, the presence of sandy deposits in this type of channel, particularly under the embankments, has proved to be favourable for the variety and complexity of the benthic families. Sections on the basin bottom composed of compounded stones were the least inhabited, from the point of view of the occurrence of macrozoobenthos, but they offer a far more favourable environment than the sequential stone pavement built in the old-style channel regulation.

Our study makes evidence available for decision makers dealing with nature-close torrent control.

ACKNOWLEDGEMENTS

The paper was supported by the Czech Ministry of Agriculture, National Agency for Agriculrtural Research (NAZV), Projects QI91 C008 Optimalisation of technical erosion control measures and QJ1220033 Water regimes optimalisation on the Morava river valley. The team of authors fully acknowledges this support.

REFERENCES

Abbott MB, Refsgaard JC. 1996. *Distributed Hydrological Modelling*. Kluwer Academic Publishers: Dordrecht.

Allan JD. 1995. *Stream Ecology: Structure and Function of Running Waters*. Springer: Dordrecht; 388.

Aquaveo. 2010. *Aquaveo SMS*. Aquaveo: Provo, Utah, United States. http://www.xmswiki.com/xms/SMS:SMS.

Beven KJ. 2006. *Rainfall–Runoff Modelling. The Primer*. John Wiley & Sons: Chichester.

ter Braak CJF, Smilauer P. 2002. *CANOCO Reference Manual and CanoDraw for Windows User's Guide: Software for Canonical Community Ordination (Version 4.5)*. Microcomputer Power: Ithaca.

Brookes A, Shields FD, Jr. 1996. *River Channel Restoration*. J. Wiley & Sons: Chichester. ISBN 0-471-96139-6, 433 s.

Brunner GW. 2010. HEC-RAS computer program (2010): version 5.1.v. US Army Corps of Engineers Hydrologic Engineering Center (HEC), Davis, CA95616-4687, USA.

Chin A. 2003. The geomorphologic significance of step-pools in mountain streams. *Geomorphology* **55**: 125–137.
Chin A, Gregory KJ. 2001. Urbanization and adjustment of ephemeral stream channels. *Annals of the Association of American Geographers* **91**: 595–608.
Chin A, Anderson S, Collison A, Ellis-Sugai BJ, Hlatiner JP, Hogervorst JB, Kondolf GM, O'Hirok LS, Purcell AH, Riley AL, Wohl E. 2009. Linking theory and practice for restoration of step-pool streams. *Environmental Management* **43**: 645–661.
Comiti F, Mao L, Wilcox A, Wohl E, Lenzi M. 2007. Field-derived relationships for flow velocity and resistance in high-gradient streams. *Journal of Hydrology* **340**(1–2): 48–62.
Comiti F, Mao L, Lenzi MA, Siligardi M. 2009. Artificial steps to stabilize mountain rivers: a post project ecological assessment. *River Research and Applications* **25**: 639–659.
Computer Aided Design. 2012. *AutoCAD Civil 3D, 2012 Manual*. San Rafael: USA.
Computer program. 2001. HEC-RAS (Hydrologic Engineering Center's River Analysis System), version 3.0.1, III 2001.
Cook AC. 2008. *Comparison of One-dimensional HEC-RAS with Two-dimensional FESWMS Model in Flood Inundation Mapping*. Purdue University: West Lafayette, Indiana.
COUNCIL DIRECTIVE 98/83/EC. 3 November 1998. On the quality of water intended for human consumption.
Diez-Hernandez JM. 2008. Hydrodynamic ecohydraulic habitat assessment aimed at conserving and restoring fluvial hydrosystems. *Revista Ingenieria E Investigacion* **28**(2): 97–107.
Doledec S, Lamoroux N, Fuchs U, Merigoux S. 2007. Modelling the hydraulic preferences of benthic macroinvertebrates in small European streams. *Freshwater Biology* **52**: 145–164.
Gordon ND, McMahon TA, Finlayson BL. 1996. *Stream Hydrology – An Introduction for Ecologists*. J. Wiley & Sons: W. Sussex, England, 526 s.
Hauer C, Mandlburger G, Habersack H. 2009. Hydraulically related hydro-morphological units: description based on a new conceptual mesohabitat evaluation model (MEM) using lidar data as geometric input. *River Research and Applications* **25**: 29–47.
Hradek F, Kovar P. 1994. Computation of design rainfall intensity. *Vodni hospodarstvi (Water resources)* **11**: 49–53.
Jahring SC, Lorenz AW. 2008. Substrate-specific macroinvertebrate diversity patterns following stream restoration. *Aquatic Sciences* **70**: 292–303
Just T, Matousek V, Fischer D, Karlik P. 2005. Water restorations and their role in flood control. 3. ZO ČSOP Horovice region, 359 p.
Kovar P. 1992. Possibilities of determining design discharges and small catchments using KINFIL model. *Vodohospodarsky casopis (Water Resousces Journal)* **40**: 197–220.
Kovar P, Krovak F. 1998. DOS-T 04.02.01. Recommended Technical Standard. Riverengineering, CKAIT, 13 pp.
Kovar P, Krovak F. 2002. Torrent control, teaching materials FLD CULS. ISBN 80-213-0888-5, 45 pp.
Kovar P, Krovak F. 2011. Nature close torrent control in Ore Mountains. IAHS Conference HydroEco, Proceedings, Vienna, 1.–5. 5. 2011, s. 386.
Kovar P, Cudlin P, Herman M, Zemek F, Korytar M. 2002. Analysis of flood events on small river catchments using the KINFIL model. *Journal of Hydrology and Hydromechanics SAV SR, Bratislava* **50**(2): 157–171.
Kozarek JL, Hession WC, Dolloff CA, Diplas P. 2010. Hydraulic complexity metrics for evaluating in-stream brook trout habitat. *Journal of Hydraulic Engineering-asce* **136**(12): 1067–1076.
Kram P, Hruska J, Shanley JB. 2012. Streamwater chemistry in three contrasting monolithologic Czech catchments. *Applied Geochemistry* **27**: 1854–1863.
Lai YG. 2008. *SRH-2D Version 2: Theory and User's Manual*. U.S. Department of the Interior, Bureau of Reclamation: Denver.
Lange G, Lecher K. 1993. *Gewässerregulung, Gewässerfplege*. Paul Parey: Hamburg und Berlin, ISBN 3-490-17916-1.
Lellak J, Kubicek F. 1991. Hydrobiology. Karolinum, Praha, 260 s.
Lenzi MA. 2002. Stream bed stabilization using boulder check dams that mimic step-pool morphology features in northern Italy. *Geomorphology* **45**(3–4): 243–260.
Morel-Seytoux HJ, Verdin JP. 1981. Extension of the SCS rainfall runoff methodology for ungaged watersheds. Report FHWA/RD-81/060, U. S. National Technical Information Service, Springfield, Virginia.
Morgan RPC, Nearing MA. 2011. *Handbook of Erosion Modelling*. NSERL, Wiley-Blackwell: Chichester.
Novak L, Iblova M, Skopek V. 1986. *Riparian Vegetation*. SNTL: Praha.
Pasternack GB, Bounrisavong MK, Parikh KK. 2008. Backwater control on riffle-pool hydraulics, fish habitat quality, and sediment transport regime in gravel-bed rivers. *Journal of Hydrology* **357**(1–2): 125–139.
Pastuchova Z, Greskova A, Lehotsky M. 2010. Spatial distribution pattern of macroinvertebrates in relation to morphohydraulic habitat structure: perspectives for ecological stream assessment. *Polish journal of Ecology* **58**: 347–360
Peckarsky BL. 1984. Sampling the stream benthos. In *A Manual on Methods for Assessing Secondary Productivity in Freshwaters*, 2nd edn, Downing JA, Rigler FH (eds). IBP Handbook #l7. Blackwell Scientific Publications: Oxford; 131–160.
Ponce VM, Hawkins RH. 1996. Runoff curve number: has it reached maturity? *Journal of Hydrologic Engineering* **1**(1): 11–19.
R Development Core Team. 2009. *R: A Language and Environment for Statistical Computing*. R Foundation for Statistical Computing: Vienna.
Ramakrishna DM, Viraraghavan T. 2005. Environmental impact of chemical deicers – a review. *Water, Air, and Soil Pollution* **166**: 49–63.
Roni P, Bennett T, Morley S, Pess GR, Hanson K, Van Slyke D, Olmstead P. 2006. Rehabilitation of bedrock stream channels: the effects of boulder weir placement on aquatic habitat and biota. *River Research and Applications* **22**(9): 967–980.
Samaj F, Valovic J, Brazdil R. 1983. Daily depths of extreme rainfalls in 1901–1980. Sbor. prac SHMU, Alfa, Bratislava.
Singh VP. 1996. *Kinematic Wave Modeling in Water Resources: Surface-water Hydrology*. John Wiley & Sons, Inc.: New York; 1399. ISBN 0-471-10945-2.
Sundermann A, Antons C, Cron N, Lozenz AW, Hering D, Haase P. 2011. Hydromorphological restoration of running waters: effect on benthic invertebrate assemblages. *Freshwater biology* **56**: 1689–1702
Tejnecky V, Bradova M, Boruvka L, Nemecek K, Sebek O, Nikodem A, Zenahlikova J, Rejzek J, Drabek O. 2013. Profile distribution and temporal changes of sulphate and nitrate contents and related soil properties under beech and spruce forests. *Science of the Total Environment* **442**: 165–171.
U.S. SCS. 1986. Urban hydrology for small watersheds. U.S. Soil Conservation Service, Technical Release **55**(13), USDA, Washington, D.C.
US Army Corps of Engineers. 2000. *Hydrologic Modeling System HEC-HMS – Technical Reference Manual*. Hydrologic Engineering Center – US Army Corps of Engineers: Davis, CA.
USDA SCS. 1972. National engineering handbook – section 4: hydrology. Washington DC. ISBN 9787368433.
Vassova D, Kovar P. 2011. Program DES_RAIN. Available on http://fzp.czu.cz/vyzkum/.
Vrana I, Vanicek J, Kovar P, Brozek J, Aly S. 2012. A group agreement-based approach for decision making in environmental issues. *Environmental Modelling & Software* **36**(2012): 99–110.
Waal LC, Large ARG, Wade PM. 2000. *Rehabilitation of Rivers*. J. Wiley & Sons. ISBN 0-471-95753-4, 331 s.
Wetzel RG. 2001. Limnology. 3th edition. Academic Press: San Diego; 1006 pp.
WFD EC 2000/60/ES. 2000. Directive of the European Parliament and the council establishing a framework for community action in the field of water policy, 2000/60/ES.
Wilcox AC, Peckarsky BL, Taylor BW, Encalada AC. 2008. Hydraulic and geomorphic effects on mayfly drift in high-gradient streams at moderate discharges. *Ecohydrology* **1**: 176–186
Yu G, Wang Z, Zhang K, Duan X, Chang T. 2010. Restoration of an incised mountain stream using artificial step-pool system. *Journal of Hydraulic Research* **48**(2): 178–187.

PŘÍLOHA č. 2

Environ Monit Assess (2016) 188: 74
DOI 10.1007/s10661-015-5080-7

Water balance analysis of the Morava River floodplain in the Kostice-Lanžhot transect using the WBCM-7 model

Pavel Kovář · Darina Heřmanovská · Pavel Hadaš · Michaela Hrabalíková · Jitka Pešková

Received: 11 December 2014 / Accepted: 22 December 2015 / Published online: 5 January 2016

Abstract The study area of the Morava River floodplain is situated between the rivers Morava and Kyjovka in the reach from Hodonín to Lanžhot. This experimental area was chosen because during the last 30 years, there has been a serious problem with the frequent occurrence of hydrological extremes, such as floods and droughts. Dry seasons have a very negative impact on the floodplain forest and have been caused mainly by regulation of the Morava River channel in the 1970s. Since flooding in the catastrophic year 1977, a part of this area has served as a polder for flood impact mitigation of the urbanised area of the town of Lanžhot. Management and farming practices have been heavily affected by the enormous economic and ecological damage due to long-term flooding of agricultural land. The purpose of this study is to assess the extent to which the precipitation in the growing season of the dry years 2003 and 2011 was deficient, in comparison with the normal year 2009, through a study of the actual evapotranspiration caused by the significant drought in the Morava floodplain. A similar but converse situation in the wet year 2010 was also analysed, with the aim to show the differences in the components of the water balance equation in the growing seasons of all the extreme years tested here. The daily data from the Kostice climatological station were processed using the WBCM-7 model, where the input parameters were calibrated by the fluctuation of the groundwater table in the control borehole.

P. Kovář (✉) · D. Heřmanovská · M. Hrabalíková · J. Pešková
Faculty of Environmental Sciences, Czech University of Life Sciences Prague, Kamýcká 129, 165 21 Praha 6, Suchdol, Czech Republic
e-mail: kovar@fzp.czu.cz

P. Hadaš
University of Central Europe, Kráľovská 386/11, 909 01 Skalica, Slovakia

Keywords Drought · Flood · Hydrological extremes · Hydrological processes · Water balance equation

Introduction

In the past, the Morava River flowed along a meandering stream route. Once or twice a year, in spring or in summer, it usually flooded. The extent of the overbanks remained acceptable, and there was no serious damage. At the end of the 1970s, however, a project to regulate the river was implemented, with adjustments to the river meanders and dredging of the river bottom. Dikes were built along the river to provide protection against higher discharges than design Q_{100} within the dike cross section. The run-off became faster and led to lowering of the groundwater and thus to more frequent dry periods, as a reverse event to flooding (Soukalová 2012). Figure 1 presents the recorded groundwater hydrographs caused by significant floods, where the depletion curves have negative consequences in water-scouring river bed and deepening groundwater levels along alluvial plains due to a leakage through the geological quarternary river bed. For this reason, a new

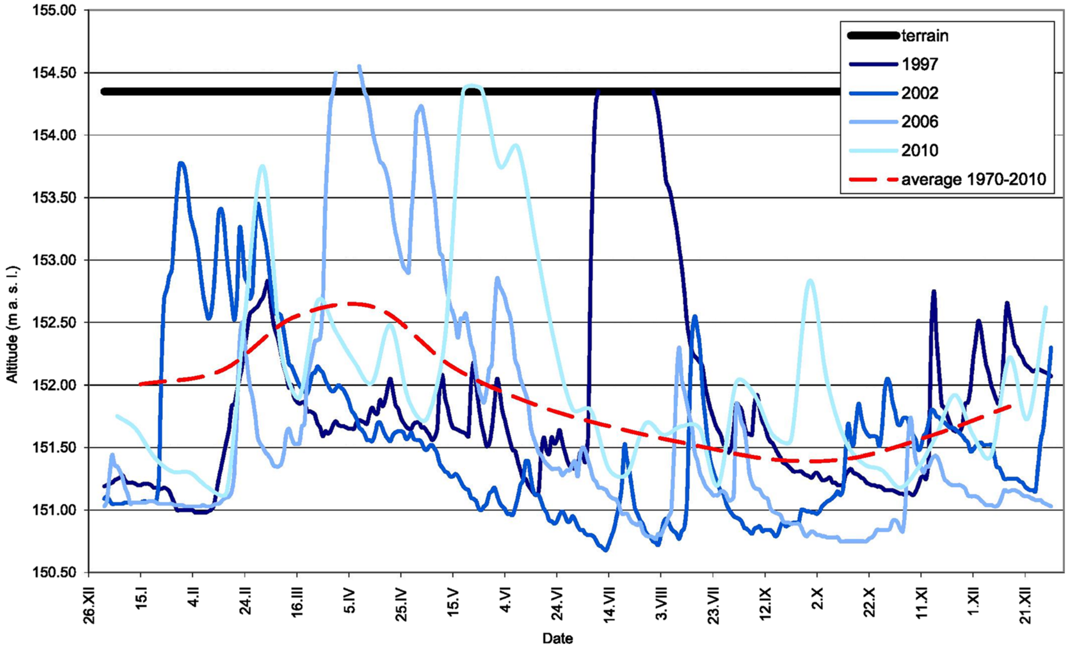

Fig. 1 Groundwater hydrographs in the test borehole VB0241 Lanžhot (Soukalová 2012)

water supply conduit, called the Spářavka channel, was built in the 1980s. The Spářavka channel supplies the forested area downstream and the municipal heating plant in the town of Hodonín. This new source of cooling water, with a stable regulated discharge of $Q = 3.0\ m^3\ s^{-1}$, supplies the alluvial plain and is a major source of water for the new restoration system and for additional irrigation. An optimal water regime for the forest, meadows and agricultural crops, i.e. proper water management, should be adopted in this regulated area. In order to ensure an adequate water regime, it is very useful to create a water balance simulation model.

We have learnt a lot of lessons from human-induced changes to catchment characteristics and their impact on the hydrology in the area. Impact research has been the focus of field experiments (Vázquez-Suñé et al. 2005; Brown et al. 2005) and of simulation models. Hydrological models are widely used in water and environmental resource management. They can mostly be classified into two groups: (1) conceptual models and (2) physically based models. To address the question of human impact on hydrological functioning, the models need to describe the dominant physical processes. Physically based models, like the well-known SHE (Abbott et al. 1986a, b), MIKE-SHE (Refsgaard and Storm 2005) and ECOMAG (Motovilov et al. 1999), are usually very time-consuming and data-intensive, when used in a fully distributed manner. Conceptual models are frequently applied in operational practice. However, they usually neglect the spatial variability of the parameters and state variables. They are often calibrated using measured stream flow data. Models of this type include HBV (Bergström 1995), SAC-SMA (Burnash 1995), TOPMODEL (Beven et al. 1995), SWAT (Arnold et al. 1998) and AFFDEF (Moretti and Montanari 2007). The parameters of models of this kind often cannot be measured in the field or lack physical meaning. These models also suffer from lack of parameter identifiability and from equifinality.

Recharge estimation is essential for proper management of a catchment area. The group of water balance models based on the water balance equation, e.g. simplified DHVSM (Andrew and Dymond 2007), HIDROMORE (Sánchez et al. 2010) or the WBCM model (Kovář and Vaššová 2010), can therefore be used to improve water regimes quantitatively.

This paper provides a comparison of the water balance in the growing season (April 1 to October 31) in dry years 2003 and 2011. For floods, wet year 2010 was selected and was compared with normal year 2009, on the transect from the Kostice climatological station to groundwater table recording borehole VB 0360 at

Lanžhot. These four characteristic years were used to compute the requirements for an optimal water regime, in which forest, meadows and agricultural crops would grow with support from science-driven water management.

Materials and methods

Area of interest

The area of interest within the Moravian alluvial plain lies on the right bank, in the reach between the towns of Hodonín and Lanžhot, which are 12 km apart. This area is about 3.0 km in width and 1.0 km in length, i.e. 3.0 km^2. The entire Morava River catchment from the upper water divide down to the Lanžhot gauge is 9722 km^2. The average annual temperature is 9.5 °C, with average annual precipitation of 533 mm. The rainfall maxima occur in June and in July. The average annual number of rainy days is around 120. The recent dry periods are shown in Table 1. The hydrological conditions are controlled by the Morava River, which completely influences the groundwater regime. The historical changes to the river channel can be observed in the river's alluvial plain, in particular the changes introduced by the regulation measures carried out in the 1970s. The wetlands and wet meadow area were considerably reduced by shortening the meanders (by about 22 % in our reach). Forest, as a relatively stable land component, was also reduced. Since the 1970s, this area has therefore been losing its earlier retention capacity. As was mentioned above, due to the reduction in the length of the river, the amount of water infiltration has diminished, resulting in lowering of the groundwater table.

Figure 2 shows the situation of the land area with three transects of climatic stations: Mikulčice—borehole VB0356 (Mikulčice), Týnec—borehole VB0359 (Tvrdonice) and Kostice—borehole VB0360 (Lanžhot). From these profiles, we have selected the Kostice transect for this paper. The Kostice transect is an area of 3 to 12 km^2 that reflects the physiographic characteristics of the area as far as soil, climate, altitude and land use are concerned. Due to substantial change of land use in the Mikulčice region, in contrast to the permanent grassland growing in the Kostice vicinity, the Mikulčice environs is forested. This fact obviously caused small differences in seasonal values of the potential evapotranspiration on the Mikulčice station.

Human intervention in the natural water regime of the floodplain was in connection with factors such as soil fertility, good status of forests in the past and urbanisation. These impacts probably led to differences between the potential and actual evapotranspiration subsidy of lower soil moisture content, lower groundwater storage and higher direct run-off. These components of the water balance equation, deprived of their past homogeneous continuity, can also be considered as an impact on climate change, and the consequences of the changes should be added to the right side of the water balance equation.

Model WBCM-7

A water balance of a particular area in a given time span can be described by the equation (in mm)

$$SP = SQ + SAE + ASM + GWR - BF \tag{1}$$

where SP is rainfall, $SQ = SOF + BF$ is total run-off, SAE is actual evapotranspiration, ASM is change of soil

Table 1 Hydrologic data for the recent dry periods in 1976, 2003 and 2011 of the Morava River alluvial plains

Year	Precipitation (mm)	Potential evapotranspiration (mm)	Actual evapotraspiration (mm)	Evapotranspiration coefficient (–)	Water balance deficit (mm)
1976	452	707	495	0.70	−212
2003	293	669	309	0.46	−360
2011	364	639	367	0.57	−272

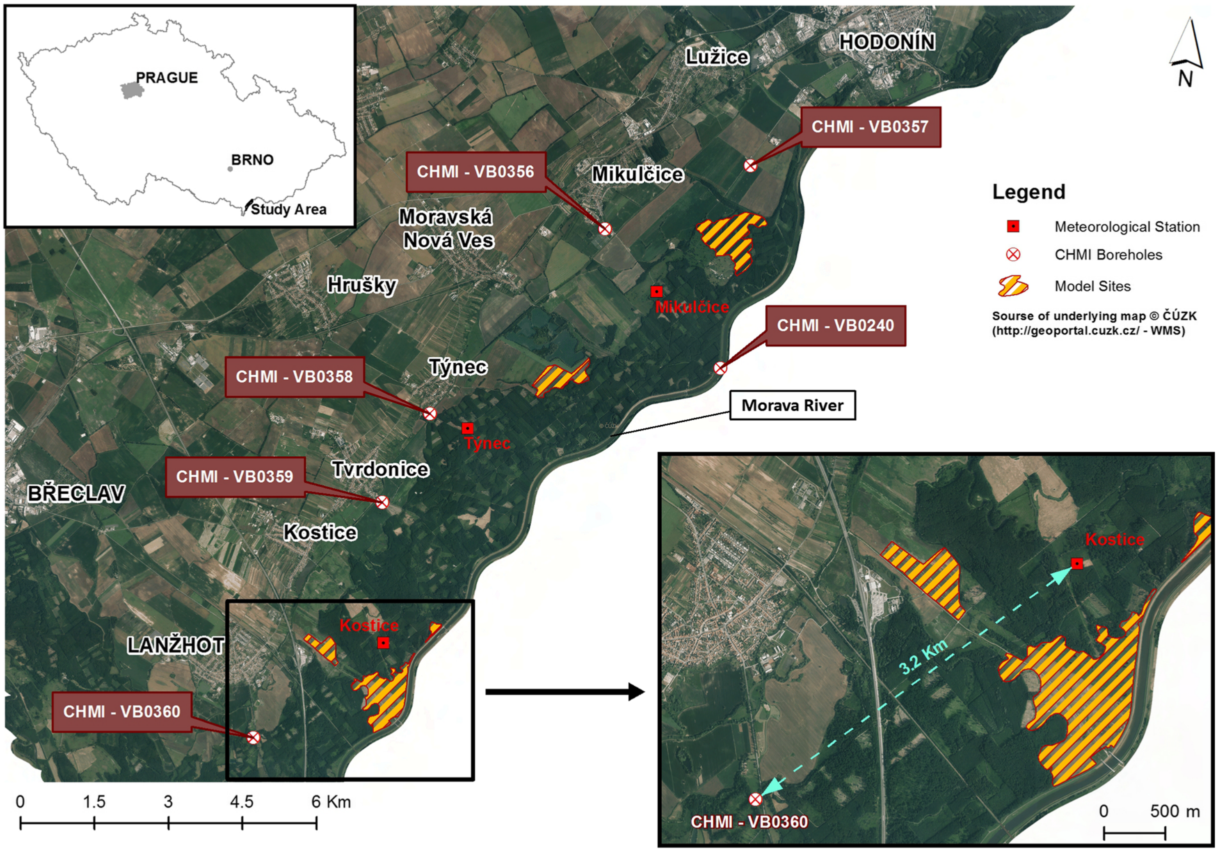

Fig. 2 Orthophotomap of the area of interest area (Morava River floodplain between Hodonín and Lanžhot), with the climatological stations (Mikulčice, Týnec and Kostice) connected by transects with their corresponding boreholes (e.g. Kostice station to borehole VB0360 Lanžhot)

moisture content, *GWR* is groundwater recharge, *BF* is baseflow and *SOF* is direct run-off.

The net change in subsurface storage is calculated from (in mm)

$$SNGRWR = SGWR - BF = ASM + GWR - BF \qquad (2)$$

where *SNGWR* is the net change in subsurface storage and *SGWR* is the change in subsurface storage.

The aim of implementing the WBCM-7 model was to quantify the water balance. It is a combined model with the unsaturated soil zone as a distributed part and other zones conceptually structured. In principle, it is based on the integrated storage approach. Each storage element represents the natural storages of interception, the soil surface, the root zone and the whole unsaturated zone and the active groundwater zone. The model with a daily step computes the storage of each zone and treats their daily values, including input and output rates, in line with physical regularities, as reflected by the system of recurrent final difference and algebraic equations balancing the following processes (Kovář et al. 2004; Kovář 2006): (1) potential evapotranspiration, interception and throughfall; (2) surface runoff recharge; (3) root soil moisture zone dynamics; (4) soil moisture content and actual evapotranspiration and (5) groundwater dynamics, baseflow and total flow.

The WBCM-7 model has 11 parameters, but only three of them are to be optimised (Kulhavý and Kovář 2000): SMAX and GWM parameters representing the maximum capacity of unsaturated and saturated zones, respectively, and BK, the transformation parameter of the baseflow process.

The individual parameters have the following physical meaning representing

AREA	Catchment area (km^2)
FC	Field capacity of unsaturated zone (−)
POR	Total porosity (−)
KS	Hydraulic conductivity ($mm\ h^{-1}$)
DROT	Average depth of the root zone (mm)
WIC	Upper limit of interception (mm)
APLHA	Non-linear filling function exponent (−)
SMAX	Maximum capacity of unsaturated zone (mm)
GWM	Maximum capacity of groundwater zone (mm)
BK	Baseflow transformation parameter (day)
CN	Curve number (USDA NRSC) (−)

The modified Penman-Monteith method (Penman 1963; Monteith 1965) and also the Priestley-Taylor method (Priestley and Taylor 1972), or the Turc method (Turc 1961), were used for computing the daily potential evapotranspiration values. The model unit that computes the actual interception and throughfall is based on a simulation of the irregular distribution of the local interception capacities around their mean value, WIC.

The US Natural Resources Conservation Service method, based on curve number (CN) assessment (NRCS 1986), was used for quantifying direct run-off. The standard procedure for the initial CN value was accepted, and the daily storages of the active zone, SS, were computed by this procedure. The recharge of the root zone, and thus of all unsaturated zones, depends greatly on the previous soil moisture content and is controlled by the KS of the field capacity of unsaturated zone (FC) parameters. The evaluation procedure is based on the assumption that the distribution of the local FC values around their average is linear.

Figure 3 provides a description of the filling function principle, wherein rainfall input recharges the balance with a positive water surplus. The exhaustion function with negative input represents prevailing evapotranspiration in the daily step. This is applied for the root zone and also for the lower layer of unsaturated soil. Parameters P2 and P7 are based on particular soil retention curves: P2 ≅ 0.2, P7 ≅ 0.7 (loamy soils), 0.6 (for clay soils) and 0.8 (for sandy soils). Parameter P1 ≅ 0.1 describes very dry conditions for stomata transpiration. There is also a possibility to substitute linear soil retention curves by a non-linear curve introducing the parameter alpha (see Fig. 3).

Figure 4 provides a deep infiltration (i.e. percolation) and its dynamics through baseflow and upward capillary flux for evaporation. The resulting equations are included in Appendix 1. Simultaneously, the exhaustion from this zone by evapotranspiration is computed. To simulate this procedure, use is made of the proportions between the actual evapotranspiration and the potential evapotranspiration according to the soil moisture content and according to the particular physical properties of the soil. The saturated zone is filled with groundwater recharge and is depleted through baseflow. Automatic optimisation is applied where the efficiency of the model can be controlled either through the output discharges or through the fluctuations of the groundwater table. The parameters (SMAX, GWM and BK) were optimised by minimising the sum of least squared differences between the computed decade and the observed decade (10 days) groundwater depths in the control borehole.

The adequacy and the accuracy of the simulated decadal groundwater fluctuation in the control borehole were evaluated using the Nash-Sutcliffe coefficient of determination *RE* (Nash and Sutcliffe 1970), defined by the formula

$$RE = 1 - \frac{\sum_{i=1}^{N} \left(GWT_i - GWTC_i\right)}{\sum_{i=1}^{N} \left(GWT_i - GWT_p\right)} \tag{3}$$

where GWT_i is observed groundwater table for the decade i (m a.s.l.), $GWTC_i$ is computed groundwater table for the decade i (m a.s.l.), GWT_p is mean observed decadal groundwater table for the vegetation period (m a.s.l.) and N is number of decades over the vegetation period.

Input data

The water balance for the vegetation period in 2003, 2009, 2010 and 2011 was simulated by the WBCM-7 model. This model requires the antecedent 5-day (or 30-day) precipitation and the physiographical characteristics of the catchment, e.g. catchment area, land use and CN classification. The hydrophysical properties of the soil are also needed (Table 2).

At this point, daily values for precipitation, temperature, relative air humidity, sunshine duration, global radiation and wind speed were applied

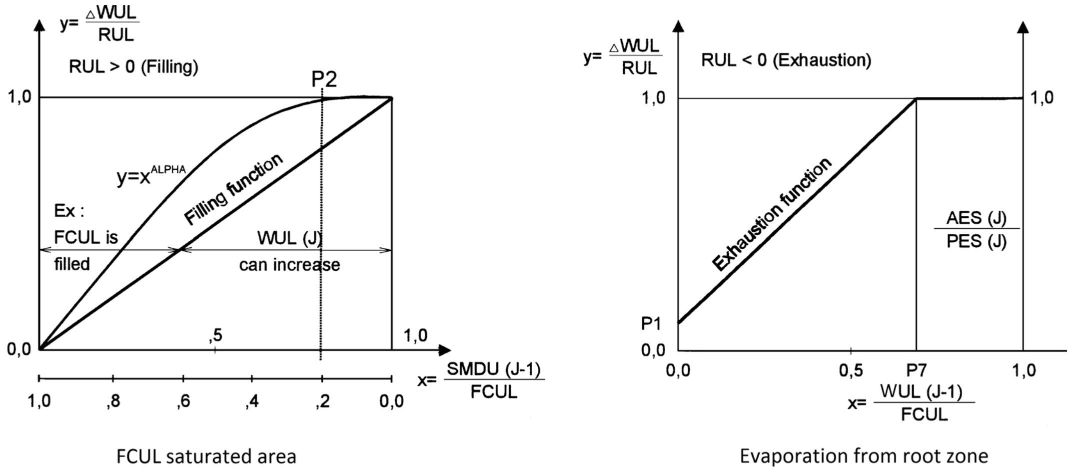

Fig. 3 Filling and exhaustion function in the WBCM-7 model

(Fig. 5). The Turc method (Hadaš 2004) was applied for the daily potential evapotranspiration values. There were some small differences in the input data. The potential evapotranspiration values measured at the climatological stations Kostice and Mikulčice differ, due to the specifics of land use in both locations. Whereas there are mostly meadows around Kostice, Mikulčice is surrounded by forests. The observed groundwater table fluctuation data were the last variables to control the correctness of the simulation procedure, which is assumed to be close to the computed procedure, to confirm the goodness of fit of the simulation. Like groundwater recharge, flow and storage are slow water balance processes. The time step is one decade (10 days) for the criteria function to optimise three parameters (SMAX, GWM and BK).

Results

The water balance was simulated for years 2003 (dry), 2009 (normal), 2010 (wet) and 2012 (dry). Our interest was focused on the dry years, as the aim of our study is to protect the alluvial plain forest from drought.

The water balance simulation of the vegetation periods in dry years 2003 and 2011 are the most important episodes in our study. These years show the importance of precipitation as the fundamental component of the water balance equation. The overview of the seasonal values of the water balance components in the four years mentioned above (2003, 2009, 2010 and 2012) is shown in Table 3.

The differences in rainfall, *SP*, and in water deficits between potential and actual

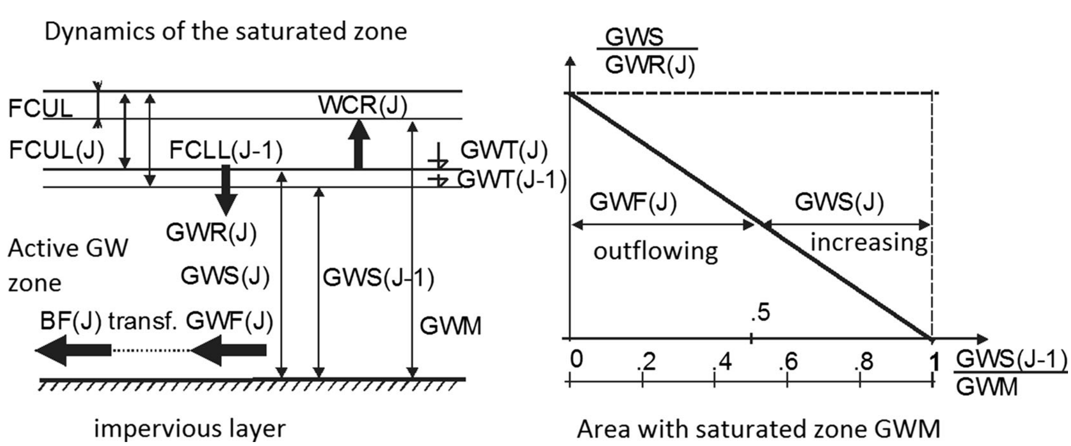

Fig. 4 Dynamics of the saturated (groundwater) zone in the WBCM-7 model

Table 2 Soil parameters for the transect Kostice-Lanžhot VB0360

Soil parameter	Value
Field capacity FC ($\%_{vol.}$) in depth 0.25–0.30 m	36.0[a]
Total porosity POR ($\%_{vol.}$) in depth 0.5–0.6 m	44.0[a]
Saturated hydraulic conductivity KS (mm h^{-1})	3.42[b]

[a] Average value of five measurements

[b] Average value of four measurements

evapotranspiration (*SPE−SAE*) clearly show the character of each year (dry or wet). The second indicator is the net change in subsurface storage (*SNGWR*), which is a figure that usually expresses a deficit in growing periods.

Figure 6 shows the major graphs produced in this study, which express the decadal water balance for the tested growing seasons. They are arranged as graphs sequentially step by step

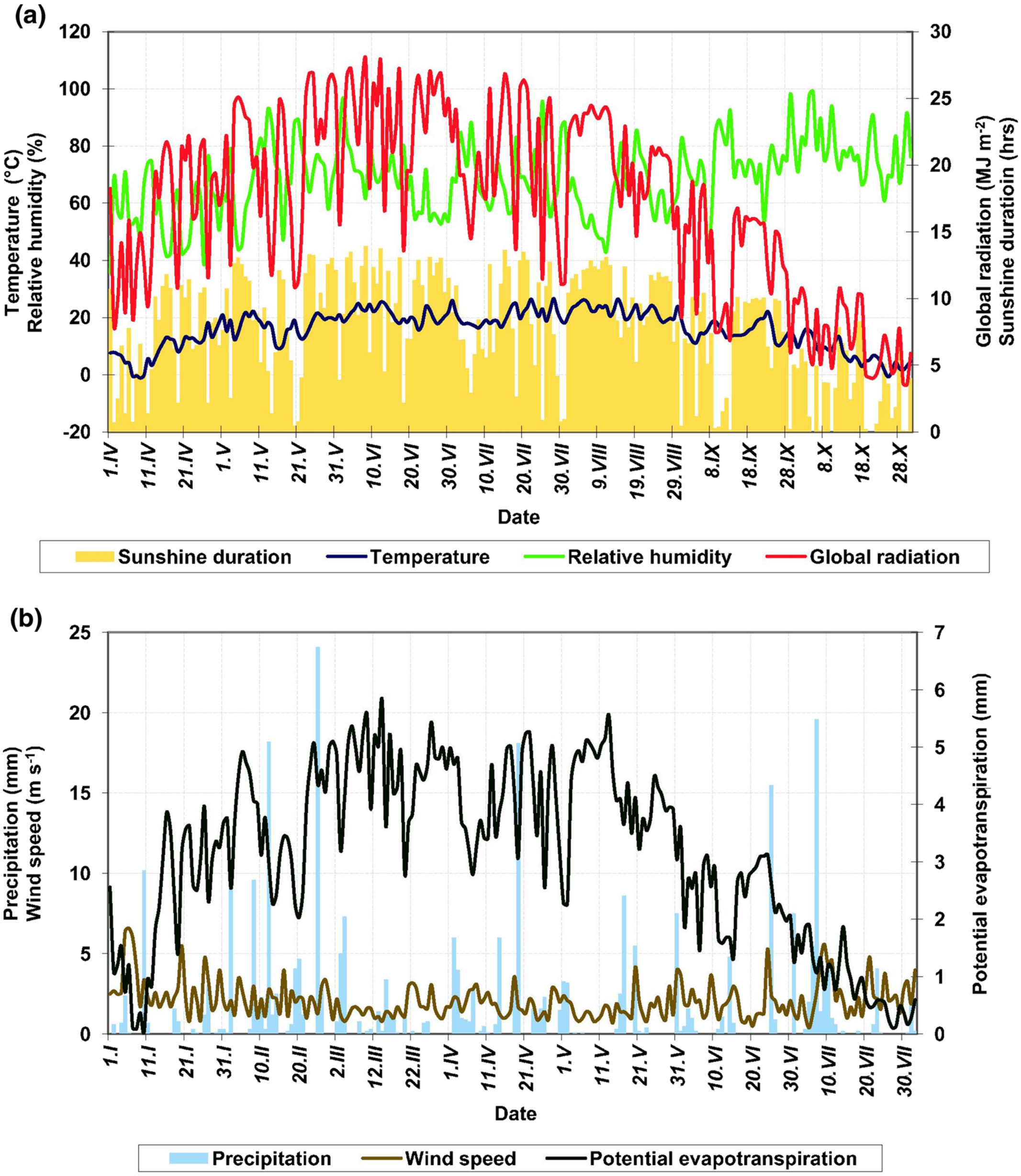

Fig. 5 Input data to WBCM-7: **a** average daily temperature, relative humidity, global radiation and duration of daily sunshine and **b** daily precipitation, wind speed and potential evapotranspiration at the Kostice station (1 January–31 December 2003)

Table 3 Seasonal water balance components of the transect Kostice-Lanžhot used and computed by WBCM-7 for the vegetation period of years 2003, 2009, 2010 and 2011

Water balance component (in mm)		Year			
		2003	2009	2010	2011
Rainfall	SP	292.8	485.1	680.3	364.1
Potential evapotranspiration	SPE	669.0	646.8	592.3	639.6
Actual evapotranspiration	SAE	309.6	395.0	432.9	367.3
Interception	SAIR	141.2	160.8	167.7	129.4
Infiltration	SRECH	136.3	243.9	403.0	201.0
Total run-off	SQ	87.6	191.1	292.1	118.7
Direct run-off	SOF	36.5	112.2	125.4	39.8
Baseflow	BF	51.1	78.9	166.7	78.9
Change of soil moisture	ASM	−66.5	−65.9	−23.1	−75.5
Groundwater recharge	GWR	15.4	42.8	144.8	32.0
Change in subsurface water storage	SGWR	−51.1	−23.1	121.7	−43.5
Net change in subsurface storage	SNGWR	−102.2	−102.0	−45.0	−122.4
Difference in water balance equation	DIF	−2.2	1.0	0.3	0.5

subtracting the water balance components on the right side of the equation for each decade, i.e. (1) SP, (2) $SP-SAE$, (3) $SP-SAE-SOF$, (4) $SP-SAE-SOF-SGWR$. The different components are shown in different colours—rainfall is a broken line between vertical ordinates, while other components occupy areas in the graph and are subtracted in downward direction. If the actual evapotranspiration in a certain decade is less than the rainfall, it is placed in a negative area, below the horizontal zero axis in Fig. 6. A significant direct run-off area was observed in June 2009 and in May and June 2010. The last component $SGWR$ expresses the subsurface water storage as the sum of the water in both the unsaturated and saturated zones $(ASM+GWR)$.

Negligible imbalances can be found in a few decades, when they are considered separately. These imbalances (DIF) are computed by

$$DIF = SP-SQ-BF-SAE-(ASM+GWR) \qquad (4)$$

The very small differences (DIF) are due to the fact that all balance components are calculated independently by the model, without forcing the balance processes to close at the end of each day. However, these imbalances, which are usually found for the entire vegetation periods, with values lower than 1.0 %, indicate that the model parameterisation is satisfactory.

The sum of the imbalances (i.e. differences) is then expressed by

$$SDIF = \sum_{i=1}^{N} DIF_i \qquad (5)$$

where $SDIF$ is the total difference between the left and right balance equation for the annual growing period (mm) and DIF_i is the difference between the decadal left and right balance equation in decade i (mm). These differences can also be expressed as a percentage (Table 4).

Figure 7 presents the control graphs, which confirm the acceptability of the observed and computed groundwater fluctuation pairs in Lanžhot borehole VB0360. The compatibility of the simulated groundwater levels with observed values is also given in Table 4, using the Nash-Sutcliffe coefficient.

In addition, three tables provide the values of non-optimised parameters (Table 5), the initial values of the starting conditions (Table 6) and automatically optimised parameters (Table 7). The baseflow depletion process in the vegetation period of particular years is compared in Fig. 8.

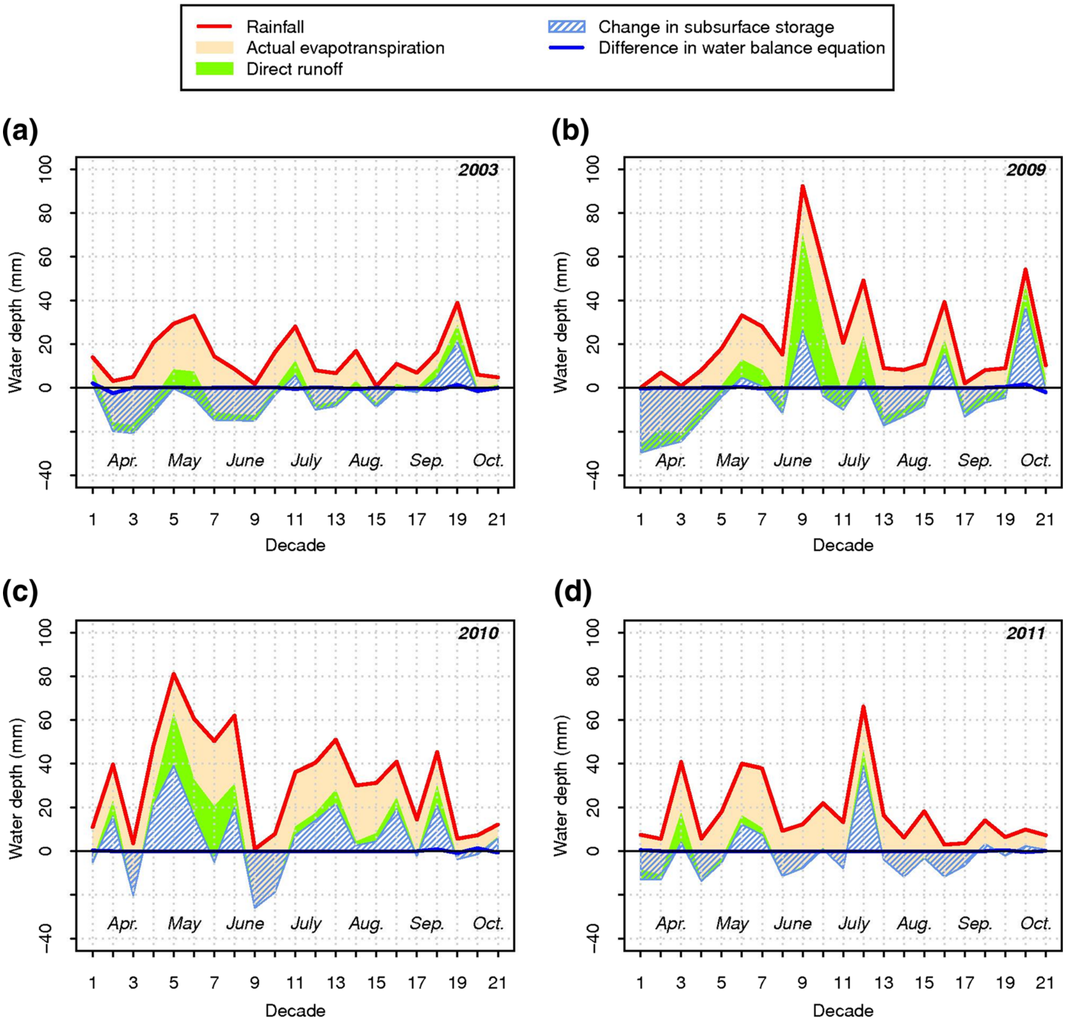

Fig. 6 Seasonal water balance (April 1 to October 31) in the Kostice-Lanžhot transect computed by the WBCM-7 model: **a** year 2003, **b** year 2009, **c** year 2010 and **d** year 2011

Discussion

The analysis of the water balance equation leads to the mass conservation equation, which can be derived from Eq. (1):

$$(ASM + GWR) = SP{-}SQ{-}BF{-}SAE \tag{6}$$

All variables are understood to be functions of time, averaged over the whole catchment area (Kirchner 2009). According to Kirchner's analysis, Eq. (6) should take into account how its individual terms can be measured to find the degree of uncertainty of their values. Precipitation (*SP*) calculations are local and are consequently loaded by the highest bias; the *SAE* data depend on the evapotranspiration method that will be used. However, global radiation data and unsaturated soil moisture parameter measurements ensure reliability only when they are measured in areal transects that are not

Table 4 Goodness of fit criteria to implementation of the WBCM-7 model for vegetation periods of 2003, 2009, 2010 and 2011

Year	Coefficient of determination (–)	Difference in depth (mm)	(%)	Verbal classification
2003	0.92	−2.24	−0.77	Very good
2009	0.89	0.95	0.20	Good
2010	0.92	0.26	0.04	Very good
2011	0.95	0.50	0.14	Excellent

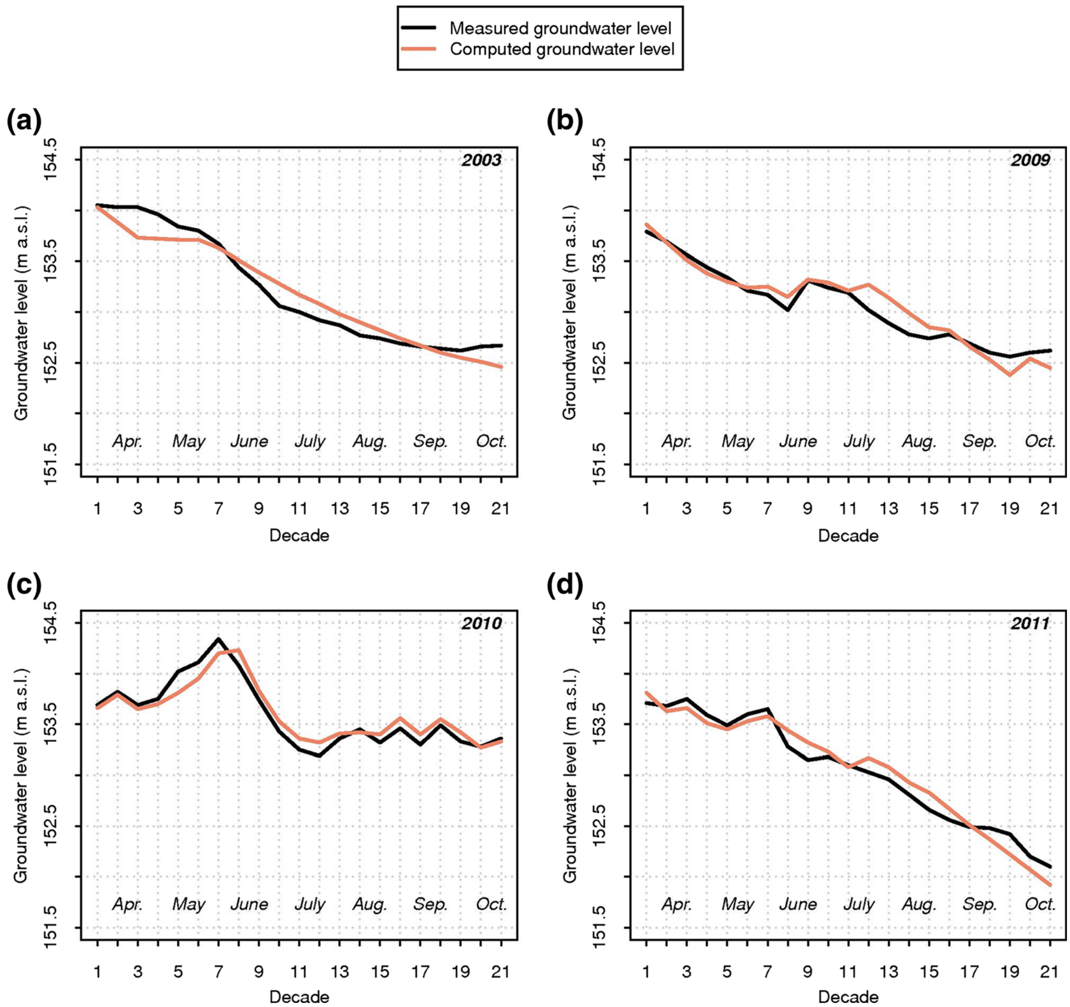

Fig. 7 Comparison of observed and simulated groundwater levels in borehole VB0241 Lanžhot for the vegetation season (April 1 to October 31): **a** year 2003, **b** year 2009, **c** year 2010 and **d** year 2011

too poorly selected. The soil moisture dynamics (*ASM*) is then computed by data calculations. The components of direct run-off (*SQ*) and baseflow (*BF*) cannot be calculated directly. Instead, we applied the measured groundwater tables. These values also depend on the selection of borehole sites. This problem was also described by Banks et al. (2011), when they assessed the spatial and temporal connectivity between surface water and groundwater in a regional catchment. Implementation of soil moisture assimilation data was

Table 5 The values of non-optimised parameters of the WBCM-7 model for transect Kostice-Lanžhot VB0360

Parameter	Value
Total porosity POR (%)	45.0
Field capacity FC (%)	36.0
Saturated hydraulic conductivity KS (mm h^{-1})	8.0
Curve number CN (–)	68.0

Table 6 The initial values of variables for transect Kostice-Lanžhot VB0360 used for the WBCM-7 model

Year	Antecedent precipitation API (30) (mm)	Upper layer soil moisture WUL (0) (mm)	Groundwater table GWT (0) (m a.s.l.)	Baseflow discharge BF (0) (mm day^{-1})
2003	5.9	120.0	154.05	1.0
2009	101.0	150.0	153.79	1.5
2010	12.3	120.0	153.69	1.5
2011	49.8	130.0	153.71	1.0

Table 7 The values of the automatically optimised parameters for transect Kostice-Lanžhot VB0360 used of the WBCM-7 model

Year	Average values of parameters		
	SMAX (mm)	GWM (mm)	BK (days)
2003	289.0	592.0	4.1
2009	297.0	606.0	3.8
2010	312.0	621.0	3.5
2011	285.0	597.0	4.0

described in a similar way by Han et al. (2012), who investigated how surface layer soil moisture data affect every hydrological process at catchment scale.

When comparing the input data of the potential evapotranspiration values (SPET) from the Kostice station (meadow prevailing land use) and the Mikulčice stations (riparian forest land use), we were confronted with some unexpected results. Table 8 provides the seasonal values of SPET and the actual evapotranspiration (SAE) in dry years 2003 and 2001 and in the more balanced year 2009. Surprisingly, much bigger differences were provided by Brauman et al. (2012), who measured higher values of potential evapotranspiration from pastures in a tropical region (Hawaii), than from forests. Obviously, the interaction of aerodynamic control on SPET was characterised by low wind speeds and low vapour pressure deficit (Brauman et al. 2012). In our case, besides a difference in land use, the lower floodplain acts as storage of flood water from the Morava River. This can contribute to the occurrence of more peak floods downstream (i.e. at Kostice station) than upstream (i.e. at Mikulčice station). Table 8 on the SAE output data in 2009 and in 2011 provides similar values, as have been presented in the paper concerning the effect of plains in Ethiopia (Dessie et al. 2014).

Evapotranspiration is a key component in water balance. However, it is not always featured in dryland hydrological modelling. Potential evapotranspiration is often represented with an empirical method, as the Hargreaves formula (e.g. Gunkel et al. 2015; Schmidt 2014) or the Penman-Monteith method (e.g. Smiatek et al. 2014). Land use representation, where vegetation prevails as a single uniform cover, is questionable for drier areas (Zhou et al. 2006).

The first reason why the efficiency coefficient computations of seasonal balances were processed from the groundwater table fluctuation, rather than from the discharges in the outlet, is explained above. The second reason is that the large disadvantage of the Nash-Sutcliffe efficiency between observed and computed values is calculated as squared values. Thus, larger values in time series are strongly overestimated, whereas lower values are neglected (Legates and McCabe 1999). The shape of the hydrograph, when discharges are used, usually leads to overestimation during peak flows and an underestimation during low flow conditions. Consequently, the Nash-Sutcliffe is not very sensitive to systematic modelling of groundwater table

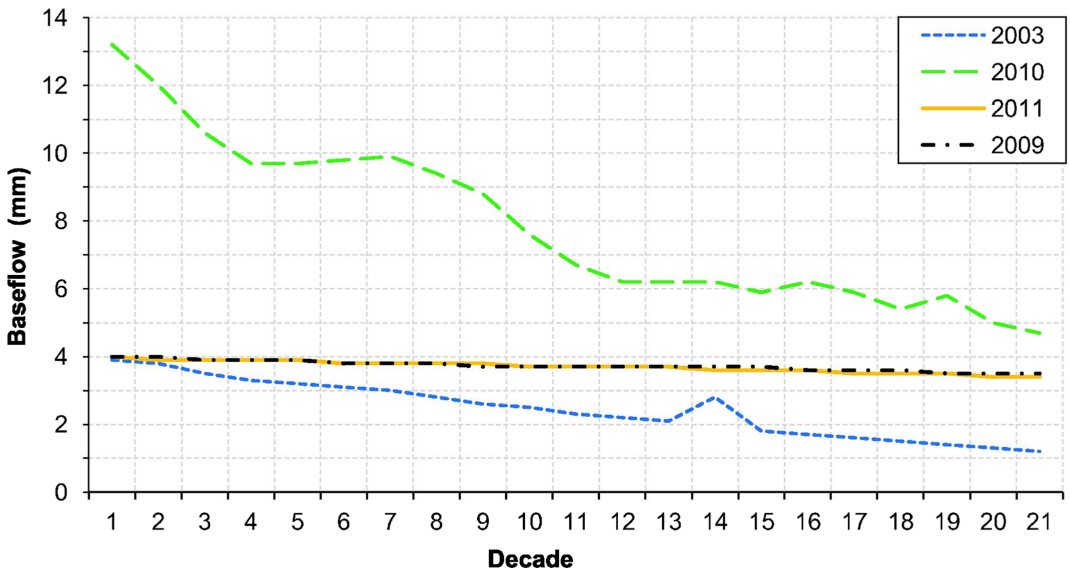

Fig. 8 Baseflow depletion process in the vegetation periods 2003, 2009, 2010 and 2011

Table 8 Comparison of SPET and SEA computed seasonal values at Kostice station (meadows) and Mikulčice station (forest)

Year	Potential evapotranspiration SPET (mm)			Actual evapotranspiration SAE (mm)		
	2003	2009	2011	2003	2009	2011
Kostice (meadows)	669.0	646.8	639.6	309.6	395.0	367.3
Mikulčice (forest)	665.0	643.5	633.1	300.3	354.7	321.2

fluctuation (Krause et al. 2005) that we have used as a criterion.

Conclusions

This paper has compared the water balance in the growing seasons in two distinct dry years (2003 and 2011), in one wet year (2010) and in one normal year (2009). The water balance data was measured on the Morava River floodplain and was computed using the WBCM-7 model. The innovations in water balance modelling can be assessed as follows:

- The climate data measurements and the data collection are done using state-of-the-art technology. A meteorological station with an automatic measurement system is used, using a charger connected with a solar panel. With a time step of 15 min, the climate data is measured by the ALA and VIRRIB devices, for the WBCM-7 model. The groundwater tables are measured in daily steps but are computed in decades.
- A comparison cannot be made with the earlier WBCM model series (i.e. WBCM-2 to WBCM-6), which is applicable only on a gauged catchment. The new version of the WBCM-7 model is also adapted for subcatchment areas equipped with boreholes for measuring the fluctuations of groundwater tables. If this area plays the role of an alluvial plain with a lower position of the river bed, the river works as a header.
- The parameter optimisation procedure in the WBCM-7 model has a two-criterion optimisation system. The first step is to minimise the difference between the measured water balance and the computed water balance, including the measured components. The second step is to achieve the best goodness of fit of the decadal groundwater tables. These two criteria should be used together.
- This paper has provided a specific hydrological study, as background for the follow-up irrigation systems engineering project, planned as a future improvement for the water regimes in the area.

Acknowledgments Field studies, model improvement, assessment and evaluation have been supported by a grant from the Ministry of Agriculture, the Czech Republic, Project NAZV, QJ 1220033 'Optimization of water regime on the Morava river floodplain'.

Appendix 1

The explanation of the symbols to Fig. 3 and Fig. 4:

Fig. 3:

RUL (J) = THR (J) − OF (J) − PES (J) (mm)

RUL (J): Positive (filling) or negative (exhausting) functions (mm)

THR (J): Throughfall, OF (J): overlandflow, PES (J): potential soil evaporation

FCUL: Field capacity of upper layer (incl. root zone, in mm)

SMDU (J) = FCUL − WUL (J): Soil moisture deficit (mm)

ΔWUL = WUL (J) − WUL (J-1): Soil moisture content in 1 day (mm)

AES (J): Actual soil evaporation (mm)

J: The day index (−)

Fig. 4:

Resulting equations:

GWS (J) = GWS (J-1) + GWR (J) × (1.0 − (GWS (J-1)) / GWM

GWR (J) = (RECH (J) − AES (J)) × (1.0 − FCLL (J-1) − WLL (J-1)) / FCLL (J-1)

GWF (J) = (GWR (J) × (GWS (J-1) / GWM)

GWT (J) = GWT (J-1) − ((GWS (J) − ((GWS (J) − GWS (J-1)) / POR) / 10.0

BF (J) = BF (J-1) × exp (−1.0 / BK) + GWF (J) × (1.0 − exp (−1.0 / BK))

GWS (J): Groundwater storage (mm)

GWR (J): Groundwater recharge (mm)

RECH (J): Infiltration recharge (from the CN method, in mm)

GWF (J): Groundwater flow (mm)

GWT (J): Groundwater table (m above sea level (m a.s.l.))

GWM: Maximum capacity of active groundwater zone (mm)

FCLL (J): Field capacity of lower layer

BF (J): Baseflow (transformed from groundwater flow, in mm)

WCR (J): Water capillary rise (if groundwater is shallow, in mm)

References

Abbott, M. B., Bathurst, J. C., Cunge, J. A., O'Connell, P. E., & Rasmussen, J. (1986a). An introduction to the European Hydrologic System—Système Hydrologique Européen, SHE, 1: history and philosophy of a physically based, distributed modelling system. *Journal of Hydrology, 87*, 45–59.

Abbott, M. B., Bathurst, J. C., Cunge, J. A., O'Connell, P. E., & Rasmussen, J. (1986b). An introduction to the European Hydrologic System—Système Hydrologique Européen, SHE, 2: structure of a physically based, distributed modelling system. *Journal of Hydrology, 87*, 61–77.

Andrew, R. M., & Dymond, J. R. (2007). A distributed model of the water balance in the Motueka catchment, New Zealand. *Environmental Modelling & Software, 22*, 1519–1528.

Arnold, J. G., Srinivasan, R., Muttiah, R. S., & Williams, J. R. (1998). Large area hydrologic modeling and assessment part I: model development. *Journal of the American Water Resources Association, 34*(1), 73–89.

Banks, E. W., Simmons, C. T., Love, A. J., & Shand, P. (2011). Assessing spatial and temporal connectivity between surface water and groundwater in a regional catchment: implications for regional scale water quantity and quality. *Journal of Hydrology, 404*(1-2), 30–49.

Bergström, S. (1995). The HBV model. In V. P. Singh (Ed.), *Computer models of watershed hydrology* (pp. 443–520). Highlands Ranch, Colorado, USA: Water Resources Publications.

Beven, K. J., Lamb, R., Quinn, P., Romanowicz, R., & Freer, J. (1995). TOPMODEL. In V. P. Singh (Ed.), *Computer models of watershed hydrology* (pp. 627–668). Highlands Ranch, Colorado, USA: Water Resources Publications.

Brauman, K. A., Freyberg, D. L., & Daily, G. C. (2012). Potential evapotranspiration from forest and pasture in the tropics: a case study. *Journal of Hydrology, 440–441*(2012), 52–61.

Brown, A. E., Zhang, L., McMahon, T. A., Western, A. W., & Vertessy, R. A. (2005). A review of paired catchment studies for determining changes in water yield resulting from alterations in vegetation. *Journal of Hydrology, 310*(1-4), 28–61.

Burnash, R. J. C. (1995). The NWS river forecast system—catchment modelling. In V. P. Singh (Ed.), *Computer models of watershed hydrology* (pp. 311–366). Highlands Ranch, Colorado, USA: Water Resources Publications.

Dessie, M., Verhoest, N. E. C., Admasu, T., Pauwels, V. R. N., Poesen, J., Adgo, E., Deckers, J., & Nyssen, J. (2014). Effects of the flood plain on river discharges into Lake Tana (Ethiopia). *Journal of Hydrology, 519*(2014), 699–710.

Gunkel, A., Shadeed, S., Hartmann, A., Wagner, T., & Lange, J. (2015). Model signature and aridity indices enhance the accurancy of water balance estimations in a data-scarse Eastern Mediterranean catchment. *Journal of Hydrology: Regional Studies, 4*(2015), 487–501.

Hadaš, P. (2004). Water balance of the riparian forest of southern Moravia in the year 2003. In J. Rožnovský & T. Litschman (Eds.), *Extrémy počasí a podnebí* (pp. 24–25). Brno: The Czech Bioclimatic Society.

Han, E., Merwade, V., & Heathman, G. C. (2012). Implementation of surface soil moisture data assimilation with watershed scale distributed hydrological model. *Journal of Hydrology, 416–417*, 98–117.

Kirchner, J. W. (2009). Catchment as simple dynamical systems: catchment characterization, rainfall-runoff modelling and doing hydrology backward. *Water Resources Research*. doi:10.1029/2008/WR006912.

Kovář, P. (2006). The extent of land use impact on water regime. *Plant, Soil and Environment, 52*(6), 239–244.

Kovář, P., & Vaššová, D. (2010). Impact of arable land to grassland conversion on the vegetation-period water balance of small agricultural catchment (Němčický Stream). *Soil and Water Research, 5*(4), 128–138.

Kovář, P., Cudlín, P., & Šafář, J. (2004). Simulation of hydrological balance on experimental catchments Všeminka and Dřevnice in the extreme periods 1992 and 1997. *Plant, Soil and Environment, 50*(11), 478–483.

Krause, P., Boyle, D. P., & Bäse, F. (2005). Comparison of different efficiency criteria for hydrological model assessment. *Advances in Geosciences, 5*(89–97), 2005.

Kulhavý, Z., & Kovář, P. (2000). *Use of water balance models for small catchments*. Praha: VÚMOP Praha.

Legates, D. R., & McCabe, G. J., Jr. (1999). Evaluating the use of "goodness of fit" measures in hydrologic and hydroclimatic model validation. *Water Resources Research, 35*(1), 233–241.

Monteith, J. L. (1965). Evaporation and environment. In G. E. Fogg (Ed.), *The state and movement of water in living organisms* (pp. 205–234). UK: Academic Press for the Society for Experimental Biology.

Moretti, G., & Montanari, A. (2007). AFFDEF: a spatially distributed grid based rainfall–runoff model for continuous time simulations of river discharge. *Environmental Modelling & Software, 22*, 823–836.

Motovilov, Y. G., Gottschalk, L., Engeland, K., & Belokurov, A. (1999). *ECOMAG: regional model of hydrological cycle*. Oslo: University of Oslo.

Nash, J. E., & Sutcliffe, J. V. (1970). River flow forecasting through conceptual models. Part I—a discussion of principles. *Journal of Hydrology, 10*, 282–290.

NRCS. (1986). *Urban Hydrology for Small Watersheds. Technical Release 55 (13)*. Washington D.C: U.S. Department of Agriculture.

Penman, H. L. (1963). *Vegetation and hydrology*. Harpenden, U.K: Technical Committee 53, C. Bureau of Soils.

Priestley, C. H. B., & Taylor, R. J. (1972). On the assessment of surface heat flux and evaporation using large-scale parameters. *Monthly Weather Review, 100*, 81–82.

Refsgaard, J. C., & Storm, B. (2005). MIKE SHE. In V. P. Singh (Ed.), *Computer models of watershed hydrology* (pp. 809–846). Highlands Ranch, Colorado, USA: Water Resources Publications.

Sánchez, N., Fernández, J. M., Calerab, A., Torres, E., & Gutiérrez, C. P. (2010). Combining remote sensing and in situ soil moisture data for the application and validation of a distributed water balance model (HIDROMORE). *Agricultural Water Management, 98*, 69–78.

Schmidt S. (2014). Hydrogeological characterisation of karst aquifer in semi-arid environments at the catchment scale-example of the Western Lower Jordan Valley. In: PhD. Thesis. University of Göttingen, Germany.

Smiatek, G., Kunstmann, H., & Heckl, A. (2014). High-resolution climate change impact analysis on expected future water availability in the Upper Jordan catchment and the Middle East. *J. Hydrometeor., 15*, 1517–1531.

Soukalová, E. (2012). *Groundwater regimes in the confluence of the Morava and Thaya rivers*. Brno: ČHMÚ Brno.

Turc, L. (1961). Evaluation des besoins en eau d'irrigation, evapotranspiration potentielle. *Annales agronomiques, 12*, 13–49.

Vázquez-Suñé, E., Sánchez-Vila, X., & Carrera, J. (2005). Introductory review of specific factors influencing urban groundwater, an emerging branch of hydrogeology, with reference to Barcelona, Spain. *Hydrogeology Journal, 13*(3), 522–533.

Zhou, M. C., Ishidaira, H., Hapuarachchi, H. P., Magome, J., Kiem, A. S., & Takeuchi, K. (2006). Estimating potential evapotranspiration using Shuttleworth-Wallace model and NOAA-AVHRR NDVI data to feed distributed hydrological model over the Mekong River basin. *Journal of Hydrology, 327*(1-2), 151–173.

PŘÍLOHA č. 3

doi: 10.17221/119/2013-SWR

Computation Method of the Drainage Retention Capacity of Soil Layers with a Subsurface Pipe Drainage System

Jitka PEŠKOVÁ and Jakub ŠTIBINGER

Department of Land Use and Improvement, Faculty of Environmental Sciences, Czech University of Life Sciences Prague, Prague, Czech Republic

Abstract

Pešková J., Štibinger J. (2015): Computation method of the drainage retention capacity of soil layers with a subsurface pipe drainage system. Soil & Water Res., 10: 24–31.

Methodological procedure for determining the drainage retention capacity (DRC) of surface layers under conditions of unsteady-state groundwater flow was demonstrated. DRC of the drainage system can be defined as a groundwater reservoir situated between the soil surface and the intermediate position of a parabola shaped water table above the drain level. Computation of DRC is based on analytical approximation of the subsurface total drainage discharge in unsteady-state groundwater conditions. DRC formula can serve as a simple tool for immediate estimation that requires only minimum amount of basic information (drainage design parameters, soil hydrology data). DRC is an important phenomenon of drainage policy, an inseparable part of drainage processes, which can mitigate negative impact of climate dynamics. A properly applied drainage policy, with the possibility of manipulating the retention capacities in the soil layers, can significantly improve soil and environmental protection. In agriculture, DRC extended by a drainage system can mitigate the negative effects of hydrological extremes such as floods and droughts.

Keywords: agricultural areas; groundwater reservoir; hydrological extremes; unsteady-state groundwater conditions

One of many reasons of floods and water logging is a very low infiltration ability and especially unsatisfactory drainage capacity of surface layers in landscape (Deasy *et al.* 2014). Good infiltration and drainage conditions of surface layers in landscape cannot definitely eliminate floods, but can considerably mitigate their negative impacts (Hümann *et al.* 2011). The primary purpose of subsurface drainage systems is facilitation of agricultural production (Blann *et al.* 2009). Consequently, drainage outflow also results in the formation of retention space above the drainage system. The conception of the drainage retention capacity (DRC) is a new term, which represents hydrophysical characteristic of porous soil environment in a drainage hydrology area. DRC is directly dependent on drainage system parameters with a favourable effect on mitigating the negative impact of floods. The negative impact of extreme runoff, resulting in floods, can be reduced by taking the precautions (Kabat *et al.* 2004).

The present drainage study is aimed at establishing a methodological procedure leading to a direct computation of the retention capacity of surface layers under unsteady-state groundwater conditions. The method is based on a mathematical and physical description of the unsteady-state groundwater flow using the Boussinesq equation with an analytical solution.

Analytical solutions of unsteady-state groundwater flow are verified procedures that have been presented e.g. by Zavala *et al.* (2007); Fuentes *et al.* (2009), Singh (2009), and Dan *et al.* (2013).

The determination of DRC of surface layers with the use of subsurface pipe drainage systems is based on the analytical solution of subsurface total drainage quantity in a non-steady state drainage flow

doi: 10.17221/119/2013-SWR

and in such a form it is being published for the first time herein.

MATERIAL AND METHODS

Fundamental principles, definitions, and equations. We assume a fully saturated soil profile with a high position of the water table level that is identical with the surface. For this soil profile, there is a subsurface pipe drainage system with drain spacing L (m), drain diameter r_0 (m), and drain depth h_d (m). The depth of the impervious floor below the level of the drain = 1 m (see Figure 1). Symbol h_0 (m) means the initial water table level (m) at time $t = 0$, and because the water table level is identical with the soil surface, the expression $h_0 = h_d$ is valid.

The water table level, drained by the subsurface pipe drainage system, begins to decrease from h_0 (m). In this case no recharge to the water table has been recorded and it means that the unsteady-state drainage flow principles can be applied.

DRC developed by operation of the subsurface pipe drainage system in unsteady-state groundwater conditions can be defined as a free gravity water drainable pore space under the surface. This drainable pore space, which does not contain any gravity water, is limited from above by the soil surface level and by parabola shaped water table situated above the drains from below (Figure 1). Determination of DRC is based on analytical approximation of subsurface total drainage quantity in unsteady-state groundwater conditions (Stibinger 2003). The solution coming from Boussinesq equation (1904) describes the unsteady-state saturated groundwater flow without any recharges to the water table:

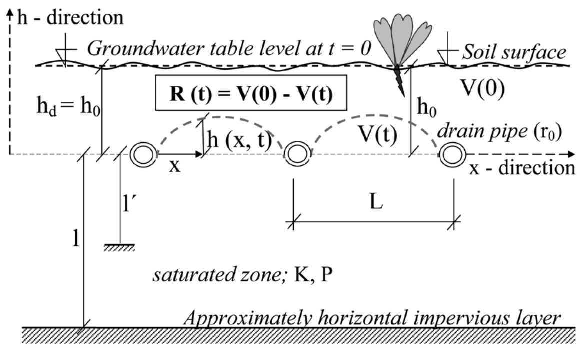

Figure 1. Height of the groundwater table h (x, t) at the distance $x > 0$ at the time $t > 0$, at saturated unsteady-state groundwater conditions and retention capacity of surface layers $R(t)$ at the time $t > 0$

$$HK\frac{\partial^2 h}{\partial x^2} = P\frac{\partial h}{\partial t} \tag{1}$$

where:
h – height of the water table level (m)
H – constant representing the average depth of the aquifer (m)
K – hydraulic conductivity (m/day)
P – drainable pore space, effective drainage porosity (–)
x – horizontal x-direction (x-coordinate) (m)
t – time (days)

The volume of the soil gravity water above the next two parallel drains at the time $t = 0$ can be expressed as

$$V(0) = h_d \times P \tag{2}$$

where:
$V(0)$ – volume of the soil gravity water above the level of the parallel horizontal subsurface drainage pipe system (at the time $t = 0$), expressed in m per unit surface area

Next step of the process will be clarified in the same way at the time $t > 0$.

The area above the next two parallel drains with drain spacing L (m) at the time $t > 0$ is approximately

$$\int_0^L h(x,t)dx \quad (\mathrm{m}^2)$$

and in the same way as Eq. (2), Eq. (3) can be modified into:

$$V(t) = (P/L)\int_0^L h(x,t)dx \tag{3}$$

where:
$V(t)$ – volume of soil gravity water (water quantity) above the level of the parallel horizontal subsurface drainage pipe system (at the time $t > 0$), expressed in m per unit surface area

The expression

$$\int_0^L h(x,t)dx$$

can be modified into:

$$\int_0^L h(x,t)dx = \frac{8h_0 L}{\pi^2}e^{-at} = \frac{8h_d L}{\pi^2}e^{-at} \tag{4}$$

Parameter a represents drainage intensity factor

$$a = \frac{\pi^2 KH}{L^2 P} \quad (1/\mathrm{day}) \tag{5}$$

By substituting the end of Eq. (4) into Eq. (3), we can define the formula for expressing $V(t)$ (m) and Eq. (3) can be written as:

doi: 10.17221/119/2013-SWR

$$V(t) = \frac{8h_d P}{\pi^2} e^{-at} \tag{6}$$

The retention capacity of soil layers $R(t)$ (m) created by the hydraulic function of the subsurface pipe drainage system at the time $t > 0$ and expressed in m per unit surface area is shown in Figure 1.

Retention capacity of soil layers $R(t)$ (m) is actually the released space under the surface. It is the difference between the volume of the soil gravity water $V(0)$ (m) at the time $t = 0$ and the volume of soil gravity water $V(t)$ (m) at the time $t > 0$, which can be expressed as:

$$R(t) = V(0) - V(t) \tag{7}$$

After substitution of Eq. (2) and Eq. (6) into Eq. (7) and rearrangements, the equation for estimation of retention capacity of soil layers $R(t)$ (m) can be defined as:

$$R(t) = h_d P(1 - \frac{8}{\pi^2} e^{-at}) \tag{8}$$

At this moment it is important to note, that the expression $h_0 = h_d$ is valid just for the case when position of the water table level is high and identical with the surface. But it means that the final formula (8) for approximation of the retention capacity of soil layers $R(t)$ (m) can also be written as:

$$R(t) = h_d P(1 - \frac{8}{\pi^2} e^{-at}) = h_0 P(1 - \frac{8}{\pi^2} e^{-at}) \tag{9}$$

From the way of derivation of retention capacity of soil layers $R(t)$ (m), which leads to Eqs (8) and (9), and from the analysis and equations presented above, the expression for approximation of retention capacity of soil layers $R(t)_1$ (m) was extrapolated in a case where $h_d > h_0$ is valid. This equation can be expressed as:

$$R(t)_1 = P(h_d - h_0) + h_0 P(1 - \frac{8}{\pi^2} e^{-at}) \tag{10}$$

After rearrangements Eq. (10) is as follows:

$$R(t)_1 = P(h_d - h_0 \frac{8}{\pi^2} e^{-at}) \tag{11}$$

By approximation made in Eqs (8) and (11) with the knowledge of the basic subsurface drainage system parameters (L, r_0, h_d) and soil hydrology characteristics (K, P, h_0), it is possible to evaluate retention capacity of soil layers $R(t)$ (m) for a case where $h_0 = h_d$ is valid as well as $R(t)_1$ (m) for a case where $h_d > h_0$ is valid, at the time $t > 0$.

Dieleman and Trafford (1976) showed that all formulas and expressions derived from Boussinesq equation, which includes Eqs (8)–(11), are valid at a certain time, which was defined as:

$$\tau(\text{days}) = 0.4\,(-)/a\left(\frac{1}{\text{days}}\right) \tag{12}$$

It should be kept in mind, that $R(t)$ (m) and $R(t)_1$ of the approximations (9) and (11) represent, from the physical point of view, a scalar. This means that volume, quantity, amount of drained space or mass is in this case expressed in length units (m).

RISWC experimental drainage field in Středočeská pahorkatina Upland (Czech Republic). Measured real values of the subsurface drainage discharges were obtained from the experimental field area, owned by the Research Institute for Soil and Water Conservation (RISWC) Prague-Zbraslav, Czech Republic (Soukup *et al.* 2000). From the geological point of view, the parent rock of the Cerhovice brook watershed area is formed of shale. All soil layers have low permeability, and the approximate depth of the impervious barrier is more than 1.0 m below the soil surface. The approximately 41.0 ha experimental field area is drained by a subsurface pipe drainage system. The thickness of the low permeable soil profile = 0.90 m, and the initial water table level h_0 = 0.50 m. The horizontal parallel systematic drainage system with drain spacing L = 11 m, average drain depth h_d = 0.75 m, and diameter of the lateral drain r_0 = 0.06 m is a typical shallow subsurface drainage system for heavy soils, with a low drainable pore space and hydraulic conductivity value K = 0.075 m/day, effective drainage porosity P = 0.015. The scheme of the drainage system parameters and soil conditions is shown in Figure 2.

The soil hydrology characteristics of the drained soil layers were measured in the terrain and verified

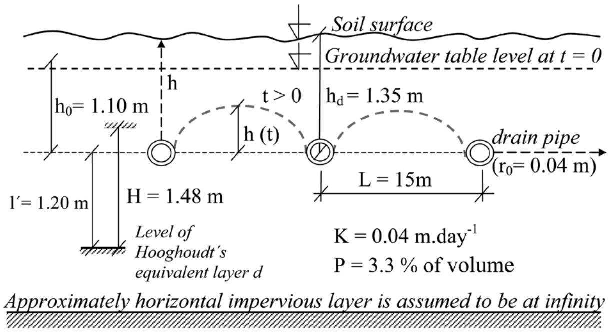

Figure 2. Drainage system parameters under unsteady-state groundwater conditions of the RISWC experimental drainage field in Prague-Zbraslav (Czech Republic)

doi: 10.17221/119/2013-SWR

in a laboratory (undisturbed core samples were used). The approximation of the hydraulic conductivity was carried out by the application of the single augerhole method, partially with the inversed single augerhole method and double ring infiltration method. The effective porosity was approximated from the soil water retention curves (Soukup *et al*. 2000).

The data used for the verification study were measured from June 2000 through July 2001. The measured subsurface drainage rate values were selected from the period May 4–17, 2001 after intensive precipitation (30 mm of recharge during May 4–6, 2001). During the drainage process, which was characterized by recession of the water table, no recharge to the water table level was recorded (e.g. through irrigation following rainfall, heavy rains or floods). The drainage process came to an end on May 29–30, 2001, when the drainage rate dropped below a value of 0.1 mm per day. The same data (Soukup *et al.* 2000) were used for approximation of subsurface drainage discharge by De Zeeuw-Hellinga theory (De Zeeuw & Hellinga 1958) and its verification (Štibinger 2009).

Experimental drainage field in the Mashtul Pilot Area (Nile Delta, Egypt). Historical data on the water table were obtained from Mashtul, situated in the Nile Delta. It was established in 1979–1980 as the Mashtul Pilot Area – Egyptian Dutch Advisory Panel (Ritzema 2009), where all variants of subsurface pipe drainage experiments in connection with crop production, soil salinity, depth of the water table, drain depth, and drain discharges for the south-eastern part of the Nile Delta were tested and verified.

The soil profile in this area can be presented as relatively homogeneous. The top clay layers are about 6 m thick, and a sandy aquifer forms the lower part of the soil profile. Low permeable (impervious), approximately horizontal layers are assumed to be at infinity. The average hydraulic conductivity value K is about 0.15 m/day for the eastern and central parts, where the data for the experiment were gathered. The continuous groundwater table level is deeper than 0.75 m below the surface. The climate of Mashtul is characterized by long dry summers and short winters, with a small amount of precipitation. The long-term annual average precipitation is 50–100 mm (Nijland *et al*. 2005; Ritzema 2007).

The results of the soil investigation by Alterra-ILRI (2008) were used to estimate the representative hydraulic conductivity value for the drainage of the experimental field, K = 0.04 m/day and the drainable pore space value P = 3.3% of volume. The approximately horizontal impermeable layer is assumed to be at infinity. Drain spacing L = 15 m, drain radius r_0 = 0.04 m, and drain depth h_d = 1.35 m are the basic design parameters of the subsurface pipe drainage system, projected and selected in steady-state drainage flow, using the Hooghoudt equation (Hooghoudt 1940). The entire geometry of the subsurface pipe drainage system of the drainage unit in the Mashtul Pilot Area is shown in Figure 3.

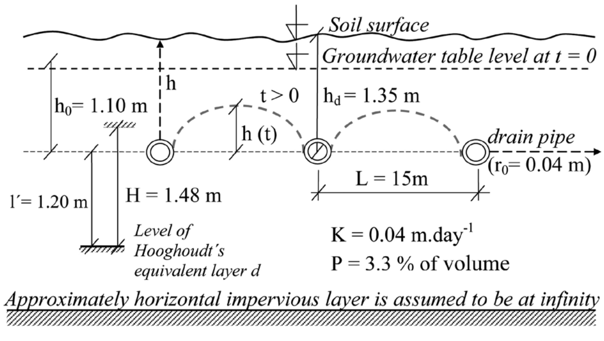

Figure 3. Subsurface pipe drainage system under unsteady--state groundwater conditions in the drainage unit of the Mashtul Pilot Area (Egypt)

RESULTS

RISWC experimental drainage field in Středočeská pahorkatina Upland (Czech Republic). The correctness of the results from the final Eqs (9)–(11) for calculations of the retention capacity of soil layers was verified using measured drainage discharge data and measured data for total subsurface drainage quantities from the RISWC experimental study area, Prague-Zbraslav.

The results of the initial hydraulic calculations from the drainage system show that the value of $l = l'$ = 0.15 m, because the lateral drains are situated very close to an impervious layer. The value of H equals to $l' + (h_0/4)$ = 0.275 (m) and indicates that the value of the drainage intensity factor a = 0.112 l/day. From the daily measured drainage rate values (mm/day) (shown in the third column of Table 1), the daily subsurface total drainage quantities were determined as well as the instantaneous retention capacity values of the soil layers (the fourth column of Table 1). The initial value for the retention capacity of the soil layers at the beginning of the drainage process, at the time t = 0, was approximated as $(h_d - h_0)\ P$ = 3.75 mm. In view of the fact that h_d = 0.75 m > h_0 = 0.50 m,

doi: 10.17221/119/2013-SWR

Table 1. Instantaneous and calculated values of the retention capacity of soil layers from the RISWC experimental field in Prague-Zbraslav (Czech Republic) and comparison of the differences between instantaneous and calculated values

Date	Time (days)	Drainage rate[1] (mm/day)	Retention capacity of soil layers[1] (mm)	Retention capacity of soil layers[2] (mm)	Differences[3] (mm)	Differences (%)
May 6, 2001	0	0.10	3.75	3.75	0.00	0.00
May 7, 2001	1	0.95	4.70	5.81	1.11	23.6
May 8, 2001	2	0.78	5.48	6.38	0.90	16.4
May 9, 2001	3	0.63	6.11	6.90	0.79	12.9
May 10, 2001	4	0.53	6.66	7.36	0.70	10.5
May 11, 2001	5	0.49	7.15	7.77	0.62	8.7
May 12, 2001	6	0.42	7.57	8.14	0.57	7.5
May 13, 2001	7	0.38	7.96	8.47	0.51	6.4
May 14, 2001	8	0.35	8.31	8.76	0.45	5.4
May 15, 2001	9	0.29	8.60	9.03	0.43	5.0
May 16, 2001	10	0.26	8.86	9.26	0.40	4.5
May 17, 2001	11	0.23	9.10	9.47	0.37	4.1

[1]instantaneous values; [2]values calculated by Eq. (11); [3]absolute magnitude

which means that $h_d > h_0$, the daily retention capacities values for the soil layers (the fifth column of Table 1) were calculated using Eq. (11).

While the water table was receding through the subsurface pipe drainage system, no recharge (e.g. rainfalls, irrigations, heavy rains or floods) to the water table level was recorded (Soukup *et al.* 2000).

Experimental drainage field in the Mashtul Pilot Area (Nile Delta, Egypt). The correctness of the results produced by the final Eqs (9)–(11) for calculating the retention capacity of soil layers was also verified using historical measured data on the water table receding from an experimental drainage field in the Mashtul Pilot Area, situated in the Nile Delta in Egypt. The historical record of the water table fluctuation data from winter 1984 and from the beginning of 1985 were used (Ritzema 2009).

Shortly after irrigation, the highest water table of 0.25 m below ground level was recorded. As the drain depth h_d = 1.35 m, this means that h_0 = 1.10 m. During the drainage process, the water table $h(t)$ falls relatively slowly with time t, following the typi-

Table 2. Instantaneous and calculated values of the retention capacity of soil layers from the Masthul Pilot Area (Nile Delta, Egypt) and comparison of the differences between instantaneous and calculated values

Date	Time (days)	Water table[1] (m)	Retention capacity of soil layers[2] (mm)	Retention capacity of soil layers[3] (mm)	Differences[4] (mm)	Differences (%)
December 6, 1984	6	0.60	31.9	26.2	5.7	17.9
December 10, 1984	10	0.43	35.5	31.1	4.4	12.4
December 13, 1984	13	0.32	37.8	34.0	3.8	10.1
December 16, 1984	16	0.28	38.6	36.2	2.4	6.2
December 20, 1984	20	0.26	39.1	38.4	0.7	1.8
December 23, 1984	23	0.26	39.1	39.7	0.6	1.5
December 26, 1984	26	0.21	40.1	40.7	0.6	1.5
December 30, 1984	30	0.19	40.6	41.7	1.1	2.7
January 2, 1985	33	0.13	41.8	42.3	0.5	1.2

[1]measured values; [2]instantaneous values; [3]values calculated by Eq. (11); [4]absolute magnitude

doi: 10.17221/119/2013-SWR

cal exponential shape, and almost reaches the drain depth level. During the test period, no precipitation was recorded in the experimental drainage unit area. The process of subsurface unsteady-state flow into the drains was therefore not influenced by any recharge to the drainage water table.

Hooghoudt equivalent depth l' (m) of the soil layer below the level of the drain was approximated using the expression presented in Dieleman and Trafford (1976); Ritzema (2007) in a simplified form:

$$l' = \frac{l}{(8/\pi) \times (l/L) \times \ln(\frac{l}{\pi r_0}) + 1} \qquad (13)$$

As the impermeable layer l (m) converges to infinity ($l > L/2$), according to Dieleman and Trafford (1976) $l = L/2$ and for the value of Hooghoudt equivalent depth d (m) we can get l' = 1.20 m. If $H = l' + h_0/2$ = 1.48 m, then the drainage intensity factor a = 0.0786 l/day. The instantaneous values for the retention capacities of the soil layers were derived from time series of the recession of the water table level (the fourth column of Table 2).

Using Eq. (11) and from the known values of h_0 = 1.1 m, h_d = 1.35 m, and a = 0.0786 l/day and for a certain time t (day), the retention capacity values for the soil layers were calculated (the fifth column of Table 2).

DISCUSSION

The initial drainage measurements for estimating and analyzing the retention capacity of soil layers during the period of subsurface flow into the drains under unsteady-state conditions were started on May 7, 2001 (t = 1) and took place in the RISWC experimental area in Prague-Zbraslav. The saturated unsteady-state drainage flow from an experimental area of 41.0 ha was terminated on May 29, 2001, when the drainage discharge dropped below a value of 0.1 mm per day.

The comparison of the instantaneous daily values for the retention capacities of the soil layers and the retention capacity values for the soil layers calculated using Eq. (11) (see Table 1) clearly demonstrates that the shape of the curve for the instantaneous daily values and the shape of the curve for Eq. (11) are the same, with only some small differences.

The small differences between the instantaneous retention capacity values and the retention capacity values calculated using Eq. (11) are characterized by the high value of determination index I_R = 0.970.

Table 1 shows clearly that the course of the time series of the differences (differences from the instantaneous retention capacity values for the soil layers minus $R(t)_1$, calculated using Eq. (11) is monotonous and slightly decreasing. This case serves as an example where the differences are inversely proportional to the retention capacity values for the surface layers. The higher the retention capacity value for the surface layers, the smaller the difference can be expected.

According to Dieleman & Trafford (1976), the validity of Eq. (11) is defined from the point of time τ = 3.57 days (calculated using Eq. (12)). This means that from approximately May 10, 2001, the 4th day (t = 4) after the beginning of the drainage process, the analytical approximation expressed by Eq. (11) will be valid, and the corresponding difference on this day, at time t = 4 days, is 0.70 mm.

This is the greatest daily difference (approximately 0.70 mm, i.e. 10.5%) for the whole 41.0 ha of the experimental drainage area in this tested time series. Other differences are smaller.

The linearization of the Boussinesq equation, which forms the basis for the other derived formulas and equations, is more correct for deeper barriers. The case presented here is a typical example of a shallow soil drainage profile.

This approximation, where parameter H has been substituted by $l' + (h_0/4)$, introduces errors into the estimations of the drain flow discharges, and even larger errors for water table elevations, as utilized in the equations for the final expression of the retention capacity of the surface layers. The initially flat shape of the water table ($h(x, 0) = h_0$ at $t = 0$ for $0 \leq x \leq L$) can also explain why the calculated values are clearly greater than the measured and fitted values at the beginning of the tested period. At the end of the demonstrated period, which is presented in Table 1, the difference makes 0.37 mm (4.1%). The greatest daily difference that is valid in this period is 0.70 mm (10.5%).

The RISWC Prague-Zbraslav records show that at the end of the unsteady-state drainage process (May 29, 2001) the difference between measured and calculated values was only 0.26 mm. This fact fully confirms the hypothesis that higher retention capacity values for the surface layers lead to smaller differences (errors).

Finally, historical drainage data from 1984–1985 are presented (Table 2) as the initial basic data for calculating the retention capacity of the surface layers using Eq. (11). Eq. (11) is valid from a certain time

doi: 10.17221/119/2013-SWR

point which was defined by Eq. (12). The data are from the experimental drainage field of the Egyptian-Dutch Advisory Panel on Land Drainage (Ritzema 2009). A comparison of the differences between the instantaneous and calculated retention capacity values for the soil layers in the Mashtul Pilot Area (Nile Delta, Egypt) is presented in Table 2.

It should be pointed out that the soil and drainage conditions in the Mashtul experimental drainage field are different from the conditions in the RISWC experimental field in Prague-Zbraslav. In the Mashtul experimental area, the drainable pore space value P is three times higher than in the RISWC experimental field, and the impervious barrier is also much deeper, tending towards infinity (Alterra-ILRI 2008; Stibinger 2011).

However, Table 2 shows results with the same characteristics both for the Mashtul and the RISWC experimental fields. It even seems that the calculated approximations used in Eq. (11) fit the instantaneous values closely, especially at the end of the test period. The suitability of the modelled formula represented by Eq. (10) is shown by the determination index with a high value of I_R = 0.956.

This means that Eq. (11) is also applicable in deeper drained soil profiles with more permeable soil conditions with higher porosity.

CONCLUSION

Based on the present results, Eq. (11) is seemingly a suitable tool for calculating the DRC of the surface layers developed by a subsurface pipe drainage system, approximating the real values.

Verifications of the simple analytical approximation of the retention capacity of the surface layers developed by a subsurface pipe drainage system calculated in Eq. (11) were carried out with data measured directly in the RISWC experimental field in Prague-Zbraslav, Czech Republic (Soukup *et al.* 2010) and in the experimental field in Mashtul, Egypt (Ritzema 2009).

The results presented here have shown good conformity between the computations and the measured data under unsteady-state drainage flow conditions in a deep soil profile with less permeable soil conditions.

The analytical approximation presented in Eq. (11) can be used as a simple tool for making an immediate estimate of the DRC value of soil layers developed by a subsurface drainage system, which can be further corrected or adjusted.

The equation should serve as a good and useful tool that requires only a minimal amount of information – basic soil hydrology data and basic design parameters of the drainage system. The verification of the field test results and measurements has shown that the equation can offer benefits to the user.

Acknowledgements. The paper was supported by the Ministry of Agriculture of the Czech Republic, Project No. QJ1220050 Strengthening of infiltration processes by runoff regulation from small catchments. The authors would like to express their many thanks to R.A. Healey for linguistic quality control of this paper.

References

Alterra-ILRI (2008): Materials from the International Course on Land Drainage, module 3: "Design, Implementation and Operation of Drainage Systems" Pre-drainage investigations for the Mahstul Pilot Area (Nile Delta, Egypt). Wageningen, Alterra-IRLI, Wageningen University and Research Centre.

Blann K.L., Anderson J.L., Sands G.R., Vondracek B. (2009): Effects of agricultural drainage on aquatic ecosystems: A review. Critical Reviews in Environmental Science and Technology, 39: 909–1001.

Dan H., Xin P., Li L., Li L. (2013): Improved Boussinesq Equation-Based Model for transient flow in a drainage layer of highway: capillary correction. Journal of Irrigation and Drainage Engineering, 139: 1018–1027.

De Zeeuw J.W., Hellinga F. (1958): Precipitation and runoff. Agricultural Journal, 70: 405–422. (in Dutch)

Deasy C., Titman A., Quinton J.N. (2014): Measurement of flood peak effects as a result of soil and land management, with focus on experimental issues and scale. Journal of Environmental Management, 132: 304–312.

Dieleman P.J., Trafford B.D. (1976): Drainage Testing. Irrigation and Drainage Paper 28. Rome, FAO.

Fuentes C., Zavala M., Saucedo H. (2009): Relationship between the storage coefficient and the soil-water retention curve in subsurface agricultural drainage systems: Water table drawdown. Journal of Irrigation and Drainage Engineering, 135: 279–285.

Hooghoudt S.B. (1940): Contribution to the knowledge of some physical parameters of the soil. Part 7. Agricultural Research Reports, 46B: 515–707. (in Dutch)

Hümann M., Schüber G., Müller Ch., Schneider R., Johst M., Caspari T. (2011): Identification of runoff processes – The impact of different forest types and soil properties on runoff formation and floods. Journal of Hydrology, 409: 637–649.

doi: 10.17221/119/2013-SWR

Kabat P., Claussen M., Dirmeyer P. *et al.* (2004): Vegetation, Water, Humans and the Climate. A New Perspective on an Interactive System. Berlin, Heidelberg, New York, Springer-Verlag.

Nijland H.J., Croon F.W., Ritzema H.P. (2005): Subsurface Drainage Practices. ILRI Publ. 60, Wageningen, Alterra.

Ritzema H.P. (2007): Subsurface flows to drains. In: Ritzema H.P. (ed.): Drainage Principles and Applications. ILRI Publ. 16, 3rd Ed. Wageningen, ILRI: 283–294.

Ritzema H.P. (2009): Drain for Gain: Making Water Management Worth its Salt: Subsurface Drainage Practices in Irrigated Agriculture in Semi-arid and Arid Regions. Leiden, CRC Press/Balkema.

Singh S.K. (2009): Generalized analytical solutions for groundwater head in a horizontal aquifer in the presence of subsurface drains. Journal of Irrigation and Drainage Engineering, 135: 295–302.

Soukup M. *et al*. (2000): Regulation and retardation of the drainage discharge from agricultural land. [Annual Report of Project EP 096000 61 50 in 1999.] Prague, Research Institute for Soil and Water Conservation Prague. (in Czech, abstract in English)

Stibinger J. (2003): Analytical approximation of subsurface total drainage quantity in non-steady state drainage flow and its verifications in heavy soils. Irrigation and Drainage Systems, 17: 341–365.

Štibinger J. (2009): Approximation of subsurface drainage discharge by De Zeeuw-Hellinga theory and its verification in heavy soils of fluvial landscape of the Cerhovice brook. Soil and Water Research, 1: 28–38.

Stibinger J. (2011): Hydraulic function of subsurface pipe drainage system on agricultural and drainage experimental field in Mashtul Pilot Area (Nile Delta, Egypt). Agricultura Tropica et Subtropica, 44: 103–112.

Zavala M., Fuentes C., Saucedo H. (2007): Non-linear radiation in the Boussinesq equation of the agricultural drainage. Journal of Hydrology, 332: 374–380.

Received for publication December 17, 2013
Accepted after corrections June 24, 2014

Corresponding author:

Ing. Jitka Pešková, Česká zemědělská univerzita v Praze, Fakulta životního prostředí, katedra biotechnických úprav krajiny, Kamýcká 129, 165 21 Praha 6-Suchdol, Česká republika; e-mail: peskovaj@fzp.czu.cz

PŘÍLOHA č. 4

Study of the evapotranspiration impact on diurnal discharges in a small catchment

Kovar P.[1], Peskova J.[1], Dolezal F.[2], Bacinova H.[1], Krovak F.[1], Mihalikova M.[2]

[1] … Faculty of Environmental Sciences, Czech University of Life Sciences Prague

[2] … Faculty of Agrobiology, Food and Natural Resources, Czech University of Life Sciences Prague

Abstract

This paper describes a new application of the Fourier series for a detailed simulation of the runoff on a catchment in dry periods when the stream flow is significantly impacted by evapotranspiration, particularly during daytime hours. Catchments can be considered as dynamic systems where evapotranspiration has an impact on streamflow day-night fluctuating discharges. Measurements of these discharges have been supported by the recent development of high-resolution sensing equipment based on the water pressure principle. Using a short time step on a small catchment, we were able to take measurements of diurnal streamflow fluctuations at any time of the day in a harmonic wave, and also to calculate the impact of the actual evapotranspiration. In parallel, we measured the free water evaporation and also the soil moisture content nearby. One of the reason of this measurement is to study a time shift of stream flow discharges delayed after water evaporation record due to hydraulic resistances. The **Fourier Series Model (FSM)** was implemented as a tool for mathematical analysis. This model provides computed discharge data through the harmonic coefficients. The major emphasis here is on the methodology of the FSM, which may be useful either for runoff simulation or for reconstructing evapotranspiration records where direct measurements are unreliable at the catchment scale.

Keywords: catchment depletion curve, evapotranspiration assessment, Fourier series, harmonic coefficients, high resolution sensing, rainless period.

Introduction

The relation between catchment vegetation and the hypodermic zone forms an important linkage in ecosystem dynamics (Balek 2006). The first publication on fluctuations of discharges due to evapotranspiration was based on observations of a small catchment in the dry year 1976 (Burt 1979). This paper also showed the harmonic process of baseflow delay, tracing lower discharge values in the daytime hours and higher values in the night hours, due to the same process of evapotranspiration. This delay of the wave-shaped depletion curve was caused by the evaporation conditions, and partly also by hydraulic roughness (Dvorakova et al., 2014). The wave-shaped curve was described by Bond *et al.* (2002). With the application of high-resolution equipment able to make precise measurements of water discharges in the outlet of a catchment, many papers describing similar discharge fluctuation records in day/night regimes began to appear early in the 21st century (Zhang *et al.* 2001; Brown *et al.* 2004; Loheide *et al.* 2005; Deutscher & Kupec 2014). Other hydrologists have described the shapes of jagged depletion curves on small catchments (Fenicia *et al.* 2006; Winsemius *et al.* 2006; Dvorakova & Zeman 2010; Dvorakova *et al.* 2012 and 2014; Kovar *et al.* 2014).

Hydrological processes in small catchments began to be analysed and described using the modern systems approach in the late 1960s, soon after systems engineering linkages and their feedback were explained and published (Kraijenhoff *et al.* 1966). Systems hydrology takes into account not only links between rainfall and runoff, but also links between runoff and evaporation (Kirchner 2006). Both of these links are important hydrological processes that can be described by a harmonic and periodic Fourier series.

The Fourier series is used to investigate an idea based on systems theory. The input to the hydrological system is a depletion curve, in the form either of a straight line or of a flat exponential curve that shows the falling limb of the hydrograph in a rainless period. The output of the system is an undulating curve caused by the maximum-minimum diurnal impact on the streamflow by evapotranspiration. The falling trend describes the depletion process. In contrast to the output curve, the input curve is not influenced by evapotranspiration. The two curves can be represented by a Fourier series with a different form and different parameters. To transform input systems into output systems, it is necessary to go through the evapotranspiration process, which turns straight-line runoff depletion into an undulating curve similar in shape to a harmonic Fourier series curve. The analysis of the process can be expressed by the mass–conservation equation (Kirchner 2009):

$$dS/dt = P - E - Q \tag{1}$$

where S is water storage, P is precipitation, E is evapotranspiration, and Q is discharge. In Eq. (1), only the discharge is an aggregated measurement for the entire catchment. The author of this analysis (Kirchner 2009) added what can be learned about catchment processes from fluctuations in streamflow, without assuming that measurements of precipitation or evapotranspiration are spatially representative. Extreme droughts are often estimated using discharge measurements during streamflow, and show harmonic evaporation rates that are orders of magnitude smaller than the levels in typical catchments (Kirchner 2009; Langhammer & Vilimek, 2008; Kovar *et al.* 2014).

A further question is whether it is better to apply the Boussinesq exponential type of curve or the regression line only for a recession curve of the Starosuchdolsky Brook catchment. The decision depends on the storage-discharge relationships, and in particular on the position of the falling limb of the hydrograph. In general, the Boussinesq exponential curve can be applied more broadly than the regression line (Brutsaert & Nieber 1977).

Methods and Materials

Fourier Series Model

The Fourier series is expressed as an orthogonal function (Hardy & Roginski 1971). The function $g(t)$, in the interval $0 < t < n$, can be exactly represented in any time t of this interval by the Fourier series:

$$g\ (t)= a_0 + \sum_{r=1}^{n-1}(a_r .\ cos\ r\ \frac{2\pi t}{n} + b_r\ .\ sin\ r\ \frac{2\pi t}{n}) \qquad (2)$$

The cosine and sine functions of this series are orthogonal to one another for any pair of limits n separately. Thus the coefficients in Eq. (2) are given by:

$$a_r = \frac{2}{n}\int_0^n g\ (t)\ .\cos r\ \frac{2\pi t}{n}\ dt \quad \text{,but} \quad \mathrm{a}_0 = \frac{1}{n}\int_0^n g\ (t)\ dt, \quad \mathrm{b}_\mathrm{r} = \frac{2}{n}\int_0^n g\ (t)\ .\sin r\ \frac{2\pi \mathrm{t}}{n}\ dt \qquad (3)$$

If the time functions of input functions $x(t)$, output functions $y(t)$,and transformation functions $u(t)$ are represented by a finite harmonic expansion of the same time duration n, we can use the coefficients *[a, b]* for *x(t)*, *[A, B]* for *y(t)*, and *[α, β]* for *u(t)*. Then, by substitution to the convolution integral, which is the expression for the output, we obtain all the coefficients that are needed. The Fourier Series Model (FSM) has been adapted from the classical Fourier series expansion, which was developed earlier for simulations of rainfall–runoff events (O'Donnell 1960). However, instead of a rainfall hyetograph as an input function, the depletion function $x\ (t)$ is used, either in the form of a line or in the form of an exponential curve approximated by the Fourier expansion with coefficients a_r, b_r, where r is the index for harmonic coefficients, see Eq. (2). Output function $y\ (t)$ is a harmonic series expansion that is transformed by the evapotranspiration process with coefficients A_r and B_r:

$$\mathrm{A_r} = \frac{\mathrm{n}}{2}\ (a_\mathrm{r}\alpha_\mathrm{r} - \mathrm{b_r}\beta_\mathrm{r}), \qquad \mathrm{A}_0 = \mathrm{n} \cdot a_0\alpha_{0,} \qquad \mathrm{B_r} = \frac{\mathrm{n}}{2}\ (a_\mathrm{r}\beta_\mathrm{r} - \mathrm{b_r}\alpha_\mathrm{r}) \qquad (4)$$

This transformation process is again linear, and is based on a Fourier series expansion for the transformation function with coefficients α_r, β_r. We solve the coefficients as follows:

$$\alpha_\mathrm{r} = \frac{2}{n}\ .\frac{a_\mathrm{r}\ \mathrm{A_r} + \mathrm{b_r}\ \mathrm{B_r}}{a_\mathrm{r}^2 + \mathrm{b}_\mathrm{r}^2} \quad \text{,but} \quad \alpha_0 = \frac{1}{n}\ .\frac{\mathrm{A}_0}{\mathrm{a}_0}, \qquad \beta_r = \frac{2}{n}\ .\frac{a_r B_r - b_r A_r}{a_r^2 + b_r^2} \qquad (5)$$

In principle, if there is given $x\ (t)$ and the corresponding $y\ (t)$ in n points for a time invariant linear system (i.e. if the time step is Δt), then $x\ (t)$ and $y\ (t)$ can be represented by $g\ (t)$ in all t–points in the discrete interval $O\ \leq t\ \leq n$. From the input data $x\ (t)$ and also from the output data $y\ (t)$ in all n points, it is easy to set up precisely the finite harmonic series with n–terms:

$$yc\ (t) = g\ (t)\ =\ a_0 + \sum_{r=1}^{n-1} a_r\ .\cos \mathrm{r}\ \frac{2\pi\mathrm{t}}{\mathrm{n}} + \mathrm{b_r}\ .\sin \mathrm{r}\ \frac{2\pi\mathrm{t}}{\mathrm{n}} \qquad (6)$$

In practice, this is a set of n simultaneous equations (for $\mathrm{t} = 0, 1, 2, \ldots (n-1)$) with n "unknown" coefficients $a_0, a_1, \ldots a_p$; $b_1, b_2, \ldots b_p$. The orthogonality property, this time with respect to summation, permits us to find the n coefficients:

$$a_r = \frac{2}{n}\sum_{r=1}^{n-1} g\ (t)\ .\cos r\ \frac{2\pi t}{n}, \quad a_0 = \frac{1}{n}\sum_{r=1}^{n-1} g\ (t), \quad b_r\ =\ \frac{2}{n}\sum_{r=1}^{n-1} g\ (t).\sin r\ \frac{2\pi t}{n} \qquad (7)$$

Series (6) can hardly be expected to fit $g\ (t)$ exactly between the given data points, where in fact $g\ (t)$ is not known, but it does fit the n data points exactly. As n is increased, the n harmonic coefficients of the finite series fitting n points approach the Fourier coefficients of the finite series fitting the function everywhere (O'Donnell 1960). By implication, we can use only harmonic coefficients as approximations for the Fourier coefficients $[a_n,\ b_n]$ and $[A_n,\ B_n]$ in Eqs. (5), and we can find only a finite number of such approximate Fourier coefficients. Therefore, we have to accept errors in the $[\alpha_n,\ \beta_n]$ coefficients of the transformation function $u\ (t)$ of the runoff to evaporation. These errors also depend on the duration of time step Δt and on the fact that we can find only a finite number of coefficients $[\alpha_n,\ \beta_n]$. If we have computed these coefficients α, β, they can be used for the transformation function:

$$u\ (t) = \alpha_0 + \sum_{r=1}^{n-1} \alpha_r \,.\cos r\ \frac{2\pi t}{n} + \beta_r \,.\sin r\ \frac{2\pi t}{n} \tag{8}$$

Then, we can proceed to compute the simulated diurnal runoff (discharge ordinates) in each time step $y\ (t)$:

$$y\ (t) = A_0 + \sum_{r=1}^{n-1} (A_r \,.\cos r\ \frac{2\pi t}{n} + B_r \,.\sin r\ \frac{2\pi t}{n}) \tag{9}$$

Starosuchdolský Brook Experimental Catchment

The Fourier Series Model methodology requires small catchments and good water-retaining soil characteristics to protect vegetation in dry conditions. The Starosuchdolsky Brook close to Prague, Czech Republic, has a small catchment area of 2.95 km^2. In such a small catchment, the differences in diurnal water discharges can be significant, usually enabling high-quality data to be gathered.

The catchment characteristics are given in Table 1 and in Fig. 1. The prevailing land use in the Starosuchdolsky Brook catchment is arable land (50% of the catchment area) and urbanized areas (38%). The forested area is a mixture of deciduous and coniferous trees. The downstream part of the catchment is environmentally protected. In both river belts there are typical local forest species, represented by *Alnus glutinosa*, *Fraxinus excelsior*, *Quercus robur*, and a small number of *Carpinus betulus*.

The morphology of the catchment has a plain character in its upper part (up to 0.05 of slope), then it goes down to the central area, which is much steeper (up to 0.30), and the outlet part again has a moderate slope. Diurnal discharge fluctuation occurs in the catchment during hot, dry summer periods, and the discharge measurements show clear day/night differences in the runoff depletion process. The deep soil moisture content of the Starosuchdolsky Brook catchment is always partially saturated, due to the deep valley morphology. The moisture content therefore contributes to the streamflow for a long time.

Table 1

Results

The Starosuchdolsky Brook catchment has been monitored since 2011. The discharge data is obtained from the water table data, which is obtained from measurements taken every ten seconds at the outlet of the catchments, using a V-notched (Thomson) weir equipped with a Vegawell 71 submersible water level gauge. The gauge measures the water pressure with high-resolution sensitivity. Among many dry episodes measured in the catchment of the Starosuchdolsky Brook, we have selected the following three episodes:

EPISODE 1:24/6 (20 h) – 29/6 (05h) 2011 (n = 106 h)

EPISODE 2: 22/5 (09h) – 29/5 (02h) 2012 (n = 162 h)

EPISODE 3: 08/8 (02h) – 16/8 (20h) 2012 (n = 211 h)

where n is the number of time steps Δt. For this study, Δt was set to one hour. The Fourier Series Model (Kovar *et al.* 2014) has recently been modified and implemented for a broader episode spectrum of measurements (Dvorakova *et al.* 2014). The free water evaporation measurements were taken at a weather station located in a grassland area about 2 km to the south of the centre of the catchment, using an EWM automatic sunken evaporation pan, developed by AS & Consulting, Melnik, Czech Republic (Bares *et al*. 2006). The geometry of EWM is derived from the standard Russian GGI-3000 evaporation pan (Gangopadhyaya *et al.* 1966; cited after Brutsaert 1982). EWM has a cylindrical design, and is made of stainless steel, with a cross-sectional area of 3000 cm^2 and a height of 60 cm, of which 10 cm extends above the ground. The water level is detected by a float, and is monitored by a digital optical position sensor with 0.1 mm resolution.

When the discharges were measured at the outlet of the Starosuchdolsky Brook catchment, priority was given to the same episodes. The aim of these measurements was to test the hypothesis that the daily catchment discharge minima correspond with the water evaporation maxima. Finally, the relation is also dependent on the soil moisture content and on the time taken for the depletion process of the surface runoff, and also the subsurface water flow. The field capacity of the soil, the lower threshold of drainable soil water, was estimated in the standard way as the soil water content corresponding to 33 kPa of suction (Romano & Santini 2002). It was found to be, on an average, 0.371 $m^3\ m^{-3}$, with a standard deviation of 0.063 $m^3\ m^{-3}$. The measurements (three replications) were performed in the laboratory on 250 cm^3 of undisturbed core samples, taken from the loamy, skeleton-rich soil of the alluvial plain at a depth of 10-15 cm. The HYPROP instrument was used. This is a piece of laboratory evaporation equipment for determining the retention curves and the unsaturated hydraulic conductivity of the soil (Schindler *et al.* 2010). The saturated water content of this soil (an estimate of the total porosity) was, on an average, 0.533 $m^3\ m^{-3}$, with a standard deviation of 0.029 $m^3\ m^{-3}$.

The three episodes discussed above are presented in this paper. First, the linear regressions and also the exponential correlation are presented to illustrate the Fourier input series, and then their coefficients a_r, b_r are computed (see Eq. 2). These input series simulate a smooth depletion process in the form of either a line (a linear function) or the exponential curve by the Boussinesq equation. The difference between these functions is very small. Table 2 presents the results of all three time episodes, using the methods of correlation analysis.

The measured discharges in their wavy line were used to compute the output Fourier coefficients A_r, B_r (Eq. 4). Then it was easy to solve the transformation harmonic coefficients $\alpha_r,\ \beta_r$ (Eq. 5), to compute the transformation function (Eq. 8), and to solve the simulated harmonic ("Fourier") series as the computed model responses of all episodes (Eq.

9). Figs. 2, 3, and 4 show the approximations of Episodes 1, 2, and 3. A comparison of the measured discharges and their computed pairs is presented Table 3a.

The efficiency coefficient (Nash & Sutcliffe 1970) computed for their goodness of fit is derived as:

$$EC = 1 - (\sum_{i=1}^{N}(Q_i - QC_i)^2)/(\sum_{i=1}^{N}(Q_i - \bar{Q})^2) \tag{10}$$

where: Q_i……measured discharge ordinates ($l.s^{-1}$)

QC_i…..computed discharge ordinates ($l.s^{-1}$)

$\bar{Q}$……mean value of the measured discharges ($l.s^{-1}$)

The Nash-Sutcliffe coefficient EC and its value for good acceptance should be $EC > 0.75$ (WMO 1992). However, the case of highly dense periodicity of the discharge fluctuation as an output function, in comparison with a line-type depletion curve as an input function, was computed once more. In addition, the influence of bias slightly reduces the acceptability level of the fit. This is the only case where episodes 1 and 2 are not within the accepted limit for goodness of fit.

There are two options for solving this problem. The first way is to select the number of harmonic coefficients, and the second way is to remove the ad hoc bias by using some smoothing approximation method. We used a polynomial series instead of a harmonic series. We selected 5-term polynomials to improve the fit and the EC values. However, this does not provide a substantial improvement, and ranks the $EC > 0.75$ (WMO 1992). Table 3b provides the correction of the bias of episodes 1 and 2, together with a new linear regression when polynomial smoothing changes the former harmonic shape. Fig. 5 and Fig. 6 test the better amendments of episodes 1 and 2. Table 4 provides a list of the transformation coefficients α_r and β_r of the Fourier series for all three episodes. The number of coefficients (rr) was adjusted according to the length of the series (n).

The last step in this study is to present how to assess the largest actual catchment-scale evapotranspiration from the free water evaporation data and the soil moisture data. The larger the catchment, the more inaccurate the results will be. For precise and reliable instrumentation, the next step is easy. The evapotranspiration values should be adjusted by the relative soil moisture content, as follows:

$$AE(i) = FWE\ (i).(SMC\ (i)/FC) \tag{11}$$

where:

$AE(i)$ … computed actual evapotranspiration (mm.h^{-1})

$FWE(i)$ … measured free water evaporation (mm.h^{-1})

$SMC(i)$ … measured soil moisture content (-)

FC … measured field capacity (-)

Fig. 7, Fig. 8 present graphs of the three episodes where all components were measured. We are aware that these results for the episodes are higher estimates of the actual evapotranspiration, as the starting point for the calculation is free water evaporation, and not potential evapotranspiration. However, in mild European climate conditions, when a few weeks pass without precipitation, an assessment of the actual evapotranspiration can be close to the values subtracted from the potential evapotranspiration (see Eq. 11). A better assessment can be provided by a water balance equation with the necessary measured components, using either seasonal Penman-Monteith potential evapotranspiration or the method proposed by Kirchner (2009), who introduced the function $g(Q)$ as the sensitivity function $g(Q) = dQ/dS$, where Q is discharge and S is water storage.

For the computed discharges in rainless periods $yc\ (t)$ in Eq. (9) we can also make use of the fundamental relationship of any linear system, viz. the convolution integral:

$$yc\ (t) = \int_0^t x(\tau) \cdot u\ (t - \tau)\ d\tau \tag{12}$$

where $x(\tau)$ is the input of depletion curve and $u\ (t - \tau)$ is a theoretical alternative of the transformation function. The rational computation requires to substitute the integral by the summation of $x(t)$ and $u\ (n - t)$ multiples within the certain limits corresponding to the duration of the event in Eq. (13):

$$yc\ (t) = \Delta\ t \sum_{t=1}^{n} (x\ (t) \cdot u\ (n - t)) \tag{13}$$

The term of addition in Eq. (13): $x(i) \cdot u\ (n - i)$ for the finite limits expressed the convolution procedure when $x\ (t)$ is not zero, then the computed runoff $yc\ (t)$ can be expressed by Eq. (9) which is the Fourier expansion.

Discussion

The diurnal discharge fluctuation during a hot and dry summer period can be observed in the measured discharge records. The discharges show a declining trend in their runoff depletion curve, but the catchment rarely becomes dry, even in a long time period. The soil zone of the catchment is always partially saturated, owing to its deep valley morphology in the Starosuchdolsky Brook plain. It therefore contributes almost permanently to the streamflow. There is still a question about the type of recession curve that should be used - whether to apply the Boussinesq exponential type of curve, or the least squares line only. Many hydrologists take the view that it depends on the storage-discharge relationships, i.e. on the position on the falling limb of the hydrograph. In general, the Boussinesq exponential curve type can be more broadly applied (Rupp & Selker 2006).

Evapotranspiration during a rainless period can be roughly assessed by discharge measurements, and also from a runoff simulation using the Fourier Series Model (FSM). The expression “roughly” means that the discharge ordinates are loaded by the hydraulic resistance impact, which calls into doubt the validity of expressing the values on the basis of computed daily values of the actual evapotranspiration, either by water balance models or much less precisely by FSM, due to the bias with which they are loaded. This bias must be taken into consideration when analysing the problem. A dynamic catchment system offers useful information on how streamflow hydrographs may be applied for reconstructing evapotranspiration records. In such a dynamic system, precipitation and evapotranspiration have comparable but opposite effects on the catchment storage, and therefore on the streamflow.

As the fluctuations in the streamflow reflect the precipitation to the catchment, it is natural to conclude that these fluctuations also reflect the evapotranspiration losses. In the past decades, hydrologists studied ways of using discharge measurements during streamflow recession to show harmonic evapotranspiration rates. The smaller the catchment, the more significant the fluctuations will be (Brutsaert 1982; Boronina *et al.* 2005; Szilagyi *et al.* 2007). Similar results were found in delay time and water-use related fluctuations by evapotranspiration of 1% to 3% in mid-Wales, in the Severn and the Wye (Kirchner 2009). The differences were evidently caused by different climatic and geographical conditions.

Figs. 1 to 3 present interesting data to illustrate what happens when evapotranspiration impacts the flow. It is practical to implement FSM based on the Fourier series, where the input coefficients (a_r, b_r) and the output coefficients (A_r, B_r) in Eq. (5) are used for computing the transformation function coefficients ($\alpha_r,\ \beta_r$). However, the results are loaded by some noise from the subsurface processes, which delay the surface discharge mainly due to hydraulic roughness (Dvorakova *et al.* 2014; Kovar *et al*. 2014). Nevertheless, the method for computing discharge ordinates undoubtedly has an excellent mathematical background (O'Donnell 1960; Hardy & Rogosinski 1971).

One more remark for discussion: the approximation of the transformation function $u\ (n-t)$ (see Eqs. (8), (9) and (13)) for the computed discharges by FSM offers a higher goodness of fit than other similar mathematical models, i.e. Laguerre functions. The FSM can be improved through the choice of the period length $n \to t$ (Kraijenhoff *et al.* 1966). Herein, the number of the Fourier´s harmonic coefficients rr can be increased up to the number of the discharge ordinates n. Fig. 9 shows the transformation function $u\ (t)$ in EPISODE 3.

For the sake of completeness, the harmonic model coefficients can also be used for computing discharge data that is missing due to a measurement failure. In this case, we can use both the input coefficients and the transformation coefficients from the time series just before the discharge measurements collapsed (Kovar & Bacinova 2015).

Conclusions

The impact of evapotranspiration on catchment runoff is an interesting but little studied hydrological phenomenon. Water use by riparian vegetation is closely linked to diurnal streamflow variability. The FSM model used in this study is based on the Fourier series, and it takes full advantage of its mathematical properties, such as harmonic functions, convolution principles, and strong convergence. The methodology based on the set of Eqs. (2) to (9) used in this study is straightforward, but it has only become applicable with the development of high-resolution measuring instruments. Complementary relations between streamflow measurements and the corresponding mathematical tool (FSM) have now been joined together to produce this methodology. This would hardly have been applicable ten years ago. All these advantages can be used in hydrology, not only for rainfall-runoff relations but also for runoff-evapotranspiration relations. Both of these hydrological attributes are well functioning dynamical systems in catchment hydrology. The assumption of a well-functioning dynamical system may not be smoothly applicable for every catchment, but in many cases it can provide a useful approximation. Thus streamflow hydrographs may also be useful for reconstructing evapotranspiration records.

Acknowledgement

This study was supported within Czech Technological Agency project TA02020402 Water Regime Optimisation to Mitigate Impacts on Hydrological Extremes. We express our gratitude for this financial support.

References

Balek, J. 2006 Small basins as a continuous source of information. Malá povodí jako trvalý zdroj informací. *J. Hydrol. Hydromech.*, Vol. **54**. No. 2: 96-105.

Bares, D., Mozny, M., Stalmacher, J. 2006 Automation of evaporation measurements in the Czech Hydrometeorological Institute. In Czech. In: *Bioklimatológia a voda v krajine.* Strečno, 11. - 14. 9. 2006. Slovak and Czech Bioclimatological Society. ISBN 80-89186-12-2. 9 p. http://www.cbks.cz/sbornikStrecno06/prispevky/PosterI._clanky/P1-16.pdf, accessed 15 May 2015.

Bond, B. J., Jones, J. A., Moore, G., Phillips, N., Post, D., McDonnell, J. J. 2002 The zone of vegetation influence on baseflow revealed by diel patterns of streamflow and vegetation water use in a headwater basin, *Hydrol. Processes*. **16**, 1671-1677.

Boronina, A., Golubev, S., Balderer, W. 2005 Estimation of actual evapo-transpiration from an alluvial aquifer of the Kouris catchment (Cyprus) using continous streamflow records. *Hydrol. Processes* **19**, doi: 10.1002/hyp.5871.

Brown, E. A., Zhang, L., McMahon, A. T., Western, W. A., Vertessy, A. R. 2004 A review of paired catchment studies for determining changes in water yield resulting from alterations in vegetation. *Journal of Hydrology* **310**: 28-61.

Brutsaert, W. 1982 *Evaporation Into the Atmosphere: Theory, History and Applications*, D. Reidel, Dordrecht, The Netherlands.

Brutsaert, W., Nieber, J. L. 1977 Regionalized drought flow hydrographs from a mature glaciated plateau. *Water Resources Res.*, **13**, 637-643, doi: 10.1029/WR013i003p00637.

Burt, T. P. 1979 Diurnal variations in stream discharge and throughflow during a period of low flow, *Journal of Hydrology.*, Vol. **41**, issue 3 - 4: 291-301.

Deutscher, J., Kupec, P. 2014 Monitoring and validating the temporal dynamics of interday streamflow from two upland head micro-watersheds with different vegetative conditions during dry periods of growing season on the Bohemian Massif, Czech Republic. *Environmental Monitoring and Assessment*, Vol. **186**, No. 6: 3837-3846.

Dvorakova, S., Zeman, J. 2010 Analysis of fluctuation in the stream water level during the dry season in forested areas, *Scientia Agriculturae Bohemica*, vol. **41**, No. 4: 218-224.

Dvorakova, S., Kovar, P., Zeman, J. 2012 Implementation of conceptual linear storage model of runoff with diurnal fluctuation of discharges in rainless periods, *Journal of Hydrology and Hydromechanics* **60**, 4: 217-226 doi: 10.2478/v10098-012-0019-y.

Dvorakova, S., Kovar, P., Zeman, J. 2014 Impact of evatranspiration on discharge in small catchments. *Journal of Hydrology and Hydromechamics*. Vol. **62**, No. 4: 285-292. doi: 10.2478/johh-2014-0039.

Fenicia, F., Savenije, H. H. G., Matgen, P., Pfister, L. 2006 Is the groundwater reservoir linear? Learning from data in hydrological modelling, *Hydrol. Earth Syst. Sci.*, **10**: 139-150.

Gangopadhyaya, M., Harbeck, G. E. Jr., Nordenson, T. J., Omar, M. H., Uryvaev, V. A. 1966 Measurement and estimation of evaporation and evapotranspiration. *World Meteorological Organization*, Tech. Note No. **83**, WMO - No. 201, TP, 105.

Hardy, G. H., Rogosinski, W. W. 1971 *Fourier series, Fourierovy řady,* SNTL/ALFA, 3rd Issue, 04-005-71.

Kirchner, J. W. 2006 Getting the right answers for the right reasons: Linking measurements, analyses and models to advance the science of hydrology, *Water Resources Research* **42**, W03S04, doi: 10.1029/2005WR004362.

Kirchner, J. W. 2009 Catchments as simple dynamical systems: Catchment characterization, rainfall-runoff modeling, and doing hydrology backward. *Water Resources Research*, Vol. **45**, W02429, doi: 10.1029/2008WR006912.

Kovar, P., Dvorakova, S., Peskova, J., Zeman, J., Dolezal, F., Suva, M. 2014 *Application of harmonic analysis for evapotranspiration of riparian vegetation in dry periods.* Proceedings of the Conference Hydrology of Small Catchments. 2 volumes.

Kovar, P., Bacinova, H. 2015 Impact of Evapotranspiration on Diurnal Discharge Fluctuation Determined by the Fourier Series Model in Dry Periods. *Soil and Water Res.* **10**, 2015 (4): 210-217, doi: 10.17221/122/2015-SWR.

Kraijenhoff van de Leur, D. A., Schulze, F. E., O'Donnell, T.O. 1966 *Recent Trends in Hydrograph Synthesis*. TNO 13., The Hague.

Langhammer, J., Vilimek, V. 2008 Landscape changes as a factor affecting the course and consequences of extreme floods in the Otava river basin. Czech Republic. *Environmental Monitoring and Assessment* **144**, 53-66.

Loheide, S. P., Butler, J. R. J., Gorelick, S. M. 2005 Estimation of groundwater consumption by phreatophytes using diurnal water table fluctuations: A saturated-unsaturated flow assessment. *Water Resources Research*, vol. **41**, W07030. doi:10.1029/2005WR003942.

Nash, J. E., Sutcliffe, J. V. 1970 River flow forecasting through conceptual models. *Journal of Hydrology* **10**, 282-290.

O'Donnell, T. O. 1960 *Instantaneous unit hydrograph derivation by harmonic analysis.* IAHS Publ. No. 51: 546–557. Vol III. Ashbrook catchment, Wallingford Research Station.

Romano, N., Santini, A. 2002 Water retention and storage: Field. In: *Methods of Soil Analysis* (J. H. Dane; G. C. Topp, Eds.), Part 4, Physical Methods. Madison: ASA; SSSA, 721-738.

Rupp, D. E., Selker, J. S. 2006 On the use of the Boussinesq equation for interpreting recession hydrographs from sloping aquifers. *Water Resources Research* **42**, W12421, doi: 10.1029/2006WR005080.

Schindler, U., Durner, W., von Unold, G., Mueller, L., Wieland, R. 2010 The evaporation method: Extending the measurement range of soil hydraulic properties using the air-entry pressure of the ceramic cup. *Journal of Plant Nutrition and Soil Science* **173**, 563-572, doi: 10.1002/jpln.200900201 563.

Szilagyi, J., Gribovszki, Z., Kalicz, P. 2007 Estimation of catchment-scale evapotranspiration from baseflow recession data: Numerical model and practical application results. *Journal of Hydrology* **336**, 206-217, doi: 10.1016/j.jhydrol.2007.01.004.

Winsemius, H. C., Savenije, H. H. G., Gerrits, A. M. J., Zapreeva, E. A., Kless, R. 2006 Comparison of two model approaches in the Zambezi river basin with regard to model reliability and identifiability, *Hydrol. Earth Syst. Sci.*, **10**, 339-352.

WMO 1992 *Simulated real-time intercomparison of hydrological models*. WMO No. 779, Operational Hydrology 38, Geneva.

Zhang, L., Dawes, W. R., Walker, G. R. 2001 Response of mean annual evapotranspiration to vegetation changes at catchment scale. *Water Resources Research* **37**, 7001-7708.

List of Figures:

Fig. 1: Selected characteristics of the Starosuchdolsky Brook catchment

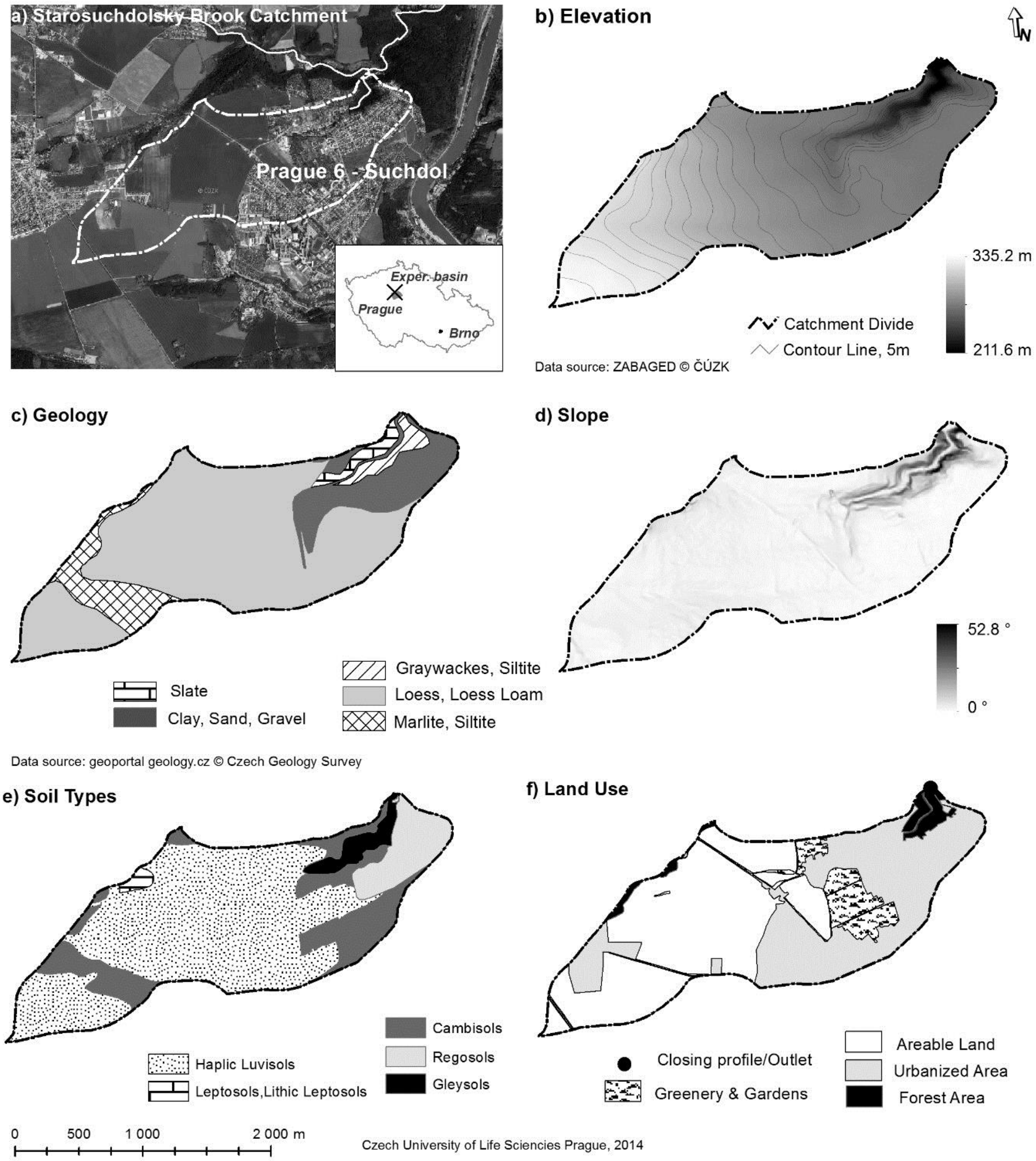

Fig. 2: Discharges in the dry period from 24/6/2011 to 29/6/2011 measured on the Starosuchdolsky Brook catchment. EPISODE 1

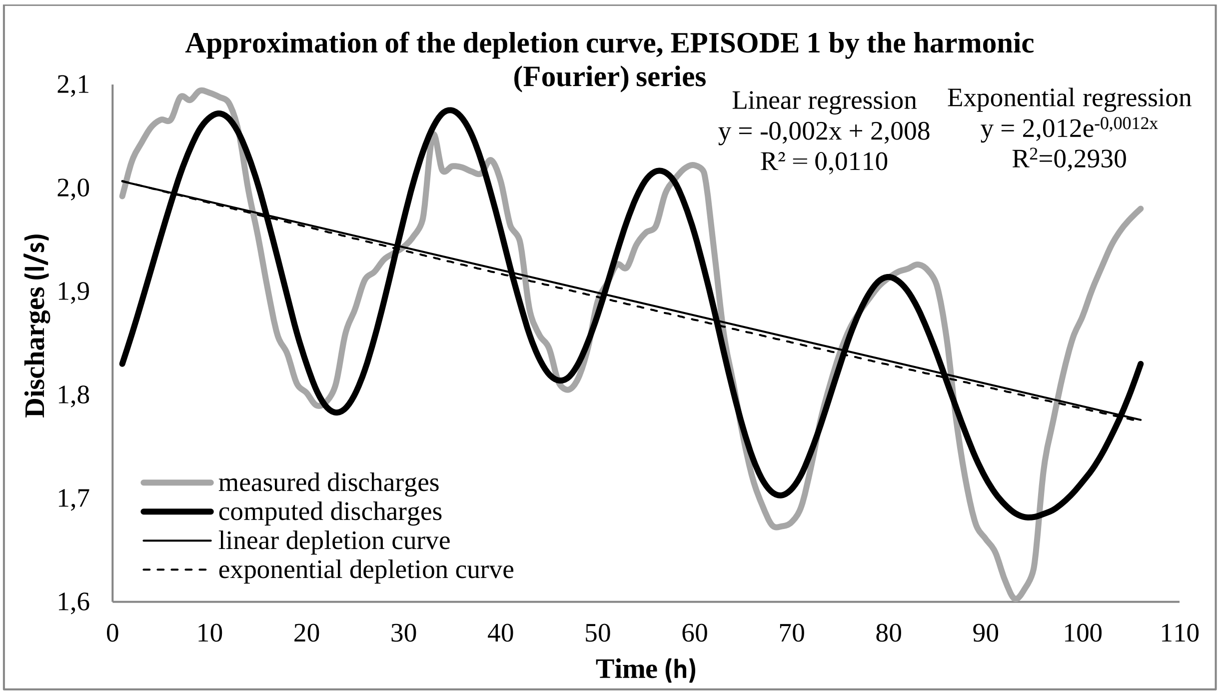

Fig. 3: Discharges in the dry period from 22/5/2012 to 29/5/2012 measured on the Starosuchdolsky Brook catchment. EPISODE 2

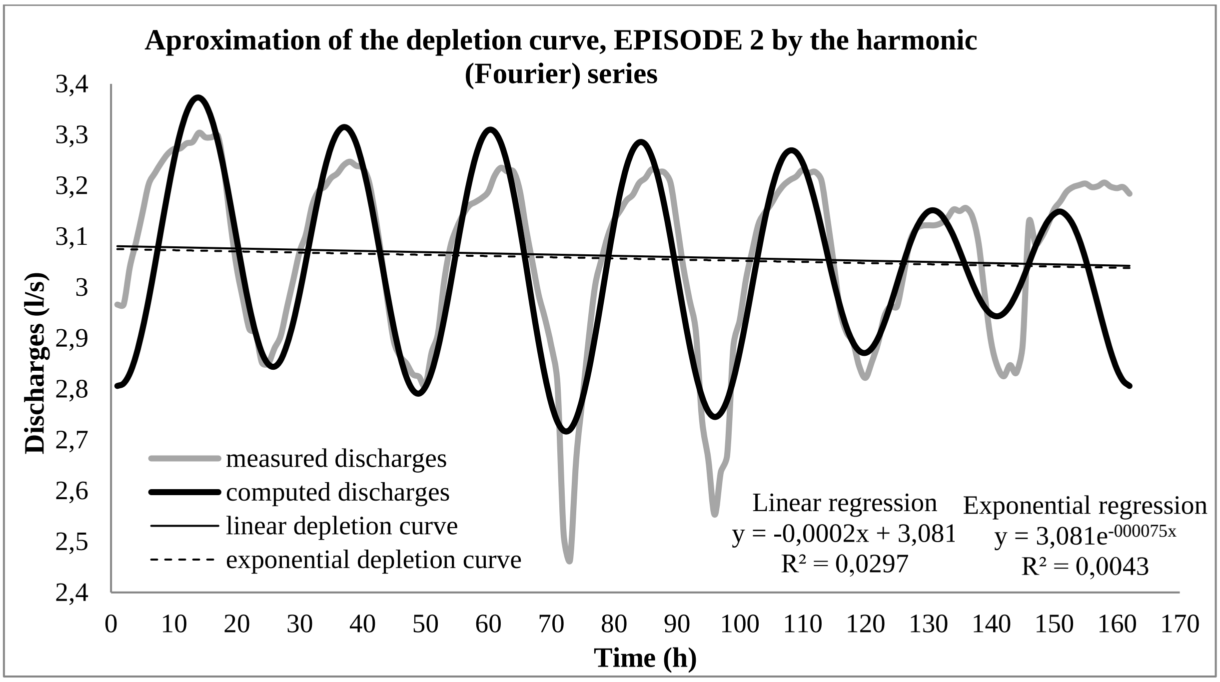

Fig. 4: Discharges in the dry period from 8/8 /2012 to 16/8/2012 measured on the Starosuchdolsky Brook catchment. EPISODE 3

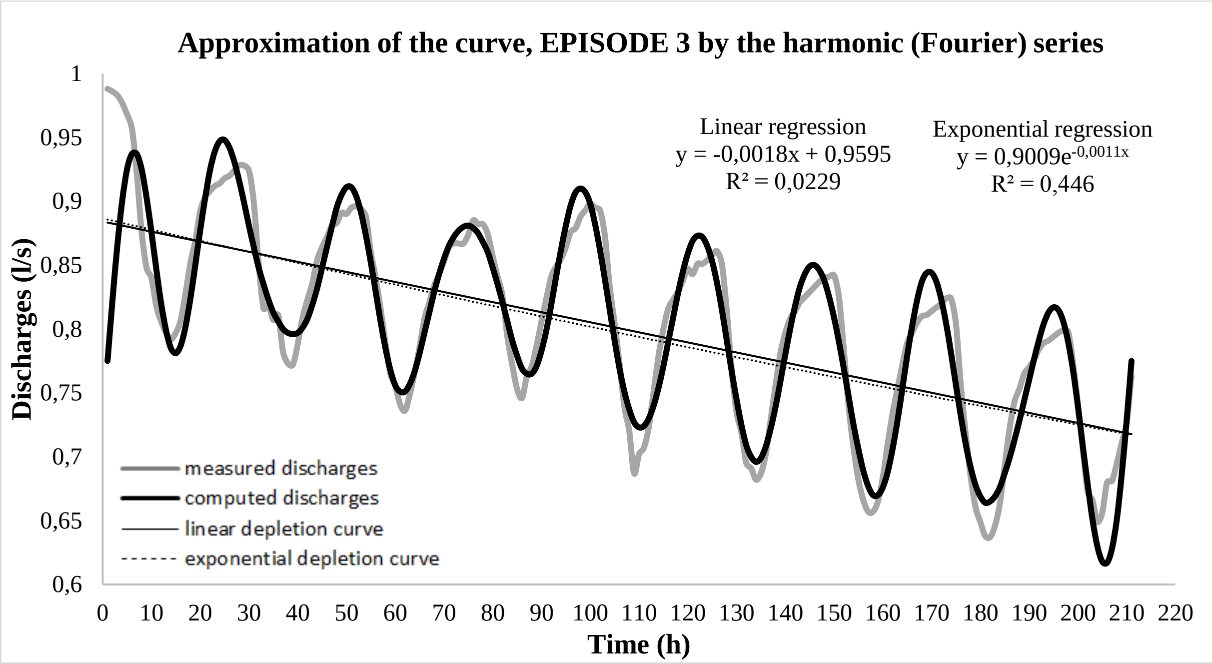

Fig. 5: Smoothing of the measured discharges by a 5-term polynomial. EPISODE 1 (bias amendment)

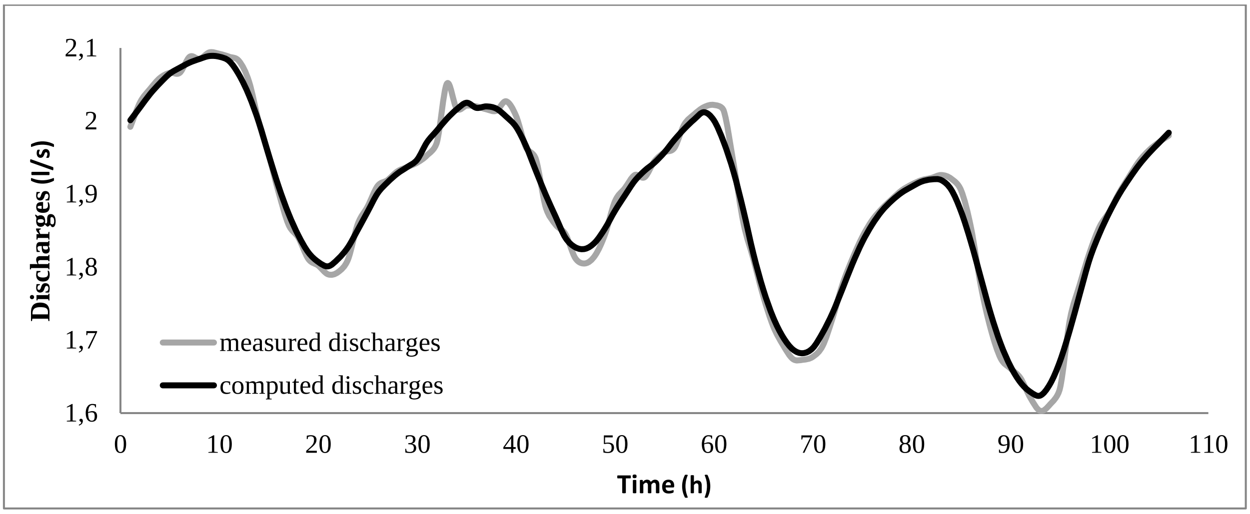

Fig. **6:** Smoothing of the measured discharges by a 5-term polynomial. EPISODE 2 (bias amendment)

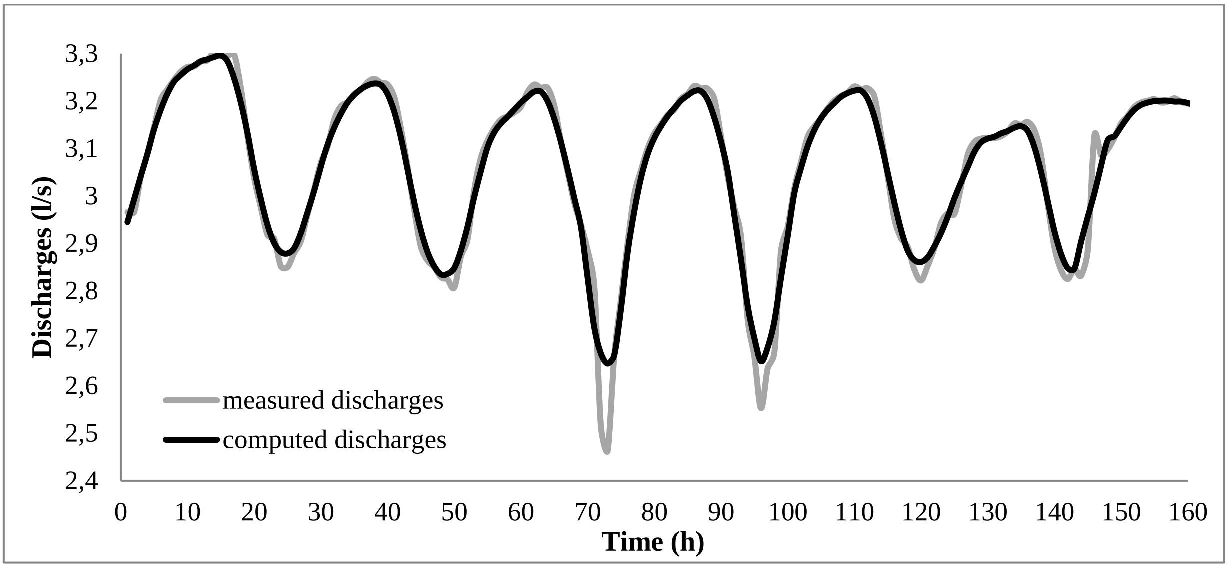

Fig. 7: An appraisal of the actual catchment-scale evapotranspiration. EPISODE 2

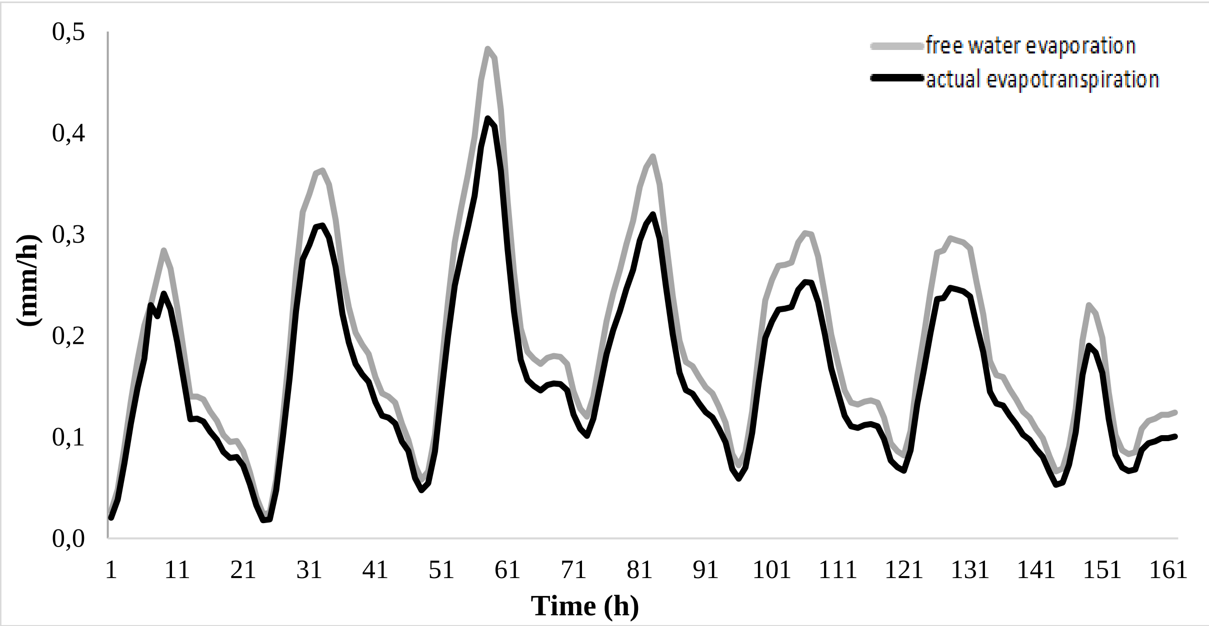

Fig. 8: An appraisal of the actual catchment-scale evapotranspiration. EPISODE 3

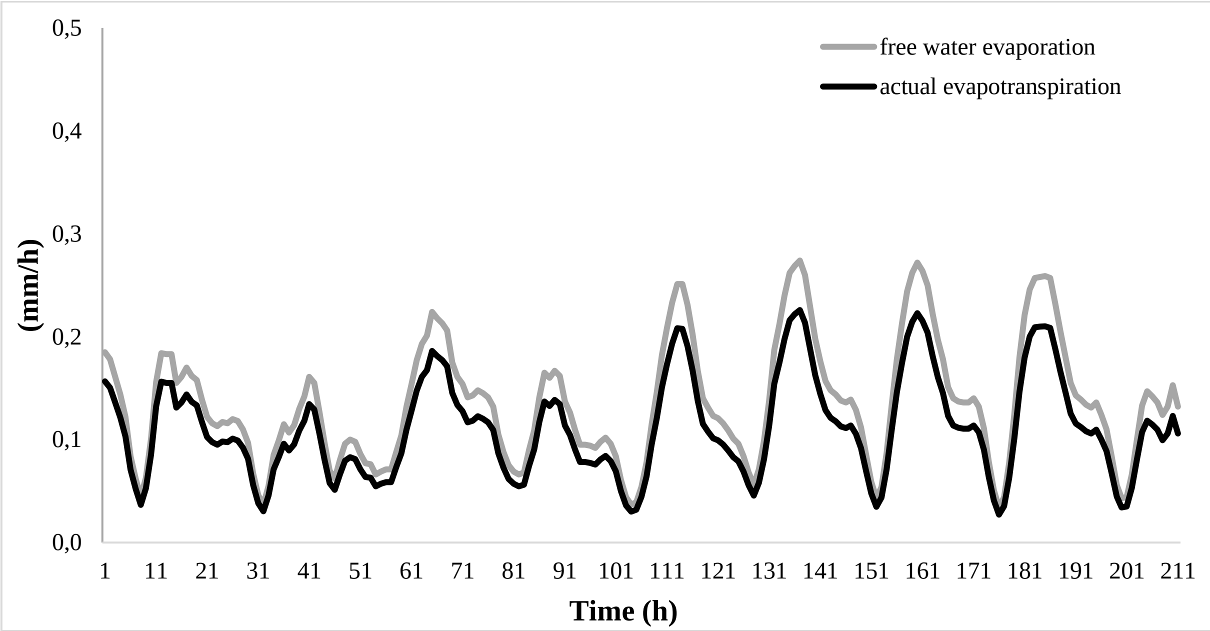

Fig. 9: Approximation of the transformation function $u\ (t)$. EPISODE 3 by the Fourier Series Model.

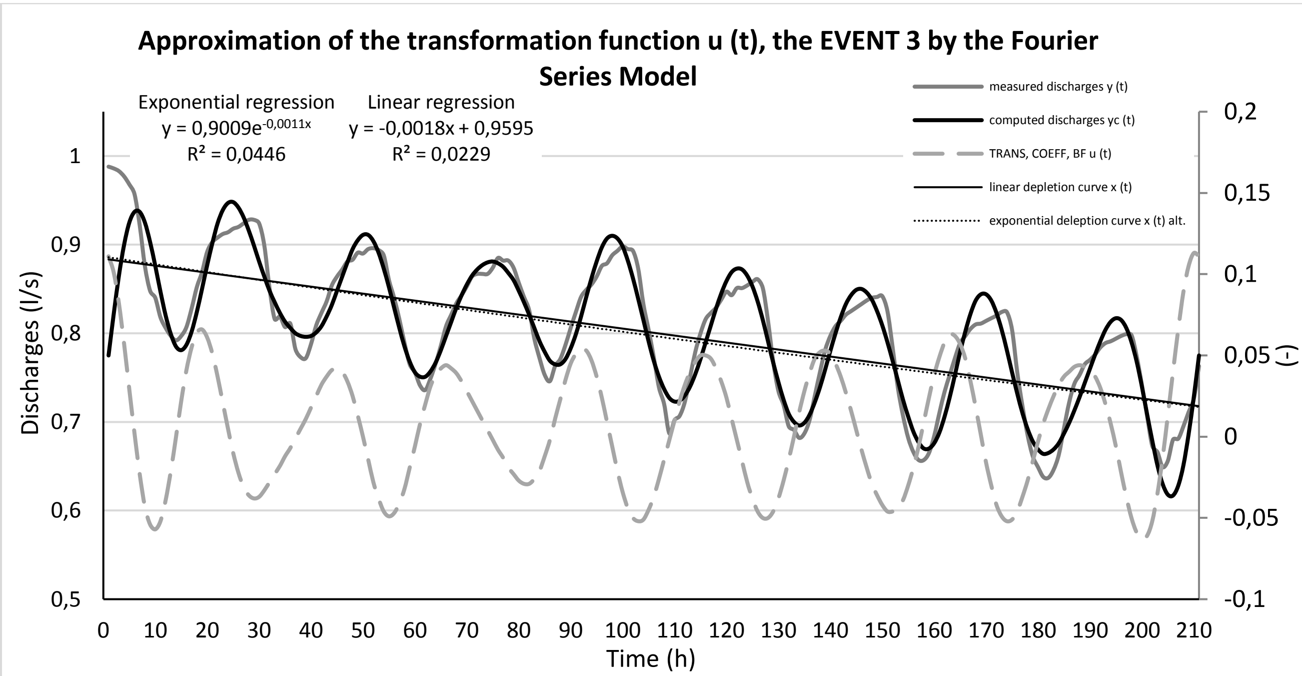

List of Tables:

Tab. 1.: Characteristics of the Starosuchdolsky Brook catchment

Physiographical factors of the Starosuchdolsky brook			
Catchment area (A, km^2)	2.95	Maximum catchment elevation ($H_{max.}$, m a.s.l.)	335
Length of thalweg (L_{th} , km)	3.7	Minimum catchment elevation (outlet) ($H_{min.}$, m a.s.l.)	211
Length of brook (L_b, km)	0.58	River network density (R_d , -)	0.33
Length of water divide (P, km)	9.1	Annual precipitation (mm)	350 - 400
Average slope of brook (J_b, %)	5.4	Annual runoff (mm)	120 - 140
Average catchment slope (J_s, %)	20	Annual average temperature (°C)	8.8
Land use categories of the Starosuchdolsky brook			
Arable land (%)	50.2	Urbanized area (%)	37.9
Forest (%)	3.5	Permanent grassland/greenery (%)	8.4

Tab. 2: Linear and exponential regressions of the depletion curves of the Starosuchdolsky Brook catchment in rainless EPISODE 1, 2, and 3

LINEAR REGRESSIONS		
	Approximated equations**: $y = a . x + b$**	
EPISODE 1	a = - 0.002195	b = 2.008608
	$R^2 = 0.011087$	
EPISODE 2	a = - 0.000240	b = 3.081071
	$R^2 = 0.029755$	
EPISODE 3	a = - 0.001822	b = 0.959497
	$R^2 = 0.022853$	
EXPONENTIAL REGRESSION		
Approximated equations (Boussinesq): $y = y_0 . e^{-\alpha.x}$		
EPISODE 1	$y_0 = 2.012123$	$\alpha = -0.001173$
	$y = 2.012123 . e^{-0.001173.x}$	
	$R^2 = 0.293019$	
EPISODE 2	$y_0 = 3.081396$	$\alpha = -0.000075$
	$y = 3.081396 . e^{-0.000075.x}$	
	$R^2 = 0.004286$	
EPISODE 3	$y_0 = 0.900967$	$\alpha = -0.001064$
	$y = 0.900967 . e^{-0.001064.x}$	
	$R^2 = 0.044559$	

Tab. 3a: Optimal number of the harmonic coefficients (rr) for the Nash-Suttcliffe coefficients for goodness of fit (EC)

EPISODE 1 (n = 106)		EPISODE 2 (n = 162)		EPISODE 3 (n = 211)	
rr	**EC**	**rr**	**EC**	**rr**	**EC**
6	0.743	7	0.726	15	0.860
5	0.725	6	0.709	14	0.858
7	0.739	8	0.716	16	0.862

Tab. 3b: Correction of the bias in Episode 1 and 2 by polynomial series smoothing

EPISODE 1 (n = 106)		EPISODE 2 (n = 162)		NEW LINEAR REGRESSION
rr	**EC**	**rr**	**EC**	**(Polynomial smoothing)**
6	0.771	7	0.742	EPI 1: a = - 0.002160
5	0.754	6	0.729	b = 2.006650
7	0.748	8	0.733	EPI 2: a = - 0.000228 b = 3.079739

Tab. 4.: Transformation coefficients α_r and β_r of the Fourier series for the episodes

Index	**EPISODE 1**		**EPISODE 2**		**EPISODE 3**	
	n = 106, rr = 6		**n = 162, rr = 10**		**n = 211, rr = 15**	
	α	**β**	**α**	**β**	**α**	**β**
0	0.010		0.006		0.005	
1	0.021	-0.001	-0.005	-0.008	0.004	0.001
2	0.007	-0.009	0.007	-0.005	0.004	-0.001
3	0.018	-0.020	0.003	-0.005	0.005	0.001
4	0.019	-0.041	0.007	-0.002	0.003	0.002
5	0.003	0.033	0.014	-0.002	0.004	0.001
6			0.005	-0.026	0.002	0.003
7			0.043	0.053	0.001	0.004
8			0.016	0.000	-0.003	0.011
9			0.014	0.006	0.039	-0.026
10					0.009	-0.008
11					0.011	-0.003
12					0.008	0.000
13					0.010	-0.002
14					0.010	0.002